ABSTRACT

SINGHI, BHAVYA. Wet Spinning of Poly (4-hydroxybutyrate) to Produce Drug-loaded Fibers for Controlled Drug Delivery Applications. (Under the direction of Dr. Martin W. King).

Polyhydroxyalkanoates (PHAs) are considered novel polymers because of their biodegradability and tunable mechanical and structural properties. A wide range of hydroxyalkanoate units, such as butyrates and valerates, are produced by bacterial fermentation. One of the PHAs which has generated a lot of interest recently is poly(4-hydroxybutyrate) (P4HB). Due to its biocompatibility and desirable polymer properties, P4HB has been introduced in the fabrication of over a dozen FDA approved medical products, such as sutures, surgical meshes and membranes, and tissue repair patches. Some studies have explored the use of PHAs for controlled release applications with thermally sensitive chemicals and drugs. Such applications include anti-bacterial sutures, drug-eluting stents and bioactive tissue engineering scaffolds. Currently, PHAs are melt spun and drawn into filaments for various applications at processing temperatures which can reach as high as 200 °C. This inhibits the drug incorporation within the polymer during the fiber spinning stage as most drugs cannot sustain such high temperatures. They therefore require a post spinning incorporation process for loading the drugs into the fibers, which typically involves coating or surface treatments where the drugs are superficially attached to the fibers, resulting in a non-uniform absorption of the drug into the fibers and an uneven and unpredictable drug release profile. This raises the need for a low temperature spinning process for PHAs, in which the drug can be incorporated into the polymer during the spinning stage, producing drug-loaded fibers with a uniform drug distribution.

The purpose of this research was to develop a wet spinning process for P4HB that can be used to prepare drug loaded fibers in a single step by adding the drug to the polymer solution prior

to the spinning stage. The primary objective was to identify suitable wet spinning conditions to form continuous P4HB fibers. After several preliminary tests, it was found that a chloroform-based spin dope with 10-15% polymer concentration was suitable for extruding continuous stretchable fibers into a coagulation bath containing reagent alcohol. Subsequently, several P4HB fibers were spun with various spin dope concentrations, coagulation bath temperatures and spin draw ratios. It was determined that the fibers spun at room temperature with 15% polymer concentration, had a significantly higher tensile strength and fiber crystallinity. The next step was to study the effect of drug incorporation on the fiber properties, which was achieved by wet spinning drug loaded P4HB fibers. Levofloxacin, a broad-spectrum antibiotic of the fluoroquinolone class of drugs, was added to the polymer solutions at different concentrations between 2-10 wt.%, and spun into fibers at different spin draw ratios. It was found that fibers spun with up to 5 wt.% drug in the spin dope and a higher spin draw ratio did not have any significant difference in the mechanical and structural properties as compared to the control fibers with no drug content. It was also determined that the limit for fiber drug incorporation was between 2-5 wt.% drug in the spin dope. Finally, an *in vitro* study with phosphate buffered saline solution was conducted to understand the drug release behavior of these fibers. It was observed that the fiber crystallinity had a more significant impact on the drug release profile than the total percent of drug incorporated into the fiber. It was also found that the fibers underwent a rapid release of the drug during the first twenty-four hours, followed by a slower release rate over the subsequent four days. The drug release profile appears to follow a logarithmic decay model with first-order release kinetics. It was concluded that P4HB can be wet spun at room temperature with drugs incorporated in the fibers during spinning and such fibers can have a predictable drug release profile over a period of five days.

Wet Spinning of Poly (4-hydroxybutyrate) to Produce Drug-loaded Fibers for Controlled Drug Delivery Applications

by
Bhavya Singhi

A dissertation submitted to the Graduate Faculty of
North Carolina State University
in partial fulfillment of the
requirements for the degree of
Doctor of Philosophy

Fiber and Polymer Science

Raleigh, North Carolina
2019

APPROVED BY:

_____	_____
Dr. Martin W. King Committee Chair	Dr. Stephen Michielsen
_____	_____
Dr. Ericka Ford	Dr. Lucian Lucia

DEDICATION

To my family and friends
To my advisor Dr. Martin W. King

BIOGRAPHY

Bhavya Singhi was born on 7th September 1992 and grew up in New Delhi, India. She moved to Mumbai, India for her undergraduate degree in Fibers and Textile Processing Technology from the Institute of Chemical Technology and completed her bachelor's in May 2014. She joined the Master of Science in Textile Chemistry program at North Carolina State University in August 2014. She interned for two months at RTI International (Raleigh, NC). She also served as the President of the Textile Association of Graduate Students (TAGS) and the Chair of the Teaching Effectiveness Committee in NCSU Graduate Student Association. She graduated with her master's degree in December 2016 and continued onto a doctoral degree program in Fiber and Polymer Science. She has focused her graduate studies on medical applications of polymeric textile materials, specifically with resorbable polymers. She has been an active participant in various events around the campus. She enjoys cooking and travelling.

ACKNOWLEDGMENTS

Firstly, I would like to thank Dr. Martin W. King who has guided me in my graduate programs for the past five years at NC State. He always encouraged me to follow my instincts and supported me through those decisions. His insights on my work have been very helpful and I am glad to call him as my mentor.

I am grateful to Dr. Stephen Michielsen, Dr. Ericka Ford and Dr. Lucian Lucia for being a part of my advisory committee and providing guidance for this study. I wish to extend my sincere gratitude to Teresa White, Judy Elson, Birgit Anderson and Ching-Chang (BB) Chung for their help in the laboratory work. I would also like to thank all the members of the Biomedical Textiles Group, especially Radhika Vaid, Harshini Ramakrishna and Tushar Bambharoliya, for their help with my experimental work.

None of this would have been possible without the constant love and support of my family. I am extremely grateful to my parents, Mr. Kamal K. Singhi and Mrs. Seema Singhi for enabling me to pursue my dreams. I appreciate my younger brother, Kaustubh Singhi for his sense of humor which helped me through some stressful times. I would also like to thank Balaji Ramasubramanian for his endless motivation and encouragement.

TABLE OF CONTENTS

LIST OF TABLES

LIST OF FIGURES

CHAPTER 1 – INTRODUCTION

1.1. RESEARCH SIGNIFICANCE

Resorbable biopolymers can be processed and spun into filament yarns using similar techniques that one would use for permanent polymers such as a melt spinning, wet, dry or gel spinning approach. While melt spinning is a preferred approach for thermoplastic polymers, those that are not thermoplastic need to be dissolved in a solvent and extruded or solution spun into filaments using a wet spinning, dry spinning or gel spinning technique. Dry spinning involves spinning into hot air to evaporate the solvent, whereas wet and gel spinning requires the polymer to be dissolved in a solvent so that after exiting the spinneret the filaments can be precipitated or solidified by a non-solvent or coagulant.

The mechanical properties, such as stiffness and tenacity, and the rate of resorption of biopolymer spun yarns are dependent not only on the type of polymer, but also on the spinning conditions used. For example, the fine structure, which represents the degree of molecular order, crystallinity and orientation of the polymer chains within the filament, is controlled at the cooling stage during melt spinning and at the coagulation / solidification phase during solution spinning. Depending on the temperature of crystallization as well as the rate of cooling or coagulation, the randomly arranged chains in the melt or solution phase have more or less time, to become ordered and aligned into crystalline zones. Furthermore, given that the outer layers of a spun filament cool or coagulate at a faster rate than the internal layer or core of each filament, it is not uncommon to find that the extent of order or the degree of crystallinity is different between the outer sheath region and the inner core, regardless of whether it is a thick monofilament (e.g. >100 microns in diameter) or a fine individual filament in a multifilament yarn (10 - 25 microns in diameter) [1].

Polyhydroxyalkanoates (PHAs) are an attractive class of biomaterials due to their desirable properties, such as biocompatibility, good tensile strength and elongation and tunable resorption profile [2]. In the past two decades, over twenty-five patents have been issued for poly-4-hydroxybutyrate (P4HB) based medical applications. In 2007 the Food and Drug Administration (FDA) approved for the first time the use of P4HB as a medical device, namely a monofilament surgical suture for use in humans. And since that time, it has approved over a dozen different products made from P4HB [3]. Some commercially available products made from P4HB are produced by Tepha Inc. and Galatea Surgical Inc., medical device companies based in Lexington, MA. They manufacture monofilament sutures, meshes, and surgical films made from their proprietary P4HB polymer, TephaFLEX® [4].

In the past few years P4HB has been studied for drug delivery applications, especially with the growing interest in controlled release drug delivery systems. The polymer can be fabricated into films, fibers and nanoparticles for targeted drug delivery. Some examples of research studies on P4HB and its drug delivery systems include cancer therapy nanoparticles [5] and drug-coated stents for coronary applications [6].

Recently, fibers have become attractive carriers for drug delivery systems due to their morphological advantage over particle-based systems. The cylindrical structure of fibers provides a high surface area to volume ratio, and they have the capability to release drugs over a larger surface area. The fiber shape and fine structure can also be modified to meet the requirements of the desired application [7]. Typically, there are two methods to fabricate fiber-based drug delivery systems: (i) surface treatment of the spun fibers with a drug solution or (ii) adding the drug to the fiber spinning dope. In the first method, the drug is usually coated onto the fibers and it is then released to the target area fairly quickly. On the other hand, when the drug is incorporated into the

polymer spinning dope prior to spinning, it is distributed more uniformly within the fiber structure and will generally provide a slower drug release profile [8].

Currently, PHAs are melt spun and drawn into filaments for various applications at high processing temperatures which can reach up to 200 °C [9]. This limits the possibility of incorporating drugs within the polymer dope prior to melt spinning as most drugs cannot sustain such high temperatures and are required to be incorporated by a post spinning process. This raises the need for a low temperature solution spinning process for P4HB that will address the major limitations associated with incorporating a drug post melt spinning, such as non-uniform drug distribution, and an uneven and unpredictable drug release profile. Although solution spinning includes dry, wet and gel spinning, dry spinning is also an unsuitable method since it requires hot air to remove the volatile solvent. Additionally, unlike conventional resorbable polymers, such as polylactide, polyglycolide and polycaprolactone, which have been studied extensively for more than four decades, PHAs have not been studied in detail. This is mainly because of their limited availability and relatively high production cost [10]. There are currently a number of reasons for studying PHAs, especially the processing of these polymers by a solution spinning approach and measuring the effect of these processing parameters on the resorption profile and the drug delivery performance.

The current work will focus on studying some of the parameters of the wet spinning process for poly (4-hydroxybutyrate) (P4HB) and developing a scalable method for the continuous extrusion of drug loaded P4HB monofilaments. The spun fibers can be potentially used for many controlled release applications, such as internal and external drug delivery systems, wound dressings and infection control with the release of antimicrobial agents.

1.2. GOALS AND OBJECTIVES

The main goal for this proposed research is to study the feasibility of producing drug loaded P4HB monofilaments in a single step using a wet spinning process, and subsequently monitoring the drug release profile. To accomplish this goal, the research effort will be divided into three projects, each with its individual aims. The work in each project will be dependent on the results of the previous project or projects. The aims of all three projects will be achieved by completing the following objectives that need to be undertaken in a particular chronological order.

Project 1: The effect of wet spinning conditions on the structure and properties of poly-4-hydroxybutyrate fibers.

As discussed earlier, currently there is no defined procedure to produce P4HB fibers through a wet spinning process. Hence, the primary task of this research study is to identify the suitable process conditions which can be used to prepare continuous wet spun monofilaments from the P4HB polymer. The parameters investigated in this project relate to the type of solvent and coagulant to be used, the spinneret hole size, the spin dope concentration, the coagulation bath temperature and the as-spun draw ratio. Based on the results of this project, a suitable combination of these parameters will be used to further produce drug loaded P4HB monofilaments. There are three objectives for this project:

Objective 1: Analyze the process conditions for the dissolution and coagulation of P4HB.

Objective 2: Assess the effect of polymer concentration in the spin dope and the temperature of the coagulation bath on the spun monofilament properties.

Objective 3: Evaluate the effect of the as-spun draw ratio of the monofilaments on the fiber structure and mechanical properties.

Project 2: The effect of drug loading on the structure and properties of wet spun P4HB fibers.

Using the wet spinning process developed in the previous project, P4HB monofilaments will be spun with the antibiotic drug, levofloxacin, added to the polymer dope solution. The effect of adding the drug to the spin dope on the fiber structure and properties will be evaluated. Additionally, the effect of the as-spun draw ratio will be studied on the drug-loaded fibers. This project has two objectives:

Objective 1: Evaluate the effect of drug concentration on the structure and properties of wet spun P4HB fibers.

Objective 2: Study the effect of the as-spun draw ratio on the fiber structure and mechanical properties of drug loaded P4HB fibers.

Project 3: Drug retention and release profiles of the wet spun drug loaded P4HB fibers

Using an *in vitro* experimental method, the drug loaded fibers will be studied for the rate of drug released into a phosphate buffer saline medium as well as the drug retained in the fiber over a specific period of time. This study will enable an understanding of the maximum loading as well as the rate and duration of drug release from these wet spun fibers. This project also has two objectives:

Objective 1: Assess the effect of the drug loading concentration on the drug retention and drug release profiles of the wet spun P4HB fibers.

Objective 2: Evaluate the effect of the as-spun draw ratio on the drug retention and drug release profiles of the wet spun P4HB fibers.

This dissertation is divided in to six main chapters, where the first chapter describes the significance of this research study, the overall goal for this study and the main research objectives for the study. The second chapter covers an in-depth literature review to provide a deeper understanding on polyhydroxyalkanoates and their applications, fiber spinning processes – specifically solution spinning of polymers, controlled release drug delivery systems, and fiber-based drug delivery systems. Chapters three, four and five provide an elaborate description on the experimental methods, their results and inferences for the three individual projects in this study, respectively. Finally, chapter six provides an overall conclusion for this research study, correlating the findings with the initial objectives stated in Chapter 1.

CHAPTER 2 – LITERATURE REVIEW

2.1. INTRODUCTION TO POLYHYDROXYALKANOATES

Polyhydroxyalkanoates (PHAs) are a class of aliphatic biopolyesters that are synthesized by bacteria as an energy reserve by fermentation of sugar and lipids [11]. They are produced in a variety of grades, with different compositions, molecular weights and other properties. The formation of a specific variety of polymer, either a homopolymer or a copolymer, depends on the type of bacteria and the conditions of polymer formation, mainly the substrate used for feeding the bacteria and the environmental conditions of their growth [2] [12]. More than 150 different monomers can be combined within this family to obtain polymers with extremely different properties. The monomeric composition of PHAs has considerable effects on their physical properties [13].

2.1.1. History of Polyhydroxyalkanoates

The presence of PHAs in bacterial cells was first mentioned in 1888, however the biochemists referred to the unknown material as ‘lipids’ [14]. The isolation and characterization of PHAs was first carried out in the 1920s, when Maurice Lemoigne identified the composition as poly-3-hydroxybutyrate (P3HB) (Figure 2.1) [15]. Although the polymer was identified early on, the scientific community was unaware of this biopolyester for a long time as Lemoigne published his work in little-read French journals [2]. After the knowledge of the existence of these polymers was realized in the 1950s, scientists have worked on determining their microbial synthesis process, types of PHAs and their properties, and their applications. In 1974, 3-hyrdoxyvalerate (Figure 2.2)

and 3-hydroxyhexanoate were identified as additional varieties of PHA, proving that P3HB was not the only existing PHA [2].

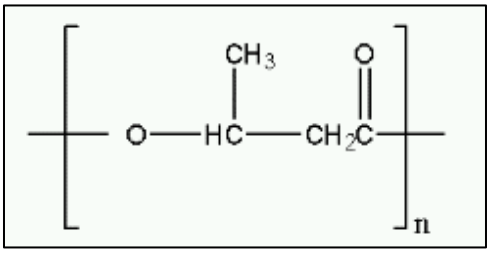

Figure 2.1. Molecular structure of P3HB [16]

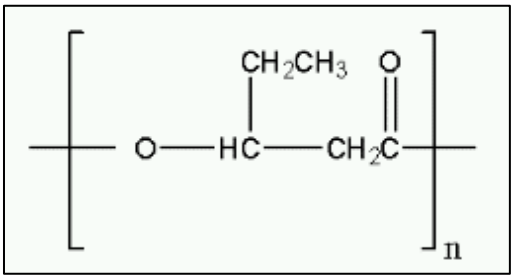

Figure 2.2. Molecular structure of P3HV [16]

The 1970s saw a tremendous growth in PHA research, with the discovery of many microorganisms that could produce the polymer and improved characterization of the materials. The importance of the relationship between PHA biosynthesis and the extra-cellular environment was realized, especially when it led to the optimization of the preparation process of PHA [17]. However, PHAs failed to be produced commercially on a large scale due to high production costs and inadequate process controllability for bulk manufacturing. This led to them being used only in laboratory experiments until the 1980s, when Biopol^{TM} – a copolymer of P3HB and P3HV, poly

(3-hydroxybutyrate-co-3-hydroxyvalerate) (PHBV) – was introduced in the market by Imperial Chemical Industries Ltd. (ICI) as a biodegradable thermoplastic polyester (Figure 2.3) [18].

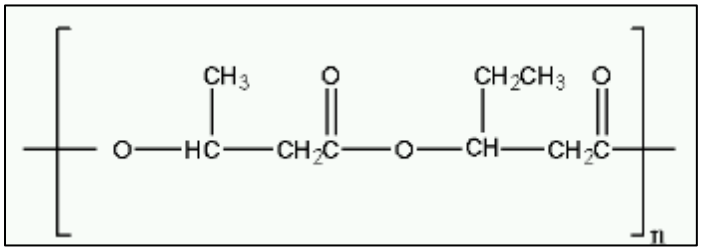

Figure 2.3. Molecular structure of PHBV [16]

Zeneca, a subsidiary for the agricultural and pharmaceutical businesses of ICI, sold the Biopol^{TM} division to Monsanto in 1996 due to economic constraints and insufficient sales [19]. Monsanto worked on Biopol^{TM} production and related copolymers in plants for various end-use applications until 2002, when it was acquired by Metabolix [20]. As seen in Table 2.1, over the past three decades, more than twenty companies have gotten involved in PHA R&D and/or commercial production [10]. The industrial production and large-scale commercialization of PHA is critically dependent on lowering the cost of production. Many scientists and engineers have been working in developing technologies to support high cell density growth, continuous fermentation with specific polymer production, improved extraction and purification, etc., which could lower the cost of high quality PHA manufacturing [21].

Table 2.1. Polyhydroxyalkanoate (PHA) R&D and commercial companies [21]

Company	Types of PHA	Production scale (tons/year)
ICI, UK	PHBV	300
Chemie Linz, Austria	PHB	20–100
BTF, Austria	PHB	20–100
Biomers, Germany	PHB	Unknown
BASF, Germany	PHB, PHBV	Pilot scale
Metabolix, USA	Several PHA	Unknown
Tepha, USA	Several PHA	PHA medical implants
ADM, USA (with Metabolix)	Several PHA	50,000
P&G, USA	Several PHA	Contract manufacture
Monsanto, USA	PHB, PHBV	Plant PHA production
Meredian, USA	Several PHA	10,000
Kaneka, Japan (with P&G)	Several PHA	Unknown
Mitsubishi, Japan	PHB	10
Biocycles, Brazil	PHB	100
Bio-On, Italy	PHA (unclear)	10,000
Zhejiang Tian An, China	PHBV	2,000
Jiangmen Biotech Center, China	PHBHHx	Unknown
Yikeman, Shandong, China	PHA (unclear)	3,000
Tianjin Northern Food, China	PHB	Pilot scale
Shantou Lianyi Biotech, China	Several PHA	Pilot scale
Jiangsu Nan Tian, China	PHB	Pilot scale
Shenzhen O'Bioer, China	Several PHA	Unknown
Tianjin Green Bioscience (+DSM)	P3HB4HB	10,000
Shandong Lukang, China	Several PHA	Pilot scale

2.1.2. Synthesis of Polyhydroxyalkanoates

PHAs are mainly produced by a combination of renewable feedstocks and biological methods. In the microbes, PHAs accumulate due to the presence of excessive carbon source coupled with a deprivation of nutrients such as nitrogen. Carbon sources that can be metabolized for the production of PHAs include fatty acids and carbohydrates [22]. PHAs accumulate as intracellular granules in many bacterial species, such as Alcaligenes, Pseudomonas, Enterobacter, Necator, Rhodobacter, Ralstonia and Cupriavidus. Microbial fermentation processes can accumulate PHAs up to 90% of the microbial dry mass. A lot of research has also been carried out on metabolically engineered microbial strains to produce PHAs with tailored process

specifications [23]. Post PHA accumulation, the biomass needs to be separated from the broth and dried, followed by PHA extraction and drying (Figure 2.4) [24].

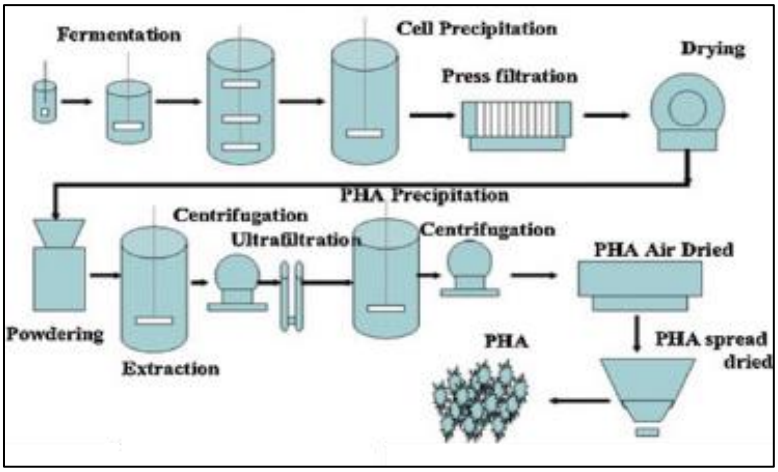

Figure 2.4. General PHA production flow [21]

Table 2.2. Recovery processes for polyhydroxyalkanoates [23]

Recovery method	Advantages	Recovery agent
Solvent extraction	High purity; endotoxin removal; limited polymer degradation	Chloroform, methanol
		Chloroform, hexane
		Chloroform, hexane
		Dichloromethane, hexane
		Chloroform
Mechanical disruption	Less use of chemicals; reduced polymer degradation	Sonication, chloroform
Chemical digestion	No polymer degradation; high purity; applicable to large volumes and high cell densities	NaClO, chloroform/ethanol
		SDS, LAS-99, ES702, AOS-04, Brij®58, NaOH
Enzymatic digestion (with or without mechanical treatment)	Good polymer recovery; high purity; reduced use of chemicals other than enzymes	Alcalase, SDS, EDTA
		Benzonase, Alcalase, lysozyme, flavourzyme; microfluidizer
Supercritical fluids	Low toxicity; low cost; high polymer purity	CO_2

The high cost of PHA production is largely due to the difficulty of efficient biomass separation and PHA extraction. Scalable processes are needed for inexpensively recovering the intracellular PHAs from microorganisms [25]. Table 2.2 summarizes some of the commonly used recovery processes for PHA extraction. A major contributor to the high cost of microbial production of PHAs is the carbon source. An alternatively cheaper route for PHA production is to use genetically modified plants with atmospheric carbon dioxide as their carbon source. This method provides advantages such as ease of harvesting and PHA extraction from the plant biomass [26]. Another method to produce PHA is *in vitro* enzymatic synthesis without the use of microbes. This is a highly selective process which would ensure well-define polymer structure. The enzyme catalyzed reactions would be carried out in ambient conditions and the polymer recovery is easily achievable. However, the production of PHAs using enzymes remains relatively expensive compared to other synthetic plastics. Production in plants is likely to become the least expensive option for certain PHAs, but it does not currently offer the molecular versatility of the polymer that can be made using microbial fermentations and enzymes [23]. Figure 2.5 provides an overview of the milestones achieved in the development of continuous process for PHA production.

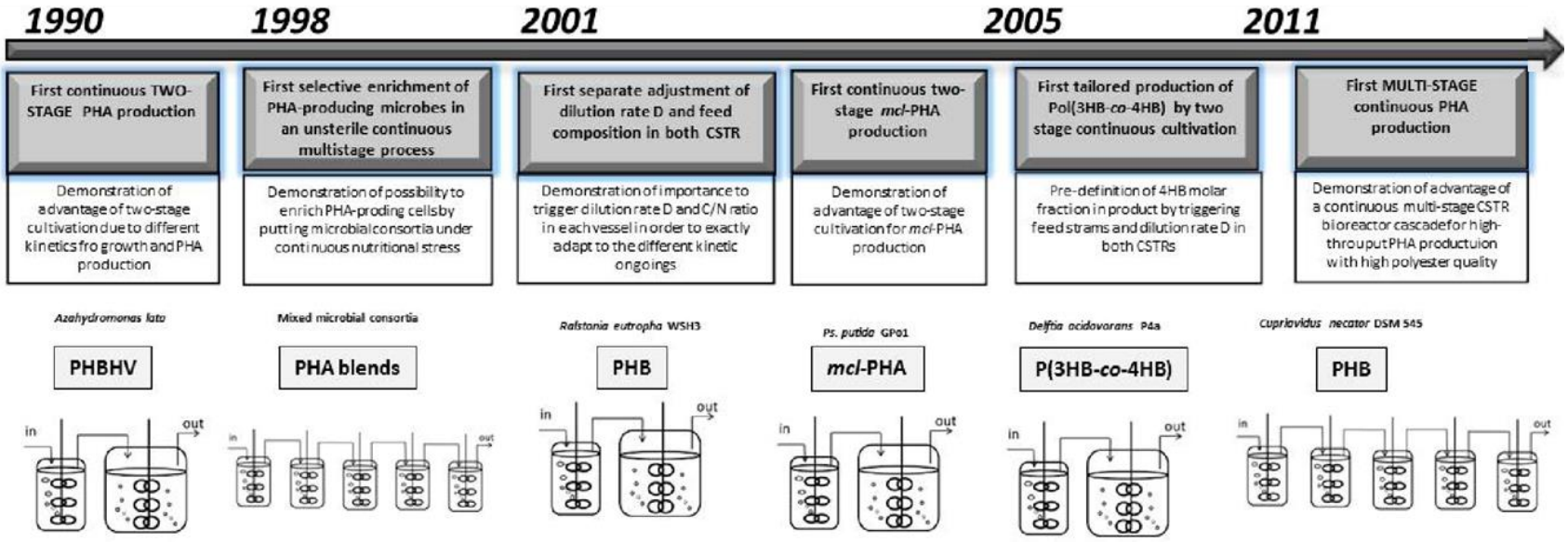

Figure 2.5. Milestones in continuous process development of PHA production [27]

2.1.3. Structure and Properties of Polyhydroxyalkanoates

PHAs are biodegradable aliphatic polyesters made from the hydroxyalkanoate monomeric group. Based on the microbial growth conditions and the species of bacteria, the molecular weight of these polymers can range between $2x10^5$ - $3x10^6$ Da [28]. Most PHAs generally consist of poly-3-hydroxy fatty acids (Figure 2.6), although there are a few with the hydroxyl group at the 4- or 5- position, like poly-4-hydroxybutyrate (P4HB) [29]. The pendant group varies between C1 to C13 and can be saturated or unsaturated. Over 150 hydroxycarboxylic acids have been identified as monomeric compounds for PHA [30].

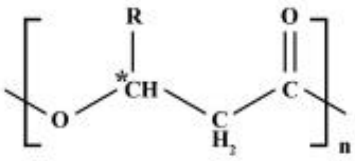

Poly(3-hydroxyalkanoate)

R group	Carbon no.	PHA polymer
methyl	C_4	Poly(3-hydroxybutyrate)
ethyl	C_5	Poly(3-hydroxyvalerate)
propyl	C_6	Poly(3-hydroxyhexanoate)
butyl	C_7	Poly(3-hydroxyheptanoate)
pentyl	C_8	Poly(3-hydroxyoctanoate)
hexyl	C_9	Poly(3-hydroxynonanoate)
heptyl	C_{10}	Poly(3-hydroxydecanoate)
octyl	C_{11}	Poly(3-hydroxyundecanoate)
nonyl	C_{12}	Poly(3-hydroxydodecanoate)
decyl	C_{13}	Poly(3-hydroxytridecanoate)
undecyl	C_{14}	Poly(3-hydroxytetradecanoate)
dodecyl	C_{15}	Poly(3-hydroxypentadecanoate)
tridecyl	C_{16}	Poly(3-hydroxyhexadecanoate)

Figure 2.6. Chemical structure of poly-3-hydroxyalkanoates [31]

Based on the number of total carbon atoms in a monomer, PHAs are classified as short chain length (scl-PHA) which have 3-5 carbon atoms, medium chain length (mcl-PHA) containing

6-14 carbon atoms and long chain length (lcl-PHA) with 15 or more carbon atoms [32]. Many bacterial species synthesize scl-PHA in the capacity of 50-80% of the cell dry mass from sugars and fatty acids [33]. The production of mcl-PHA is reported to have 20 - 30% of cell dry mass, although certain microbes can produce up to 77% [34]. Lcl-PHA has the lowest yield, mainly due to the larger molecular weight. In most bacteria which produce lcl-PHA, there are scl-PHA and mcl-PHA based byproducts [35]. Due to the high yield capacity of scl-PHAs, they are the most widely produced PHA polymers in the industry [31].

The monomer composition in the PHA polymer has the most effect on its physical and mechanical properties. The wide range of monomeric properties can lead to one PHA polymer resembling polypropylene while another PHA has elastomeric properties [29]. The structure of the PHA polymer can be controlled by adjusting the carbon substrates to attain the desired monomer content, by metabolically engineered pathways or by feeding the culture with carbon substrates with the functional side chains that can undergo chemical modifications in the secondary step [36]. The varied chemical properties arise from the length of the pendant groups, chemical nature of the groups and the distance between the ester linkages in the polymer backbone. Typically, PHAs containing shorter pendant groups (scl-PHAs) are hard and crystalline (due to a more compact structure) while those with longer pendant groups (mcl-PHAs) have elastomeric behavior (due to a more amorphous structure) [37].

Table 2.3. Comparison of PHA polymer properties [38]

Polymer	Melting point (°C)	Young's modulus (GPa)	Tensile strength (MPa)	Elongation to break (%)	Glass transition temperature (°C)
P(3HB)	179	3.5	40	5	4
P(3HB-co-3HV)					
3 mol% 3HV	170	2.9	38	–	–
9 mol% 3HV	162	1.9	37	–	–
14 mol% 3HV	150	1.5	35	–	–
20 mol% 3HV	145	1.2	32	–	–
25 mol% 3HV	137	0.7	30	–	–
P(3HB-co-4HB)					
3 mol% 4HB	166	–	28	45	–
10 mol% 4HB	159	–	24	242	–
16 mol% 4HB	–	–	26	444	–
64 mol% 4HB	50	30	17	591	–
90 mol% 4HB	50	100	65	1080	–
P(4HB)	53	149	104	1000	–
P(3HHx-co-3HO)	61	–	10	300	–
P(3HB-co-6 mol% 3HA)	133	0.2	17	680	−8
P(3HB-co-67 mol% HP)	44	–	–	–	−19
P(3HB-co-3HHx)	52	–	20	850	−4
Polypropylene	170	1.7	34.5	400	45
Polyethylene–terepthalate	262	2.2	56	7300	3400
polystyrene	110	3.1	50	–	21
LDPE	130	0.2	10	620	−30

PHB, specifically P3HB is one of the most studied and used PHA polymer. It has a melt point near 180 ºC and polydispersity index close to 2. It also has tenacity close to polypropylene, as seen in Table 2.3 [38]. It is a stiff and brittle polymer due to its shorter pendant group and high crystallinity. Modifying the side chains and the monomeric compositions of the P3HB polymer with incorporation of other hydroxyl-acid units to form PHA copolymer can impart the material with more desirable properties, such as low stiffness, improved strength and higher flexibility [29]. Based on the desired properties and production costs, only few of the PHAs, mainly poly (3-hydroxybutyrate) (P3HB), poly (4-hydroxybutyrate) (P4HB), poly (3-hydroxybutyrate-co-3-hydroxyvalerate) (PHBV) and poly (3-hydroxybutyrate-co-4-hydroxybutyrate) (P34HB) are studied extensively and produced in large quantities [39].

Another commonly studied PHA is poly-4-hydroxybutyrate (P4HB), which has shown many properties similar to other aliphatic polyesters for medical applications, such as polyglycolide (PGA) and Polycaprolactone (PCL), as shown in Figure 2.7. P4HB is a semi-

crystalline thermoplastic polymer with a melting point around 60 ºC. It can have an elongation at break of up to 1000%, especially in an unoriented structure such as films. Increase in orientation in fiber like structure lowers the elongation but increase the tensile strength. The versatility of P4HB properties and the capability to tailor this polymer into different structures for various applications can be used to develop devices for unmet medical needs [3].

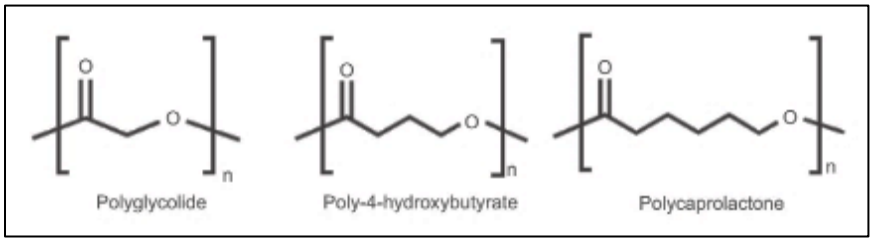

Figure 2.7. Chemical structures of PGA, P4HB and PCL [3]

2.1.4. Blends of Polyhydroxyalkanoates

Apart from copolymerizing PHAs amongst themselves, many blends with other biopolymers have also been developed to enhance material properties and offset the production costs [40]. One of the most popular blends of this polymer is of P3HB with poly (lactic acid) (PLA), another crystalline aliphatic polyester. As the production of PLA is cheaper than P3HB, the P3HB/PLA blend is also lower in cost compared to 100% P3HB. However, pure PLA is also brittle and stiff to a certain extent, which hampers the potential applications for these two polymers. It was however found that the blend of PLA with P34HB copolymer has good toughness, flexibility and high biodegradation rate [41]. P34HB/PLA blend resulted in a more favorable material with modified properties that overcame the drawbacks of the constituent polymers and provided feasible applications [40]. Polycaprolactone (PCL) is a semi-crystalline aliphatic polyester that has good mechanical properties, biocompatibility and miscibility with various polymers. PCL can

lower the elastic modulus of a P3HB/PCL blend by acting as a polymeric plasticizer, which is a good option for improving the performance of both homopolymers [42]. Another well studied blend of PHA is that of cellulose and P3HB. The β-(1, 4)-glycosidic linkages in cellulose makes it biocompatible and hydrophilic. As P3HB and ethyl cellulose (EtC) are both FDA (Food and Drug Administration) approved, their blends are researched for applications in pharmaceuticals [40]. The blend of starch, an inexpensive commodity material, and PHAs provides a good solution to make PHAs more cost effective, especially for low-end applications [43]. Chitosan is considered an important biomaterial, mainly due to its biocompatibility and antimicrobial properties. Scientists have studied blends of chitosan and PHAs for their biomedical applications [44].

2.1.5. Applications of Polyhydroxyalkanoates

In the recent years, PHAs have received much attention due to their similarities with petrochemical polymers like polypropylene, polyethylene and polystyrene. Along with good thermoplastic and mechanical properties, PHAs also possess biodegradability, biocompatibility and non-toxicity [45]. The over-dependence on the depleting petroleum resources, increased concern towards global climate change and waste disposal problems with synthetic plastics have raised the need for an alternative polymer, which can be synthesized from renewable resources, is biodegradable and has performance at par with petroleum-based plastics [39].

Table 2.4. Potential of commercialized PHA to replace petroleum-based plastics [46]

	LPDE	PP	HPDE	PS	HI-PS	PVC	PET	PA	PBT
Mirel™	++	+	++		±	+	++	±	−
Biomer®	−	++	++	+	−	−	−	−	−
Nodax™	+	++	++	−	−	+	+	−	−
Biocycle®	−	++	++	+	−	−	−	−	−

(++) Means probable; (+) means possible; (±) means doubtful; (−) means unlikely.

Table 2.4 lists certain commercially available PHA based polymers and their ability to potentially replace petroleum-based plastics for certain applications. Some of the main applications for PHAs are as a substitution for of polyethylene terephthalate (PET) and polyethylene (PE) for disposable commodity goods, such as bottles, utensils, containers, hygiene products, packaging, etc., [11]. The first commercial PHA product was biodegradable shampoo bottles by a German company, Wella AG, (Figure 2.8). However, the high production cost made long term sustainability uneconomic and the manufacturers shut down the product line [47]. Considering the cost difference between PHAs and conventional plastics, a partial substitution of polyolefin materials with PHAs is found to be a better option as it does not create a large impact on product prices yet reduces the overall carbon footprint of the products (Figures 2.9 and 2.10).

Figure 2.8. Wella shampoo bottle made from Biopol^{TM} [47]

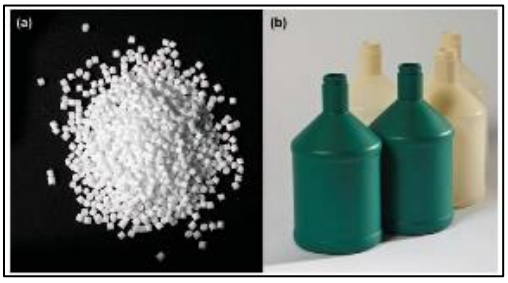

Figure 2.9. Mirel^{TM} PHA resin, Metabolix (l) and blow molded bottles (r) [47]

Figure 2.10. Packaging products made by Nodax^{TM} (poly (3-hydroxybutyrate-co-3-hydroxyhexanoate)) from P&G, USA [21]

Owing to the biocompatibility and resorbability of PHA polymers, they are promising candidates for biomedical applications such as implants, sutures, stents, tissue engineering and drug delivery [45]. Several studies have been conducted for potential applications of PHAs in tissue engineering scaffolds as they enable cell adhesion, migration and proliferation [48]. Researchers have successfully conducted experiments on in-vitro cell cultures, animal studies and a few clinical trials for use of PHB polymer and PHBV copolymer in monofilament sutures for surgical wounds and bone implants [49]. Other biomedical implants studied from PHAs are cardiovascular patches for artery augmentation, heart valve prostheses, vascular grafts, surgical meshes, ligament and tissue repair scaffolds, etc. [50].

In the past few decades, over thirty patents have been filed and/or approved for medical applications of poly-4-hydroxybutyrate (P4HB), as shown in Table 2.5. It was also the first PHA to receive FDA approval for clinical trials of P4HB based medical devices in 2007. Since then over a dozen medical device products have been fabricated from P4HB (Table 2.6) [3].

Table 2.5. U.S. patents issued and filed for medical applications of P4HB

US patent	Title
6,245,537	Removing endotoxin with an oxidizing agent from PHAs produced by fermentation (Williams et al.)
6,514,515	Bioabsorbable, biocompatible polymers for tissue engineering (Williams)
6,548,569	Medical devices and applications of PHA polymers (Williams et al.)
6,555,123	PHA compositions for soft tissue repair, augmentation, and viscosupplementation (Williams and Martin)
6,585,994	PHA compositions for soft tissue repair, augmentation, and viscosupplementation (Williams and Martin)
6,592,892	Flushable disposable polymeric products (Williams)
6,610,764	PHA compositions having controlled degradation rates (Martin et al.)
6,623,749	Medical device containing PHA treated with oxidizing agent to remove endotoxin (Williams et al.)
6,746,685	Bioabsorbable, biocompatible polymers for tissue engineering (Williams)
6,828,357	PHA compositions having controlled degradation rates (Martin et al.)
6,838,493	Medical devices and applications of PHA polymers (Williams et al.)
6,867,247	Medical devices and applications of PHA polymers (Williams et al.)
6,867,248	PHA compositions having controlled degradation rates (Martin et al.)
6,878,758	PHA compositions having controlled degradation rates (Martin et al.)
7,025,980	PHA compositions for soft tissue repair, augmentation, and viscosupplementation (Williams and Martin)
7,179,883	Medical devices and applications of PHA polymers (Williams et al.)
7,244,442	PHAs for *in vivo* applications (Williams et al.)
7,268,205	Medical devices and applications of PHA polymers (Williams et al.)
7,553,923	Medical devices and applications of PHA polymers (Williams et al.)
7,618,448	Polymeric, degradable drug-eluting stents and coatings (Schmitz et al.)
7,641,825	Method of making a PHA filament (Rizk)
7,906,135	Medical device comprising PHA having pyrogen removed (Williams et al.)
7,943,683	Medical devices containing oriented films of P4HB and copolymers (Rizk et al.)
8,016,883	Methods and devices for rotator cuff repair (Coleman et al.)
8,034,270	PHA medical textiles and fibers (Martin et al.)
8,084,125	Non-curling PHA sutures (Rizk)
US patent application	Title
20050025809	P4HB matrices for sustained drug delivery (Hasirci and Keskin)
20060177513	Embolization using P4HB particles (Martin et al.)
20060287659	PHA nerve regeneration devices (Terenghi et al.)
20070166387	Hemostatic compositions, assemblies, systems, and methods employing particulate hemostatic agents formed from chitosan and including a polymer mesh material of P4HB (Ahuja et al.)
20080183297	Method and apparatus for fitting a shoulder prosthesis (Boileau and Walch)
20080188936	System and method for repairing tendons and ligaments (Ball et al.)
20090162276	Medical devices containing melt-blown non-wovens of P4HB and copolymers (Ho et al.)
20100003300	Improved injectable delivery of microparticles and compositions therefore (Markland et al.)
20100057123	Recombinant expressed bioadsorbable PHA monofilament and multi-filament self-retaining sutures (D'Agostino and Rizk)
20110166661	Apparatus for fitting a shoulder prosthesis (Boileau et al.)
20120053689	Coatings for the manufacture and application of PHA medical devices (Martin et al.)

Table 2.6. FDA clearances of some medical products incorporating P4HB

Clearance	Date	Product	Indication
K052225	2/8/07	TephaFLEX® Absorbable Suture	Indicated for use in soft tissue approximation and/or ligation but not for use in cardiovascular or neurological surgery, microsurgery, or ophthalmic surgery
K081099	7/15/08		
K082178	10/30/08		
K070894	4/13/07	TephaFLEX® Surgical Mesh	Indicated wherever temporary wound support is required, to reinforce soft tissues where weakness exists or for the repair of hernia or other fascial defects that require the addition of a reinforcing or bridging material to obtain the desired surgical result. This includes, but is not limited to, the following procedures: vaginal prolapsed repair, colon and rectal prolapse repair, reconstructions of the pelvic floor, and sacral colposuspension
K070773	10/11/07	Model 3000 AxyaLoop™ Titanium Bone Anchor	Indicated for securing soft tissue to bone with size 2/0 synthetic non-absorbable suture or size 3/0 TephaFLEX™ absorbable suture in repairs of the extremities such as those shown below: Foot and ankle (1) hallux valgus repairs, (2) medial or lateral instability repairs/reconstructions, (3) Achilles tendon repairs/reconstructions, (4) midfoot reconstructions, (5) metatarsal ligament/tendon repairs/reconstructions Elbow, wrist, and hand (1) scapholunate ligament reconstructions, (2) ulnar and radial collateral ligament reconstructions, (3) lateral epicondylitis repair, (4) biceps tendon reattachment
K072520	11/29/07	TephaFLEX® Surgical Mesh	Indicated wherever temporary wound support is required, to reinforce soft tissues where weakness exists or for the repair of hernia or other fascial defects that require the addition of a reinforcing or bridging material to obtain the desired surgical result. The film also may help minimize the potential for tissue attachment to the device in case of direct contact with the viscera
K091633	8/07/09	TephaFLEX® Surgical Film	Indicated wherever temporary wound support is required, to reinforce soft tissues where weakness exists in the urological, gynecological, or gastroenterological anatomy or for the repair of hernia or other fascial defects that require the addition of a reinforcing or bridging material to obtain the desired surgical result. The film also may help minimize the potential for tissue attachment to the device in case of direct contact with the viscera
K093799	04/22/10	Tornier® Surgical Mesh	Indicated for use where temporary wound support is required to reinforce soft tissues where weakness exists or for the repair of hernia or other fascial defects that require the addition of a reinforcing or bridging material to obtain the desired surgical result. Tornier® Surgical Mesh is also intended for reinforcement of soft tissues, in conjunction with sutures and/or suture anchors during tendon repair surgery; including the reinforcement of rotator cuff, patellar, Achilles, biceps, and quadriceps tendons. Tornier® Surgical Mesh is not intended for use as a replacement for normal body structures or to provide the full mechanical strength to support the rotator cuff, patellar, Achilles, biceps, or quadriceps tendons. Sutures, used to repair the tear, and sutures or bone anchors, used to attach the tissue to the bone, provide mechanical strength for the tendon repair
K100876	07/14/10	MonoMax® Absorbable Suture	Indicated for use in soft tissue approximation and/or ligation but not for use in cardiovascular or neurological surgery, microsurgery, or ophthalmic surgery
K101287	8/30/10	TephaFLEX® Composite Mesh	Indicated wherever temporary wound support is required, to reinforce soft tissues where weakness exists or for the repair of hernia or other fascial defects that require the addition of a reinforcing or bridging material to obtain the desired surgical result. This includes, but is not limited to, the following procedures: vaginal prolapsed repair, colon and rectal prolapse repair, reconstructions of the pelvic floor, and sacral colposuspension
K102788	05/10/11	Tornier® BioFiber Scaffold	Same as for Tornier Surgical Mesh
K111946	09/26/11	TephaFLEX® Mesh	The TephaFLEX mesh is intended to reinforce soft tissue where weakness exists in patients undergoing plastic and reconstructive surgery or for the repair of hernia or other fascial defects that require the addition of a reinforcing or bridging material to obtain the desired surgical result

Apart from the animal studies and clinical trials, some PHA based products are available commercially in the medical field. Tepha, a medical device company manufactures many FDA approved P4HB based TephaFLEX® absorbable products, such as monofilament sutures, monofilament meshes, surgical films and composite meshes (Figures 2.11 and 2.12) [4].

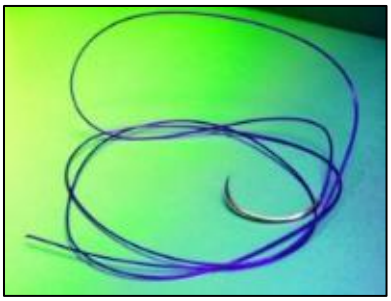

Figure 2.11. TephaFLEX® absorbable monofilament suture [4]

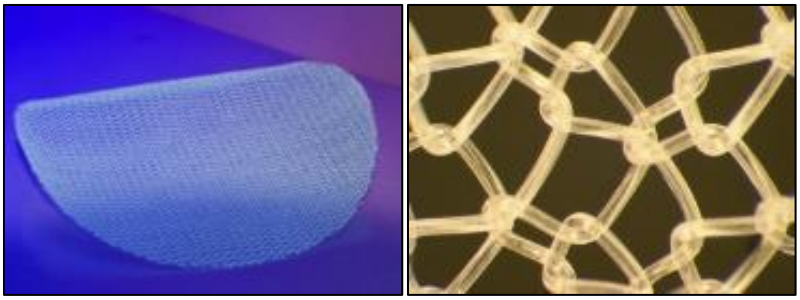

Figure 2.12. TephaFLEX® absorbable monofilament mesh (l), close-up view (r) [4]

A major application potential for PHAs is controlled release drug delivery for prolonged release of therapeutics [23]. PHB copolymer-based nanoparticle matrices have been developed for targeted treatment of cancer cells [51]. P4HB matrices coated with drugs have been developed as a local drug delivery system for fibrosis prevention in cochlear implants [52]. Other potential pharmaceutical products for PHA applications are tablets, contraceptive devices, wound dressings

and other medicinal implants [47]. Some of the other recently explored applications for PHAs are their use as a precursor to biofuels, latex in the paper industry and controlled release herbicidal agents in agriculture [23].

2.1.6. Processing of Polyhydroxyalkanoates

Generally, PHAs can be processed by methods used for other thermoplastic polymers. They can be processed into homogeneous and composite films, fibers, and particles. The conditions applied during the processing method vary based on the type of polymer, molecular weight, crystallinity and the end use application [2]. PHB is a highly crystalline linear polymer, typically with a melting point of over a 100 ºC based on the type of the polymer. Melt processing of PHB and its copolymers is the most commonly used industrial process, especially for commodity applications. Conventional technologies such as injection molding, compression molding, lamination and melt spinning can be used for melt processing of PHB and its copolymers. However, the processing conditions need to be monitored very carefully, to avoid any thermal degradation [2]. Many of the PHA applications such as plastic packaging and certain biomedical devices, require thin film formation. One of the methods to prepare PHA films is to apply a layer of molten polymer to a cool surface (4-20 ºC) slightly above the glass transition temperature of the polymer [53]. Another commonly used method for PHA film formation is solvent cast films, where the polymer is dissolved in a suitable solvent and then dried or precipitated from the polymer solution [54]. Some of the best solvents for PHAs are chloroform, dichloromethane, acetic acid, dimethyl formamide and butyl chloride, while non-solvents mostly used for precipitation of PHAs are water, methanol, ethanol, ethyl acetate and diethyl ether [2].

2.1.7. Fiber Formation of Polyhydroxyalkanoates

Traditional fiber forming techniques for polymers have been studied and modified for the preparation of PHA fibers. Fibrous PHAs are mostly used for sutures, surgical meshes and other textile based biomedical products. The most common method to spin fibers out of PHA is to carry out melt extrusion of the polymer at temperatures 15 - 20 ºC above the melting range but significantly below the degradation temperature, followed by cold or hot drawing [55]. The extruded fibers can be spun from homogeneous polymers, copolymers or a composite blend of PHA with another thermoplastic polymer. For most PHAs, a high melting point demands extrusion temperatures between 150 – 220 ºC to maintain a uniform melt flow of the polymer [56] [57]. But even for PHAs like P4HB which have a relatively low melting point (below 100 ºC), the melt extrusion is carried out at temperatures as high as 200 ºC [9]. The high temperature melt processing followed by drawing can produce fibers with high orientation and tensile strength due to their higher tendency to crystallize. However, the crystallization can sometimes lead to the formation of spherulites which increase the brittleness of the fibers and reduce their elongation. The melt spinning of polyhydroxyalkanoate fibers is widely used for manufacturing commercial products, even though it is limited by thermal and thermos-mechanical degradation during processing [56]. Melt spun PHA fibers are mostly used in application like sutures, surgical meshes and other fibrous biomedical products.

The literature also provides us data on spinning PHA fibers using volatile solvents for dissolution and methods like dry spinning and electrospinning for fiber formation. Majority of research into solution spinning of polyhydroxyalkanoates is using P3HB and P4HB polymers for producing extremely fine fibers with an average diameter in the range of 10nm to 50µm. These polymers have high solubility in halogenated solvents such as chloroform and dichloromethane,

which are typically volatile and easily removed during extrusion via dry spinning and electrospinning. The extrusion process can be carried out at ambient temperatures and prevent any thermal degradation caused during melt spinning [58] [59]. Lower mechanical properties compared to melt spun fibers are a drawback in these spinning methods. Studies have been carried out on PHB nanofibers and microfibers for applications in tissue engineering scaffolds and medical non-wovens [60]. The nanofiber membranes prepared by electrospinning are structurally similar to the extracellular matrix, which enables tissue ingrowth and cell migration [61].

2.2. OVERVIEW OF FIBER SPINNING PROCESSES

One of the oldest polymer processing techniques has been fiber formation, which has contributed significantly to the industrial development [62]. Traditionally the fiber forming processes for polymers are melt, dry, and wet spinning. All three methods involve the formation of continuous filament strands by forcing a polymer liquid material through small dies or holes in a spinneret. Melt spinning involves cooling of the molten strands to form the solid filaments, whereas dry and wet spinning involves removal of a solvent in order to form solid filaments. A fourth spinning process, called dry jet-wet spinning, commonly known as gel spinning, is also utilized for certain polymers. Dry spinning, wet spinning and gel spinning are collectively referred to as solution spinning [63]. Electrospinning, a technique to produce extremely fine fibers from polymer solutions using electrical forces, has also gathered a lot of attention in recent times [64].

2.2.1. Fiber Forming Polymers

Though the basic principle behind polymer spinning has remained the same through the years, the spinning speeds, types of polymers and processes, production efficiency and cost effectiveness have changed [65]. The fiber formation of a polymer is primarily dependent on the properties of the specific polymer. Some of the fundamental polymeric properties such as composition, molecular weight, chemical structure, morphology and crystallinity affect the spinning process as well as the final fiber produced [66].

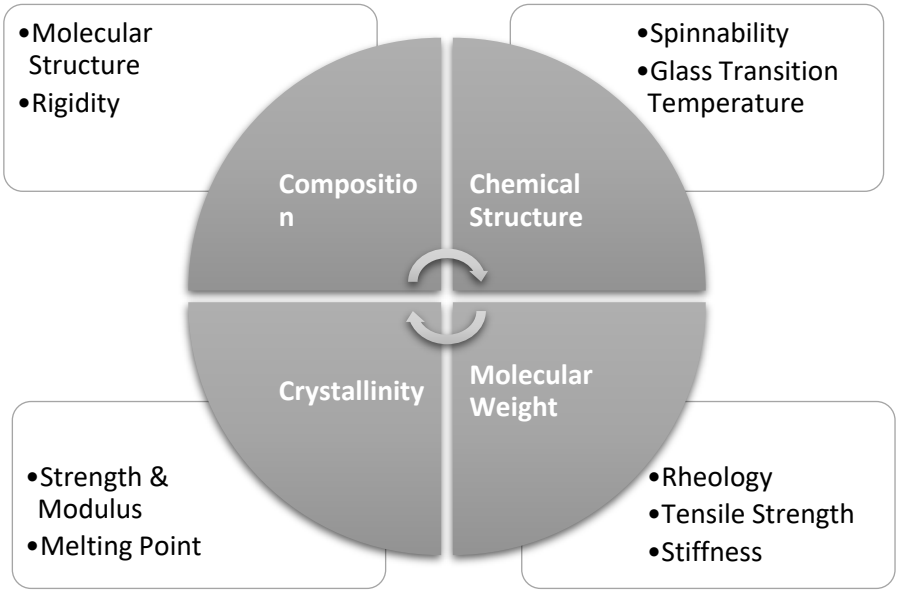

Figure 2.13. Polymeric properties that influence fiber formation

As seen in Figure 2.13, the molecular structure and the rigidity of the polymer chain is affected by the polymeric composition. The rotational freedom of the atomic groups on the polymer chain are directly related to the flexibility of the polymer. Bulky atomic groups reduce the mobility between the chain elements, which make the fiber more rigid [67]. In terms of

chemical structure, a linear polymer is always favorable for spinning. The presence of multiple functional side-groups or polymerization intermediates can undergo subsequent reactions. Over time, these reactions can lead to crosslinking or chain branching, which may result in the formation of gelled polymers that cannot be spun easily. Apart from this, the structure of the polymer chain also has significant effect on the glass transition temperature [68]. The molecular weight of the polymer influences the rheological behavior of the polymer melt or polymer solution, along with its effect on the strength and stiffness of the fiber formed. Higher molecular weight will increase the viscosity of the polymer melt or the polymer solution and can cause flow problems during spinning while a lower molecular weight might decrease the tensile strength of the fibers. As there is direct correlation between viscosity and molecular weight, it is necessary to determine an adequate compromise between the desired mechanical behavior and the polymeric rheological properties [1]. Crystallinity of the polymer is one of the most significant properties that can affect the fiber formation significantly. The combination of crystallinity and molecular orientation determine the majority of the fiber properties [69]. Figure 2.14 provides a structural diagram of the crystalline and amorphous regions in a polymer. The degree of crystallinity, which is the total percentage of crystalline regions in a polymer, directly affects the melting temperature of the polymer. A polymer with negligible crystallinity will not undergo a melt transition. Polymer crystallinity also has a direct correlation with strength and modulus, as high crystallinity means higher molecular orientation and a more compact structure [70].

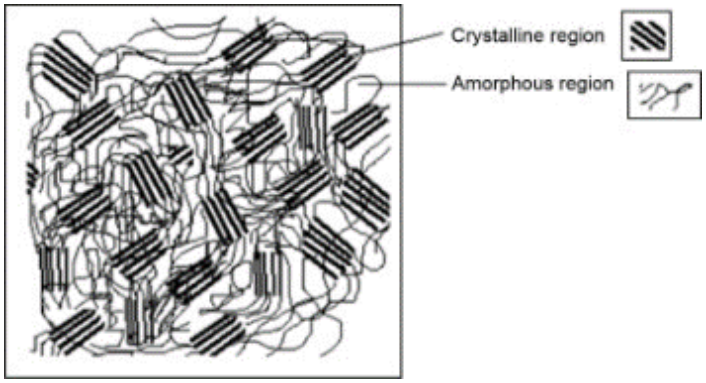

Figure 2.14. Crystalline and amorphous regions in a polymer [66]

2.2.2. Melt Spinning

The melt spinning process was first introduced in the 1930s by scientists in the DuPont Company for polyamide and subsequently polyester [71]. It was considered a revolutionary process for producing synthetic yarns.

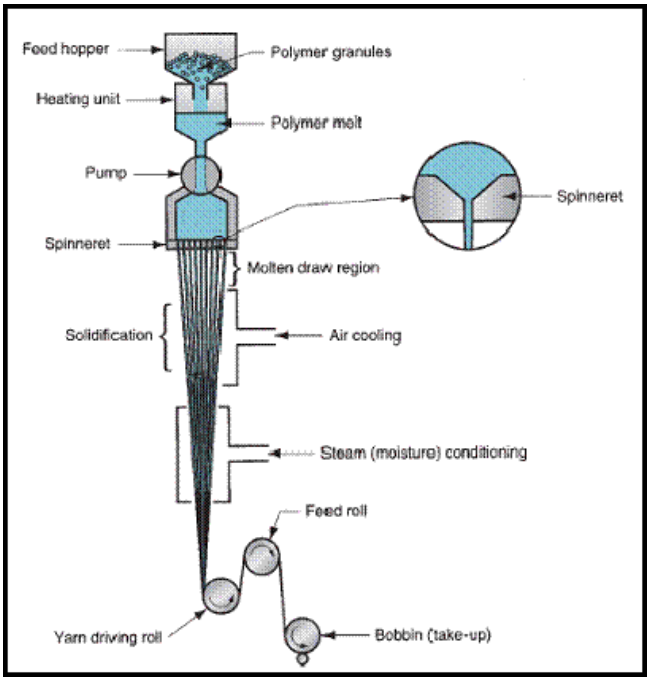

Figure 2.15. Schematic diagram of a melt spinning process [72]

A melt spinning process requires a consistent mass flow rate for the polymer melt, which is maintained by a metering pump inside the spinning head, as seen in Figure 2.15. The spinneret, which is made up of multiple capillary holes with well-defined shapes and sizes, channel the molten polymer. The polymer is extruded in the form of individual continuous filaments through the spinneret orifices, are cooled-off, solidified and collected onto a winding roll [73]. The spun filaments lack adequate strength for most applications, hence they are drawn by heating and stretching to impart additional molecular orientation and crystallinity [74]. Conventionally, melt spun fibers are wound on a bobbin after extrusion at approximately 1200 m/min and in a secondary step are drawn 3-5 times by stretching and heat treatment. However, a single step spin-draw process was developed in the late 1980s, making it a very economical method to melt spin fibers. In the single-step process, the fibers are extruded at a high speed of over 6000 m/min without fully cooling down, enabling them to be drawn during the spinning stage at temperatures between the glass transition and melting point [75].

Melt spinning is the most commonly used fiber spinning process for polymers as it does not require many raw materials, is cost effective and has a very high production rate [76]. However, due to the high temperatures sustained by the polymer during spinning, their potential degradation needs to be taken into consideration when setting the process parameters [62]. The processing of polymers with extremely high molecular weight via melt spinning is limited by the very high viscosity of the polymer melt, which makes the extrusion process difficult [75]. Moreover, the filaments need to be cooled down below the solidification point quickly, or else they may fuse with each other [73].

2.2.3. Dry Spinning

The primary steps involved in a dry spinning process involve the dissolution of the polymer in a volatile organic solvent, followed by filtration. The dissolved polymer solution is referred to as the spinning dope, which needs to be of adequate viscosity for uniform fiber formation. As seen in Figure 2.16, the dope is pumped through fine orifices in the spinneret and the extruded jets of polymer solution come into immediate contact with hot gas (air or inert gas). The stream of heated gas evaporates the solvent and solidifies the filaments without any need for further drying [77]. During the evaporation process, the solvent is first removed from the surface, forming a solid skin-like surface on the exterior of the viscous filament, followed by further evaporation from the interior during the downward passage through the gas flow [78].

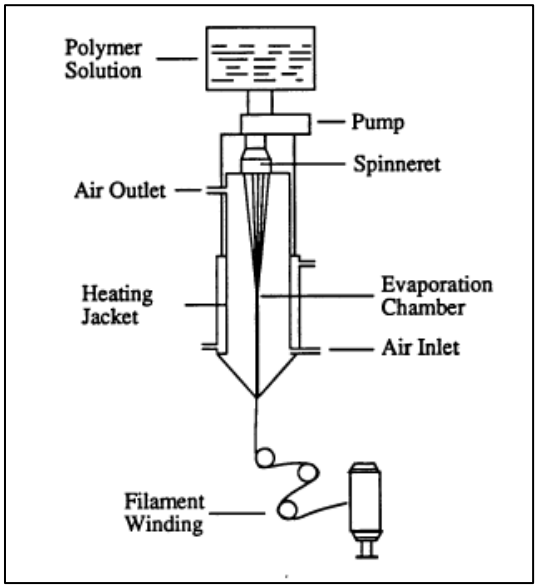

Figure 2.16. Schematic diagram of a dry spinning process [79]

The solidified filaments can be wound on bobbins and then drawn or can be simultaneously stretched in a single step spin-draw process like in melt spinning. The spinning dope for dry spinning has a concentration range of 15-40% depending on the polymer molecular weight and the viscosity of the dope. The temperature of the inlet gas can cross over 100 °C, based on the boiling point of the solvent. The spinning rate is typically in the range of 800-1000 m/min [78]. The key variables that need to be controlled during dry spinning process are the polymer solution concentration and rheology, the swelling skin friction in filament formation and the mass transfer during solidification [80].

Due to cost and environmental reasons, the recovery of the solvent post evaporation is an important process. The recovery system varies by polymer and solvent type. Apart from the recovery process, the mass transfer mechanisms involved in the solvent evaporation and filament formation, make dry spinning more complex and expensive than melt spinning [81]. The main advantages of dry spinning over melt spinning are better molecular orientation during fiber formation resulting in higher tensile strength and the ease of spinning high molecular weight polymers [82].

2.2.4. Wet Spinning

The first fiber to be spun by wet spinning was rayon, with an alcoholic solution of cellulose nitrate extruded from a nozzle dipped in cold water. Since then, a lot of natural and synthetic polymers have been spun via wet spinning [83]. Similar to dry spinning, the polymer needs to be dissolved in a suitable solvent for wet spinning as well. However, unlike dry spinning, the solvent used for wet spinning need not be volatile. The spinning dope is then pumped through the spinneret into a coagulation bath which contains a non-solvent. The interaction between the polymer solution

and the non-solvent leads to fiber formation. The fiber formation begins with the solidification of the outer layer or the skin, followed by the solidification of the core. The as-spun filaments are collected on take-up rollers, washed, dried and drawn in a continuous process (Figure 2.17) [65].

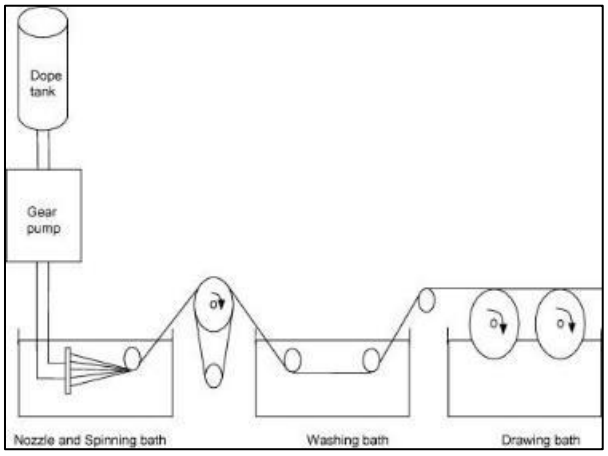

Figure 2.17. Schematic diagram of a wet spinning process [76]

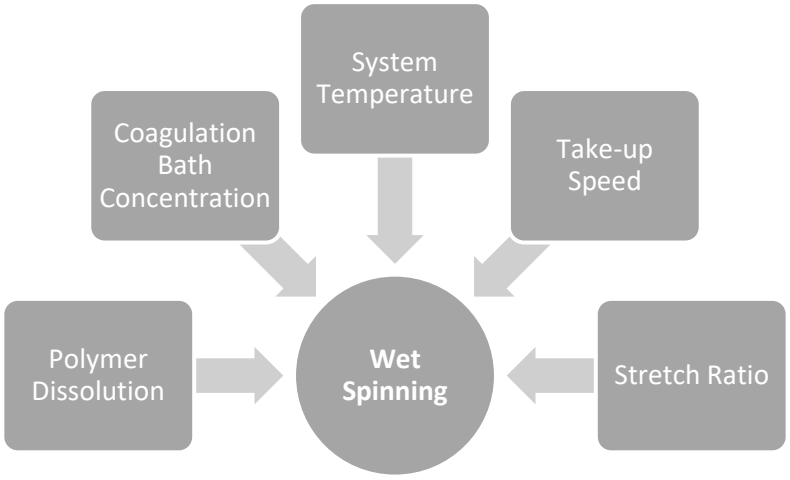

Figure 2.18. Factors affecting the wet spinning process

As seen in Figure 2.18, fiber formation in wet spinning is governed by several factors. Proper dissolution of the polymer in the solvent will ensure a uniform consistency of the dope. The solubility of the polymer in the solvent also controls the polymer concentration and the viscosity of the spin dope [77]. The concentration of the coagulation bath is an important parameter, as it affects the rate of coagulation, skin formation, fiber morphology, and fiber structure. If the rate of coagulation is too high, then the fiber will not be oriented properly before solidification while too low a coagulation rate would lead to thicker fibers [83]. The temperature of the dope and the coagulation bath are important with respect to mass transfer between solvent and non-solvent. The temperature of the system will have an effect on the shear viscosity of the spinning dope and the elongational viscosity of the filament during solidification. Higher temperature will increase the solvent and non - solvent diffusion and lead to a faster skin formation [84]. The speed of the take-up rollers is a measure of the filament residence time in the coagulation bath. Higher the speed of the take-up rollers, the shorter is the residence time. The stretch ratio affects the fiber elongation, tenacity and the molecular orientation in the filaments immediately after solidification [62].

Wet spinning has a lower spinning rate as compared to melt and dry spinning, mainly due to high fluid viscosity, which generates higher tension on the filaments. However, the wet spinning process does not require high temperatures for fiber formation. It is considered to be a much gentler spinning process. Also, the spinneret in wet spinning can have much higher number of orifices than melt and dry spinning, resulting in the production of higher denier multifilaments than other spinning processes. The wet spinning process also has the flexibility of having all spinning and post-spinning operations in a single continuous process, which can compensate for the lower spinning speeds [83].

2.2.5. Gel Spinning

Gel spinning is a technology that was developed in the 1960s mainly for spinning extremely high molecular weight polymers into high strength fibers with improved mechanical properties [85]. In this process, the polymer is dissolved in a suitable solvent to form a spinning dope. It is then extruded from the spinneret and cooled rapidly in air, water or an extractant to remove the solvent and form a gel like fiber (Figure 2.19). This fiber is then stretched to an ultra-high extension to obtain fibers with superior orientation and tenacity [86].

The gel spinning process is similar to wet spinning in most aspects, except for a few of the following differences [86]:

- Presence of an air gap between the spinneret and the extraction bath for fiber gelation.
- Temperature difference between spinning dope and extraction bath.
- Can spin ultra-high molecular weight polymers with the capability for stretching at very high draw ratios.
- Spinning dope has a lower concentration to enhance the spinning capability of the gel fiber, as highly viscous solutions will not undergo gelation properly.

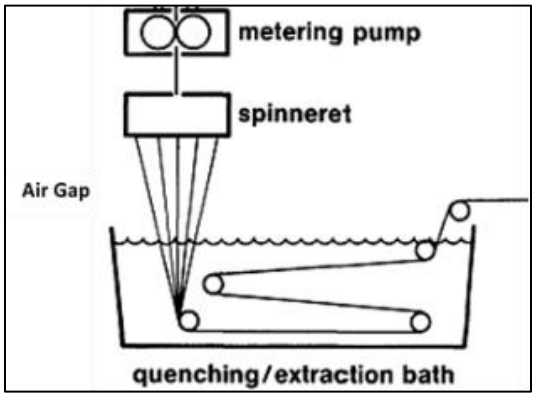

Figure 2.19. Schematic diagram of a gel spinning process [87]

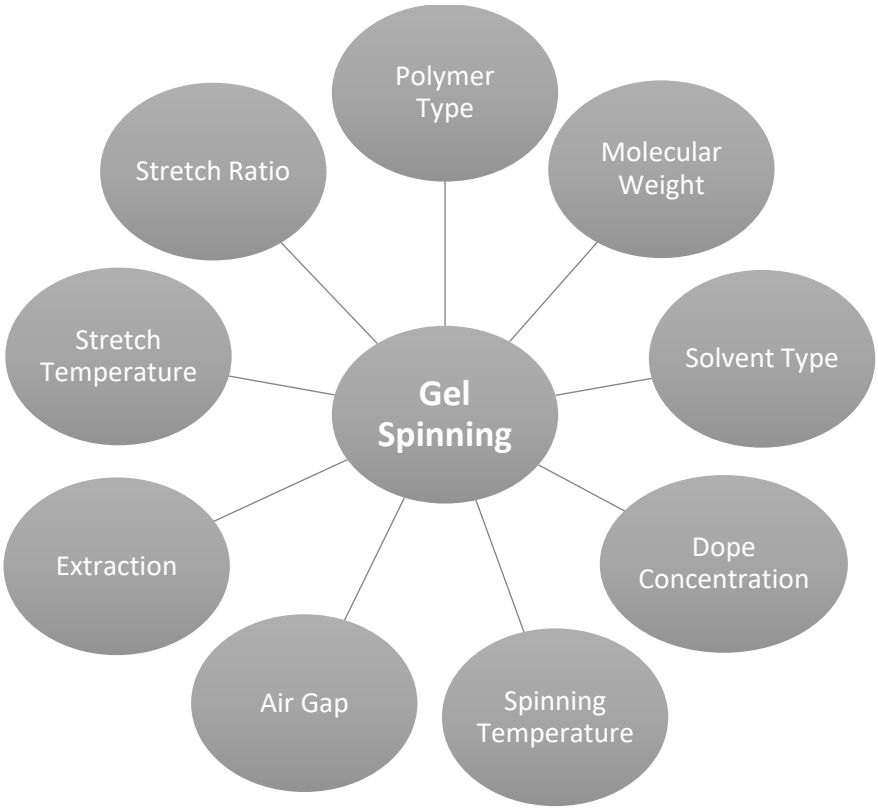

Figure 2.20. Factors affecting the gel spinning process

The fiber formation and the quality of fibers formed via gel spinning is affected by a number of factors, as seen in Figure 2.20. The polymer type and molecular weight are intrinsic polymeric properties that govern the ease of dissolution, spinnability, gel formation and fiber strength. A higher molecular weight can reduce defects in the fiber structure caused by polymer chain end groups and enhance mechanical properties [88].The type of solvent used for polymer dissolution will greatly affect the spinning stability of the gel fibers. It also affects the disentanglement of the molecular chains necessary for gel fiber stretching [86]. The spinning dope concentration controls the chain disentanglement and viscosity, which is essential to the formation of gel fibers with high molecular orientation (Figure 2.21) [85].

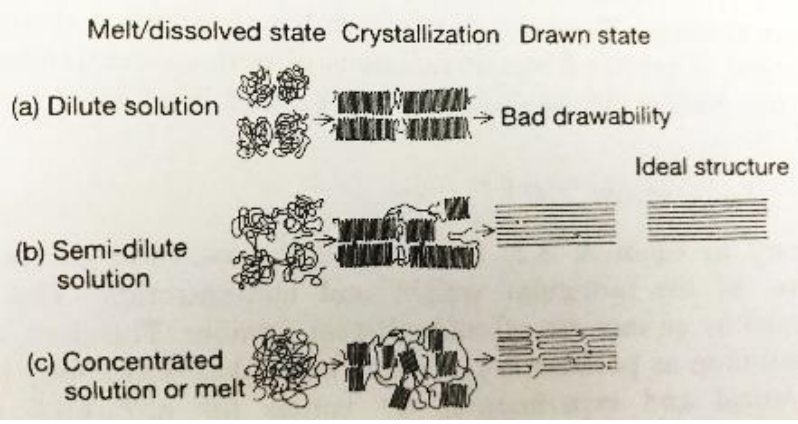

Figure 2.21. Schematic explanation of entanglement control concept [85]

The spinning temperature is correlated to the polymer dissolution and viscosity. In most cases, increasing the spinning temperature will improve the solubility of the polymer in the solvent. However, high temperatures can also lead to thermal cracking of the fiber and reduce the viscosity [86]. As the extruded solution is cooled and the solvent is extracted, the crystallization of the polymer takes place during the formation of the gel fiber. The gel structure contains dispersed crystallites that behave as pseudo-crosslinking points with entangled polymer chains between them, possessing the capability for high stretch ratios. An adequate air gap (with or without cool air flow) and suitable extractant are necessary for the development of the crystallites [85]. The stretching temperature of the gel fiber has a direct effect on the extensibility of the fiber as long as the temperature is below the melting point. Beyond the melting point, the temperature can have a detrimental effect on the strength of the fiber. The stretch ratio of the fiber has a direct correlation with the fiber crystallinity, orientation and morphology. The axial extension of the gel fiber at high stretch ratios can result in a filament with high strength and high modulus [86].

2.2.6. Electrospinning

Electrospinning technique was patented in 1934 by Formhals Anton for the production of artificial threads using an electrical field. In the past few decades, about 50 patents have been filed for electrospinning of polymers [64]. It is a relatively simple method to produce fibers in the nanometer range, which is relatively difficult by conventional spinning methods [89]. A typical electrospinning apparatus set up is shown in Figure 2.22.

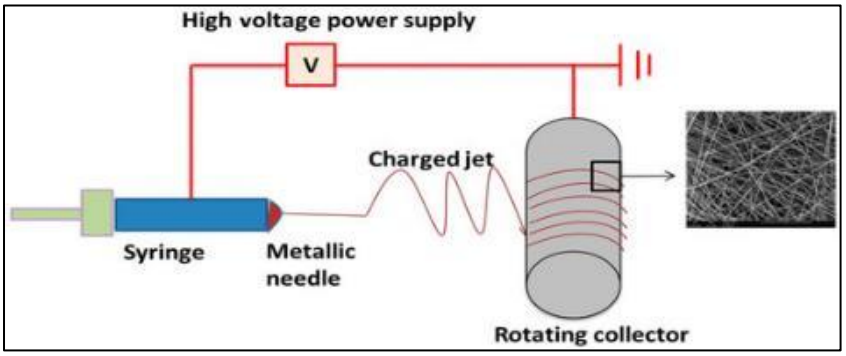

Figure 2.22. Typical electrospinning process setup [90]

The spinning is carried out at room temperature and atmospheric conditions. The electrospinning system consists of three main components, a high voltage power supply, a spinneret and grounded collecting plate. The polymer melt or solution is charged to a certain polarity with a high voltage and ejected out the spinneret at a high acceleration towards the collector. Between the capillary tip and collector, the polymer jet undergoes unstable and rapid whipping, which leads to the solvent evaporation and formation of polymeric fibers. The process is governed by many factors, classified into solution parameters (viscosity, conductivity, molecular weight and surface tension), process parameters (applied electric field, spinneret size, tip to collector distance and flow rate) and ambient parameters (humidity and temperature) [64].

Electrospun fibers have several desirable characteristics, such as their high surface area and high porosity due to their extremely fine structure. Their physico-mechanical properties are also easily tunable by manipulating the solution and process parameters to obtain desired fiber morphology and strength. They have applications primarily in the biomedical field, for tissue engineering scaffolds, wound healing, drug delivery, membranes, graft implants, etc. The electrospun fibers are also being researched for environmental engineering, defense and security, and energy storage and generation [91].

Electrospinning process can be used for both natural and synthetic polymers, as well as their blends. Natural polymers have shown to exhibit better biocompatibility and lower immunogenicity in biomedical applications. This is one of the main reasons for electrospinning of naturally polymers, such as collagen, gelatin, elastin, chitin, etc. On the other hand, synthetic polymers offer a wider scope for tailoring specific properties, such as necessary mechanical strength, desired degradation rate, and fiber structure. Biodegradable synthetic polymers like polyglycolide (PGA), polylactide (PLA), polycaprolactone (PCL) and polyhydroxybutyrate (PHB) have shown promising results with electrospun nanofibrous scaffolds [64]. But, the advantages and success of electrospinning does not surpass some critical limitation sin this process. The denaturation of natural polymers during the spinning process restricts their applications. The fine fiber structure forms a compact nanofibrous matrix with a low pore size which inhibits sell infiltration in the matrix and fails to simulate the physiological 3D tissue micro-environment. In drug delivery, the larger surface area of the fibers causes a significant burst release, which is a concern for long term release profiles. For enhanced applicability of these fibers, many innovations are being used in electrospinning. There is ongoing research for improvement of nanofiber properties and scale up of this process [64].

2.3. POLYMER DISSOLUTION AND COAGULATION PROCESS

The process of dissolving a polymer in a solvent system is the primary step of solution spinning process. A thorough understanding of the dissolution process as well as factors involved in polymer dissolution is necessary to produce a suitable spinning dope. Polymer coagulation is the process where a polymer solution is exposed to a non-solvent, leading to solvent-nonsolvent exchange and polymer precipitation. This process constitutes the most important step in the formation of filaments during wet and gel spinning processes.

2.3.1. Polymer Dissolution Process

An understanding of the polymer dissolution process can provide a path to optimize the design and processing conditions, as well as select a suitable solvent for the polymer. It plays a key role in many applications apart from solution spinning, such as film casting, microlithography, membrane formation, plastic recycling, pharmaceuticals, etc. [92]. Polymer dissolution is also vital within the field of controlled drug delivery and time-release applications. An ideal drug delivery system provides the drug only when and where it is needed, and at the required dosage level so as to elicit the desired therapeutic effect [93]. The dissolution of a polymer in a solvent involves a two-step process, the penetration of the solvent into the polymer, followed by disentanglement of the polymer chains. When an uncrosslinked, solid state polymer is in contact with a thermodynamically compatible liquid (solvent), the latter diffuses into the polymer. A gel-like layer is formed adjacent to the solvent-polymer interface due to the swelling of the polymer by the solvent interaction. The swelling of the polymer leads to deeper penetration of the solvent. After a time period, the polymer chains disentangle and the polymer is dissolved in the solvent, forming a solution, as seen in Figure 2.23 [94].

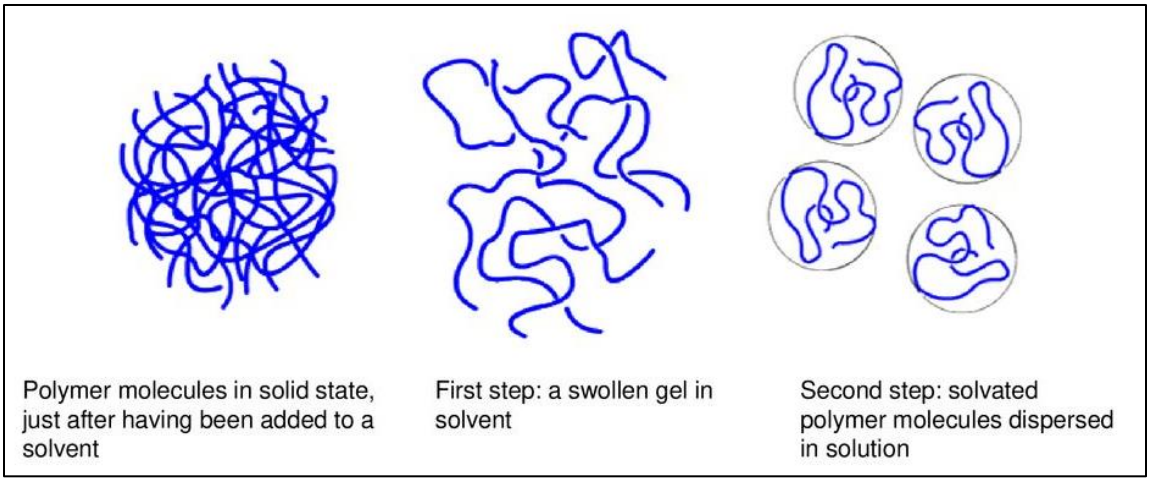

Figure 2.23. Schematic of polymer dissolution process [95]

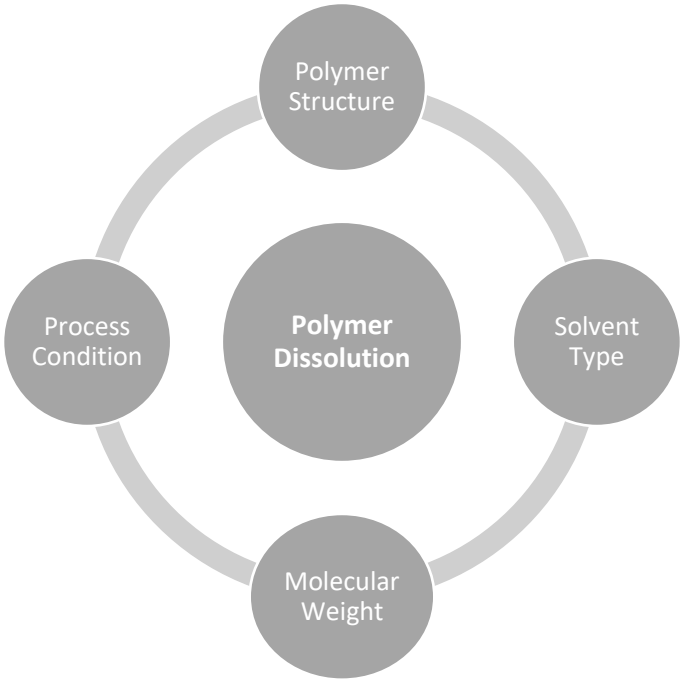

Figure 2.24. Factors affecting the polymer dissolution process

Figure 2.24 lists some of the key factors that affect the polymer dissolution process. The polymer structure is one of the most important factors regarding dissolution in a solvent. The structure of the polymer governs the penetration of the solvent in the polymer chains, which

controls the degree and rate of polymer dissolution. If the polymer has high crystallinity or a compact structure, the rate of dissolution will reduce. Also, if the intermolecular forces in the polymer chains is stronger than the polymer-solvent interactions, then the polymer chains will be unable to swell in the solvent and there will be no dissolution [94].

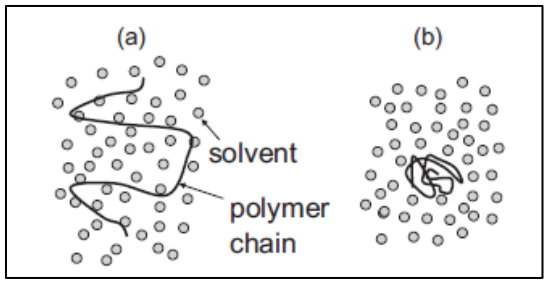

Figure 2.25. Polymer chain conformation in (a) good and (b) poor solvents [96]

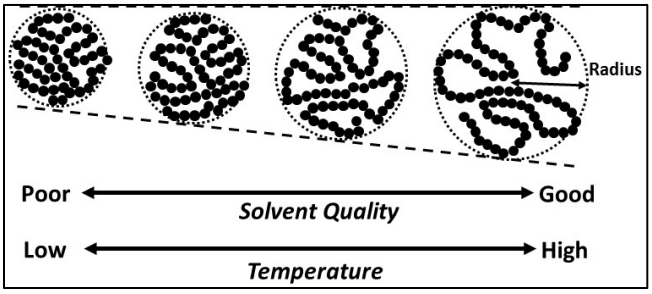

Figure 2.26. Effect of solvent and temperature on polymer chain expansion [97]

Apart from polymer structure, the type of solvent is also an important factor for polymer dissolution. Each solvent has their own diffusivity, depending on polarity, solvent strength and molecular size. A good solvent has strong affinity with the polymer segments and the solvent molecules can penetrate the polymer chains and expand the polymer chains while a poor solvent will not be able to overcome the polymer-polymer interaction and the polymers will remain coiled in the solvent, as seen in Figure 2.25 [96]. The molecular weight of the polymer has an inverse

relation to the rate of dissolution, as the longer chains have more entanglement, which leads to slower solvent diffusion. However, if the solvent is strong enough and the process conditions can enhance the solvent diffusion, then even higher molecular weight polymers can also be dissolved, as seen in Figure 2.26. Process conditions such as agitation, temperature and atmospheric exposure can directly affect rate of dissolution [94].

2.3.2. Polymer Coagulation Process

Polymer coagulation is the final step and possibly the most important in processing of polymeric materials through solution processing methods. It is defined as a process in which a homogeneous polymer solution is quenched in a non-solvent which leads to polymer precipitation. It is a non-equilibrium process, which is controlled by the rate of solvent-coagulant exchange at the polymer interface. A dense polymer "skin" or outer sheath layer is usually formed at the onset of immersing a polymer solution into a coagulant bath. The core of the polymer solution is subsequently solidified over time [98].

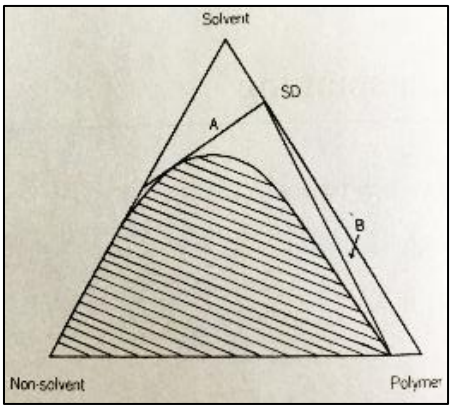

Figure 2.27. Ternary system containing polymer, solvent and non-solvent [99]

As seen in Figure 2.27, the curve represents the boundary between a homogeneous one phase system (above the curve) while the shaded area below the curve represents a heterogeneous two-phase system. The spinning dope concentration (SD) along the polymer-solvent line is of critical importance, as the shift along this line affects the concentration of the dope. In the region above line A, the polymer concentration is too low in the dope and solidification does not occur. On the right of line B, the polymer content increases and solidification occurs by gel formation. In the region between lines A and B, phase separation takes place, induced by the change of polymer solubility [99]. The homogeneous polymer solution undergoes separation due to the presence of the non-solvent, yielding a system of polymer-rich and polymer-lean phases. Upon further separation, the polymer solubility is reduced and a solid phase is formed with a specific morphology [100]. Figure 2.28 provides an overview of factors that affect polymer coagulation.

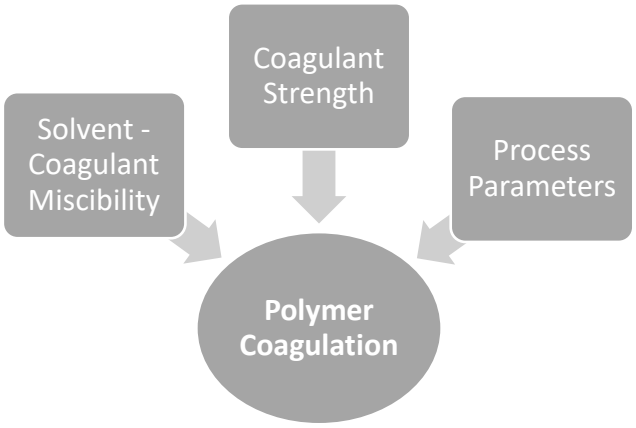

Figure 2.28. Factors affecting the polymer coagulation process

As learnt from the ternary system, solvent and non-solvent interaction is key to the polymer coagulation process. This implies that the miscibility of the solvent and the coagulant would control their interaction energy which would govern the rate of coagulation of the polymer and its

morphological structure. Lower miscibility of the solvent and coagulant will make the solvent and the polymer more similar as far as the coagulant is concerned [98]. The strength of the coagulant also controls the rate of coagulation and the formation of polymer structure. A weaker coagulant would partially dissolve the polymer in the coagulation bath, resulting in limited or no skin formation at the interface. Without sufficient skin formation, the polymer will not coagulate fast enough to form a continuous fibrous structure. External factors which can have an effect on the rate of coagulation are flow rate of polymer solution, polymer solution temperature, coagulant temperature, take-up speed and atmospheric conditions [101].

2.4. POLYMER RESORPTION PROCESS

Over the past century, many natural and synthetic polymers have been studied for biomaterials based medical applications. Initially, scientists were focused on the stability of the biomaterials rather than their biodegradability. However, since the 1960s, when Dexon®, the first synthetic resorbable suture was introduced, there has been a shift towards the study of biodegradable biomaterials or resorbable materials. Since then, the field of resorbable biomaterials has grown exponentially with the development of many synthetic biopolymers [102]. A concern often faced in regard to biomaterials is the use of the terms ‘biodegradable’ and ‘resorbable’ without fully understanding their meaning. A biodegradable process refers to the chemical degradation of a material caused in a biological environment, such as enzymes or microbes. Resorbable processes are those where the polymer is broken down mainly by hydrolysis over a period of time and the degraded products are removed from the body by cellular activity. In the case of medical devices and biomedical applications, the appropriate term for use would be ‘resorbable polymer’ or ‘polymer resorption’ [103].

2.4.1. Resorption Mechanism

As mentioned before, hydrolysis is the primary degradation mechanism for biopolymers in medical devices. Hydrolysis is a chemical process during which chain scission of a polymer occurs in an aqueous medium, dissociating into oligomers and eventually monomers. Hydrolytic degradation can be initiated by acidic, basic or enzymatic catalysts. In each of these processes, the carbon linkage in the backbone is ionized by the catalyst and the water molecule binds itself to the ionic carbon, forming an intermediate which eventually breaks into constituent monomeric chains [104]. Typically, biopolymers undergo a four-step resorption process – water sorption, molecular weight and strength loss, followed by loss of mass. Although there may be an initial strength loss that occurs due to the plasticizing effect of water (and/or biological fluids) that diffuse into the material, but as the polymer chains start to break due to the hydrolytic degradation, loss of molecular weight leads to further reduction in mechanical properties. Before total resorption of the material, changes in shape and mass are observed as the monomers get removed from the material (Figure 2.29) [105].

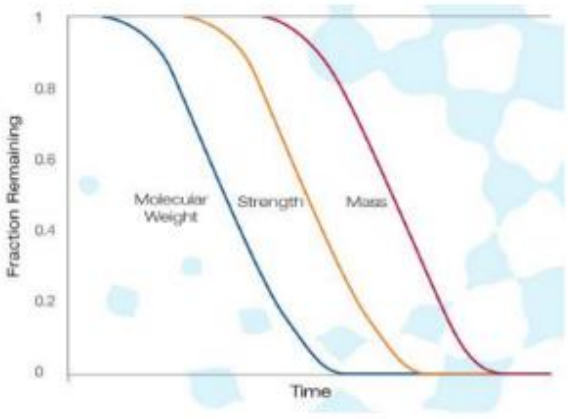

Figure 2.29. Typical bulk degradation profile for resorbable polymers [106]

2.4.2. Hydrolytic Mechanism for Resorbable Fibers

Resorbable fibers have two modes of hydrolysis – surface degradation where water does not penetrate to the interior of the material and bulk degradation where water diffuses to the core and hydrolyses the interior of the structure (Figure 2.30).

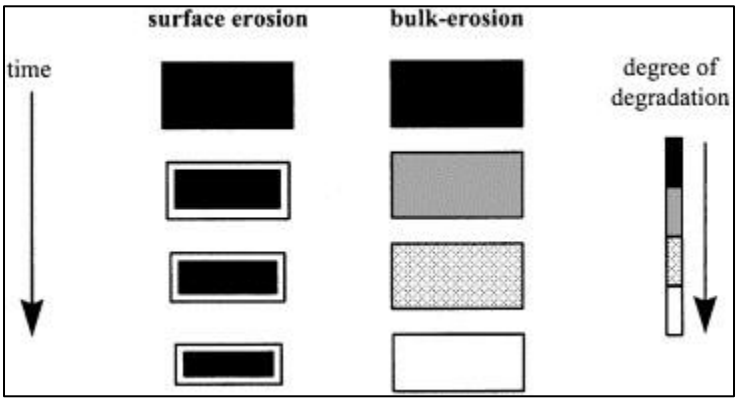

Figure 2.30. Schematic of bulk and surface degradation [107]

In the bulk degradation mechanism, apart from molecular weight, a rapid loss in strength is observed as compared to mass loss, because even though fewer intact polymer chains remain in the bulk, the monomeric chains are still present inside the fiber system. On the other hand, in surface degradation, mass loss is more prominent than strength loss as the smaller broken chains on the surface get removed quickly, but do not affect the mechanical properties significantly in the beginning. In a non-porous material, the two mechanisms occur independently, whereas in a highly porous substrate, bulk and surface degradation takes place simultaneously [107].

The balance between the rate of diffusion of water, the rate of hydrolysis of the polymeric bond and the dimensions of the structural matrix, determines the hydrolytic mechanism. The ratio of the

diffusion time to hydrolysis time gives a dimensionless number – erosion number (ε), which primarily governs the degradation mechanism [108].

Time for diffusion = $\mathbf{t_{diff} = \langle x \rangle^2 \pi / 4 D_{H2O}}$

<x>: distance of diffusion; D_{H2O}: effective diffusivity of water

Time to degrade 'n' bonds = $\mathbf{t_c = (1/k)[\ln \langle x \rangle + (1/3) \ln (N_{Av} \rho / M_0)]}$

N_{Av}: Avogadro's number; M_0: molecular weight of repeat unit;

ρ: polymer density; k: rate constant for bond hydrolysis;

Hence, $\mathbf{\varepsilon = t_{diff} / \langle t_c}$

Replacing <x> by total matrix thickness would help predict mechanism of hydrolysis.

ε > 1 bulk erosion; ε = 1 change in erosion mechanism; ε < 1 surface erosion;

For the value of <x> where ε = 1, the thickness is known as critical length ($L_{critical}$). By varying <x>, the hydrolytic mechanism of the matrix can be controlled. $L_{critical}$ for some commonly used resorbable polymers, as shown in Figure 2.31.

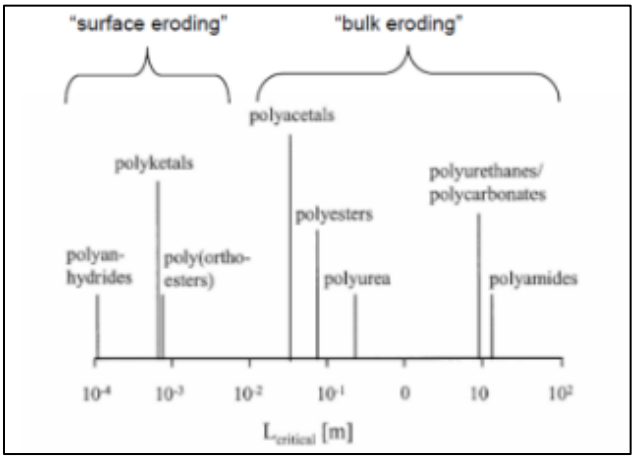

Figure 2.31. Critical thickness ($L_{critical}$) values for some resorbable polymers [109]

2.4.3. Factors affecting Rate of Hydrolysis

The rate of hydrolysis is affected by many molecular, structural and biological parameters. Some of them have a direct impact on the time taken for bond cleavage, slowing down the hydrolytic reactions, while others control diffusivity of water, hindering the hydrolysis process (Figure 2.32).

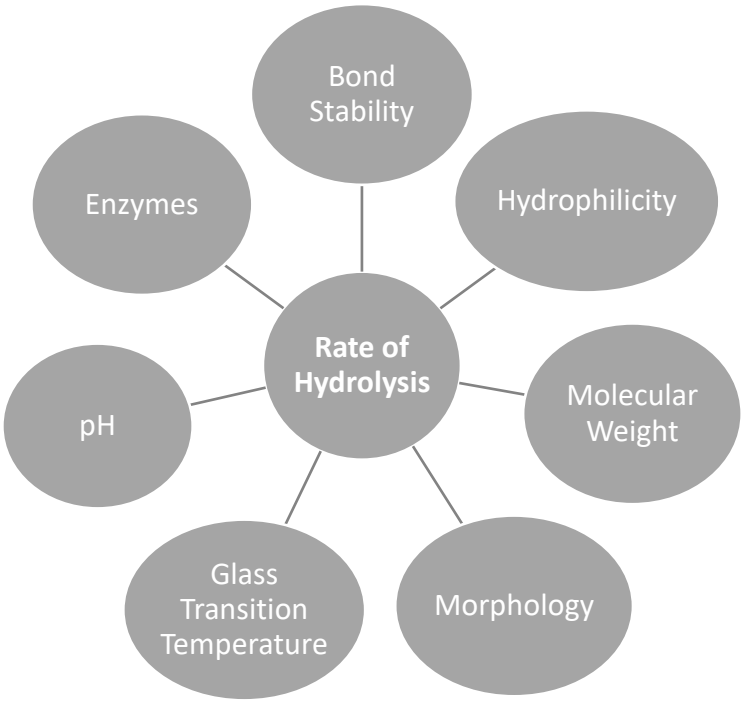

Figure 2.32. Factors affecting the rate of hydrolysis

The bond stability is determined by the susceptibility of the backbone to form ionic intermediates with water. Resonance stabilized structures have lower tendency to bind with water and are less likely to hydrolyze [110].

Rate of Hydrolysis: anhydride > ester > amide > ether

The hydrophilicity of the polymer governs its affinity towards water, which is in direct correlation with the rate of hydrolysis. Changes in molecular weight affect the architecture of the polymer and its alignment. Higher molecular weight polymers have restricted space and their proximity can create or enhance intramolecular bonding. Also, a higher molecular weight implies a higher number of bonds present in the chain, requiring more time for hydrolysis. Thus, molecular weight is inversely proportional to the rate of hydrolysis [110]. The morphology of a material mainly encompasses its crystallinity and porosity. Crystalline polymers are more aligned and oriented along the fiber axis, making the fiber more water impermeable. Although higher crystallinity doesn't necessarily imply a slower hydrolysis process, it makes the degradation process a surface phenomenon [111]. A porous structure is clearly more permeable and has a higher rate of hydrolysis. It also has a higher possibility to experience a bulk degradation mechanism. The glass transition temperature of a polymer affects its chain mobility and indirectly the diffusivity of water, which controls the rate and mechanism of hydrolysis [110]. Biological fluids in the body alter the local pH of a medical device's implant site. Additionally, cellular activity during inflammation and/or infection lowers the pH of the area and creates an acidic environment, resulting in a catalyzed rate of hydrolysis. Certain enzymes like protease, esterase, hydrolase, etc., are released in the body and can accelerate the hydrolysis of polymer chains [112].

2.5. DRUG DELIVERY SYSTEMS USING POLYMERIC FIBERS

In the recent decades, controlled drug delivery systems have gained a lot of attention due to their advantages over conventional dosage methods, such as enhanced therapeutic efficacy, lower toxicity and fewer side effects. Based on the therapeutic requirements of the controlled delivery system, the drug release period would extend from a few days to several months [113].

Figure 2.33 graphically compares conventional dosing system and controlled release dosing system on the basis of drug level in blood plasma.

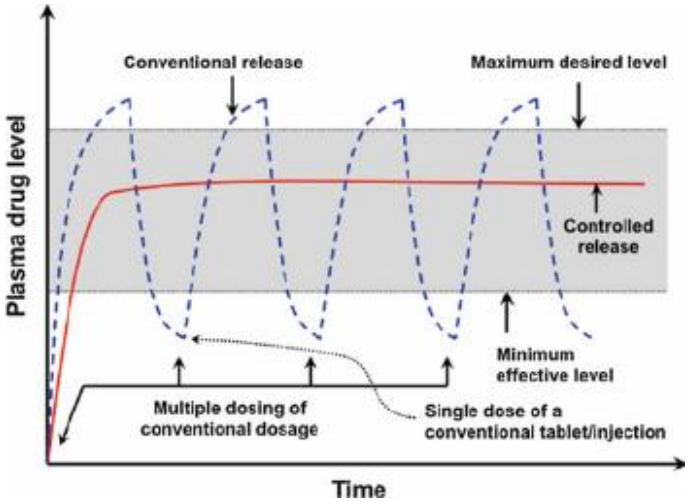

Figure 2.33. Drug levels in plasma from conventional dosing system (blue line) and controlled release system (red line) [114]

Polymers have been used in the pharmaceutical and medical industries for a long time. There are various research articles and patents from mid-20th century describing the applications of polymeric materials in pharmacology, patient-care products, medical devices and implants [115] [116]. It is only natural that polymeric materials be applied in controlled release drug delivery systems. Entrapping the drug in a polymer structure can be used to control the delivery rates reproducibly. The type of delivery carrier can govern the release rate of the drug, which can be classified as immediate, rapid, slow and prolonged [117].

The polymer-based drug delivery systems started off with the use of non-degradable materials such as silicon, polyurethane and acetate-vinylidene copolymers as these polymers were

already approved by the government regulators, were biocompatible and inert. However, their non-degradable characteristic meant the removal of the drug carrier after the required dosages are delivered. This increased the interest in biodegradable polymers for delivery systems as they do not need to be removed after the treatment. These biodegradable polymers undergo degradation and are easily expelled by the body. They also provide cost reductions and decrease the stress on the body [113]. Figure 2.34 shows the various structural forms for polymeric drug delivery systems, such as micro and nanoparticles, thin films, fibers and hydrogels.

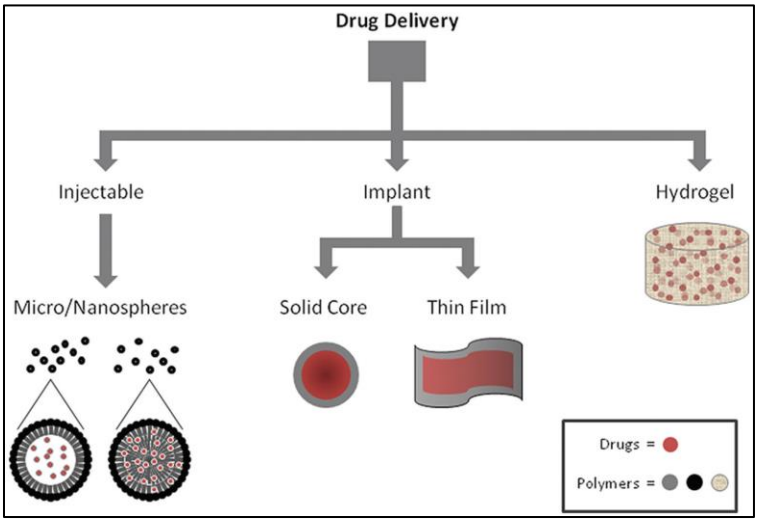

Figure 2.34. Classes of polymeric drug delivery systems [118]

An efficient drug carrier plays a major role in effective and predictable controlled drug delivery system. Factors which govern the selection of a drug carrier are – (i) drug targeting to the intended organ for maximum effect, (ii) evasion of the body immune system to reach the target, (iii) retention of the therapeutic molecules from preparation and processing to the final target and (iv) release of the drug at the destination with the intended therapeutic effect. Fiber morphology –

with their cylindrical shape and high surface area to volume ratio – make them an ideal candidate for drug delivery systems. They have the potential to release the drug in the medium over a large surface area. Also, fibers have more adjustability for drug systems as they have variable length and cross-section, unlike spherical vehicles. The versatility of fiber shape and structures (hollow, flat, ribbon-like) and their different arrangements, make them much more suitable for drug delivery than micro and nanoparticles [7].

2.5.1. Applications of Drug Loaded Fibers

Polymeric fibers have many applications in the medical field, from surgical sutures and wound dressing products to tissue engineering scaffolds and biomedical devices. In the recent years, research in the design of therapeutic fibers for use as drug delivery vehicles has increased significantly [119].

Sutures and wound dressings are the most widely used products made from textile fibers. These products are used to hold the tissue and skin together that has been separated due to an injury or surgery. The sutures alone have a market of over a billion dollars annually [120]. During wound closures, there is always a risk of infections and inflammatory reactions. In the past decade, research has been done to develop medicated sutures and wound dressing materials, made from fibers that contain bioactive compounds which can be released in a controlled time frame to support tissue repair [121]. Antimicrobial agents coated onto sutures that prevent wound/surgical site infections and consequently lead to cost savings have been commercially approved for clinical use since 2002 [122]. The success of the antimicrobial sutures led to the research advances in sutures coated with other drugs such as analgesics, anti-inflammatory, antithrombotic, antiproliferative and antineoplastic agents [123]. Figure 2.35 is a visual representation of a concept

for a PCL based suture loaded with diclofenac - an anti-inflammatory drug. A commercial example of a drug-loaded suture is Vicryl® Plus by Ethicon (Figure 2.36), where they use a polyglactin based absorbable suture coated with an antibacterial drug to prevent infections at the wound site [124].

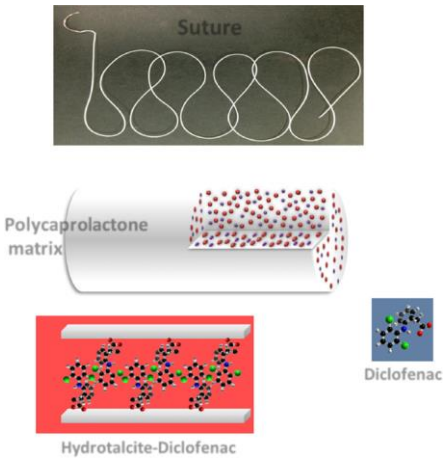

Figure 2.35. Anti-inflammatory suture concept from a research study [121]

Figure 2.36. Antibacterial resorbable sutures by ethicon [124]

Tissue engineering scaffolds serve as a 3D matrix for cell adhesion, proliferation and differentiation. The microenvironment in the scaffold can influence cellular function and tissue regeneration. Nanofibrous scaffolds incorporated with bioactive agents and drugs allow for improved cell infiltration, attachment and proliferation. The controlled release of drugs in the scaffold can accelerate the local regenerative process and reduce the concerns over undesired systemic effects of the drug in the body. Polymers commonly used for scaffold preparation are collagen, chitosan, PLA, PGA, PCL and PHB. Bioactive agents like growth factors and stem cells are attached to the scaffolds to promote tissue regeneration. Drugs like heparin are used to bind and control the delivery of growth factors in the scaffold structure [125]. Figure 2.37 shows a schematic for preparing drug-loaded PCL nanofiber scaffolds for tissue regeneration.

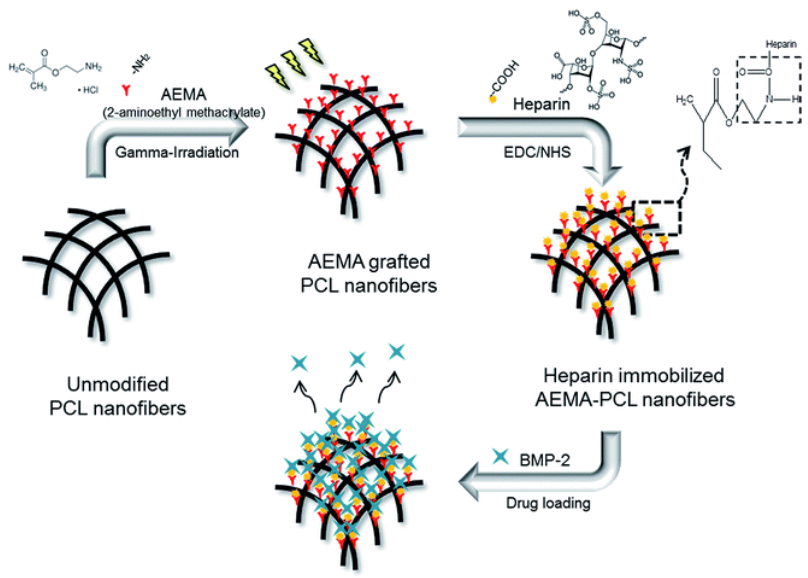

Figure 2.37. Drug loaded PCL-nanofiber scaffold from a research study [126]

2.5.2. Drug Loading in Textile Fibers

Drug-releasing fibers can be prepared with a variety of drug-loading methods such as coating, encapsulation, hollow fiber filling, bioconjugation, spinning, etc. Coating and encapsulation are two of the simplest methods for incorporating drugs in the fiber structure. Both these processes have a physical interaction of the fiber with a drug solution and get loaded onto the fiber by either surface attachment during coating or physical entrapment by diffusion. For coating the fibers with drugs, a solution is prepared with the drugs and the fibers are dipped into the solution, pulled out and dried (Figure 2.38). The drugs get affixed to the surface of the fibers due to the physical affinity between the drugs and the polymer. However, the weak physical attachments between the drug and the fiber ensures a significant drug release immediately after in vivo implantation, which makes this process unsuitable for long term drug release applications. For encapsulation of the drugs, the fibers are soaked in a drug containing solution and allowed to diffuse into the fibers. The subsequent drug release is solely diffusion controlled and dependent on the drug solubility and fiber swelling [8].

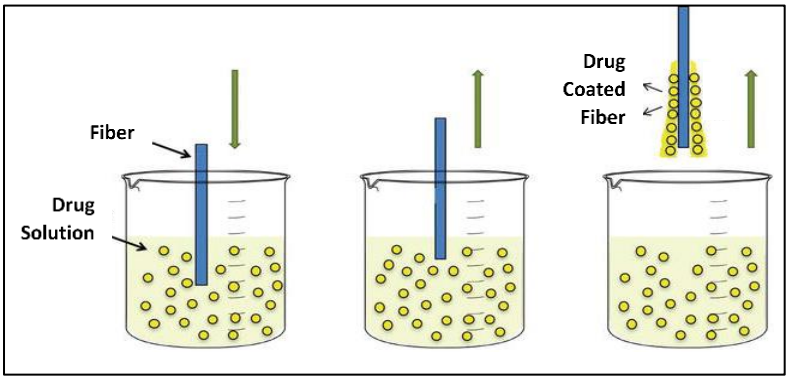

Figure 2.38. Fiber drug loading by coating method [127]

Hollow fiber drug systems can be compared to small tubes filled with a drug. The fiber was is usually made of a permeable membrane to control drug release. Typically, the drugs are first mixed with a polymer material and a drug-loaded core is prepared. Then the fiber is extruded in a coextrusion process with the drug loaded polymer forming the core of the hollow fiber while a different polymer is extruded as the outer membrane, as seen in Figure 2.39. Hollow fibers provide high drug loading flexibility and also have a higher surface area to volume ratio [8].

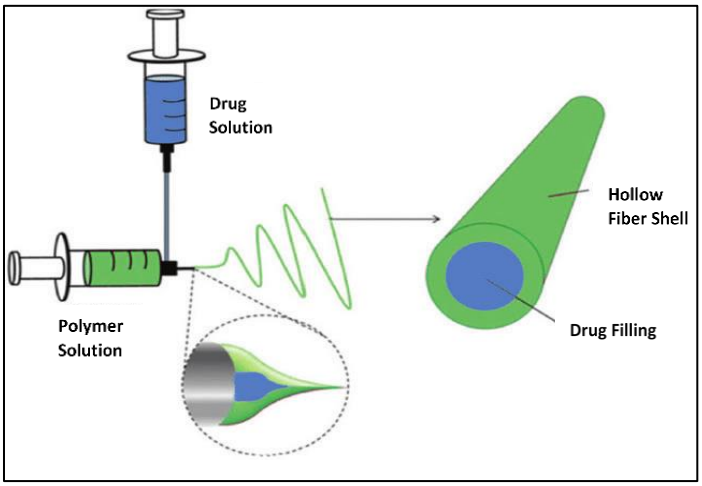

Figure 2.39. Hollow fiber with drug filling [128]

Drugs and bioactive molecules can also be attached to the fiber surface directly by bioconjugation techniques to obtain controlled release and site-specific delivery. This method requires functionalization of the fibers to allow formation of chemical or physical bonds with the drug or bioactive molecules, as shown in Figure 2.40 [8].

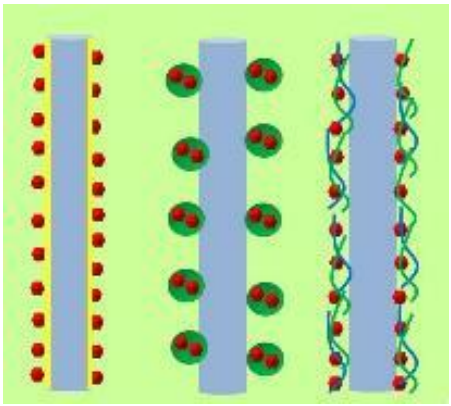

Figure 2.40. Bioconjugation of drug and bioactive agents on fiber surface [129]

2.5.3. Drug Loading during Fiber Spinning

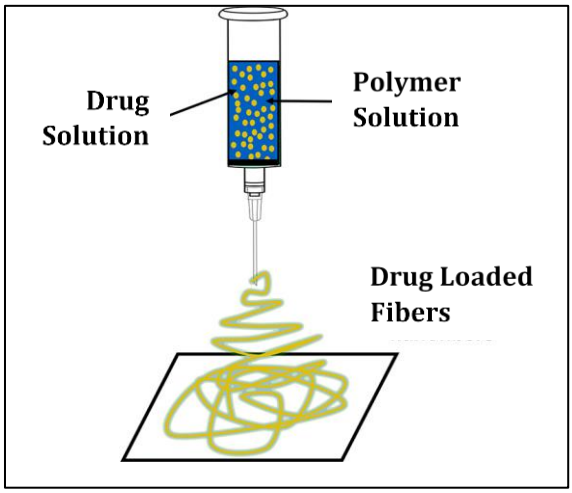

Figure 2.41. Fiber drug loading during spinning [130]

Incorporation of drugs in the fiber during the spinning stage increases the stability of the fiber-drug structure and can provide a better control of the drug loading and drug release processes. Even though melt spinning is usually unsuitable for drug loading during spinning due to the high processing temperatures, wet spinning and electrospinning can be used to produce drug loaded

fibers (Figure 2.41). In both these processes, the drugs can be added to the polymer solution before it is extruded out and the drug-loaded fibers are either coagulated in a spin bath or collected electrically. The extruded fibers have the drugs distributed throughout the fibers uniformly (Figure 2.42).

Figure 2.42. Distribution of drug molecules in a textile fiber [8]

There are numerous studies on loading various types of drugs in degradable and non-degradable fibers via wet spinning and electrospinning. Polymers such as PLA, PGA, and PCL have been used to spin fibers with drugs like levofloxacin (anti-bacterial), 5-fluorouracil (cancer therapy), ibuprofen (anti-inflammatory), etc. for sustained release [131] [132] [133]. This method of loading drugs during spinning enables the fibers to release drugs for a longer duration compared to other drug loading techniques. The incorporation of the drug in the entire structure of the fiber can allow for the use of drugs which cannot be attached to the fiber surface. This process also provides better adjustability and control of the drug delivery system parameters which require high precision [7].

2.5.4. Drug Release Mechanisms for Drug Loaded Fibers

The concept of a drug release mechanism explains the process in which the therapeutic agents are transported and delivered in vivo. This process governs the release rate of the molecules which will control the amount of drug being released from the device as well as for how long the drug will be released [134]. Some factors which influence the drug release mechanism are the composition and structure of the fiber matrix, the fiber swelling in the medium, and the fiber degradability; the pH and temperature of the medium, and the presence of enzymes; the solubility and size of the drug particles, and the interaction between drug and the fiber material [135].

In a fiber-based drug delivery system, the most relevant drug release mechanisms are immediate release, extended release and triggered/delayed release. As the name suggests, in the immediate release mechanism, the drugs have a high rate of release and the duration of drug release is relatively short. This mode is important for conditions which require an immediate action. In the extended release mode, the drugs are available for release over a prolonged period of time and rate of release is relatively lower compared to the immediate release mode. This allows to maintain a significantly lower dosing frequency. The triggered or delayed release mechanism is controlled by an environmental stimulus or external trigger and/or time. This drug release mode can be an immediate release type or a slow-release type depending upon the trigger or stimulus. The release can be triggered by a variety of factors such as changes in environmental temperature, pH, ionic strength of the surrounding tissue, etc. [136].

A common method to study drug release from fibers is to use an in vitro experimental design with the use of a saline medium, such as phosphate-buffer at 7.4 pH and a temperature of 37 ºC to mimic the typical conditions of a human body [137].

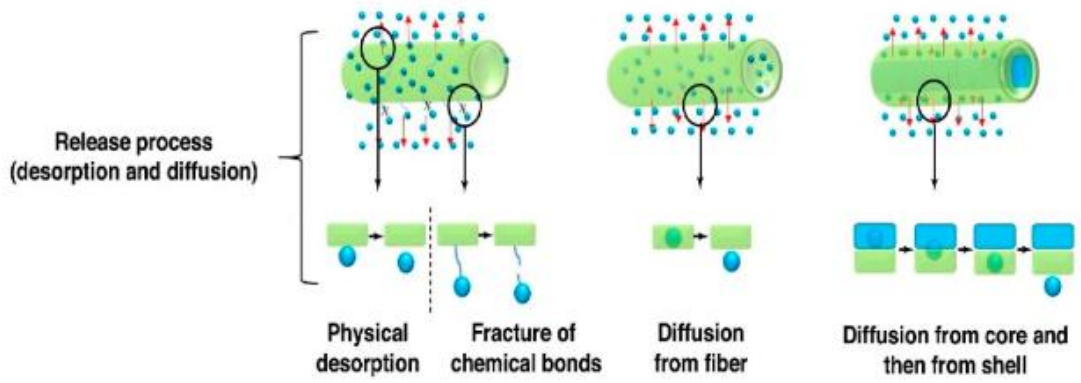

Figure 2.43. Drug release processes from non-biodegradable polymeric fibers [90]

Devices made with non-biodegradable polymeric fibers are recovered after the drug has been released via the diffusion or desorption process, as seen in Figure 2.43. Drugs are released by desorption process when the drugs are loaded onto the fiber surface via a physical or a chemical attachment, such as in coating or bioconjugation. If the drug molecules are trapped inside the fibers, via encapsulation, hollow fiber filling or spinning methods, then the drugs diffuse from the fiber. The drug release is primarily related to the thickness of the fibers and permeability of the polymeric structure. The release rate is fairly constant and is generally not affected by a concentration gradient for zero-order kinetics. On the other hand, for a first-order kinetic release, the diffusion rate is dependent on the concentration of drugs remaining in the matrix [135].

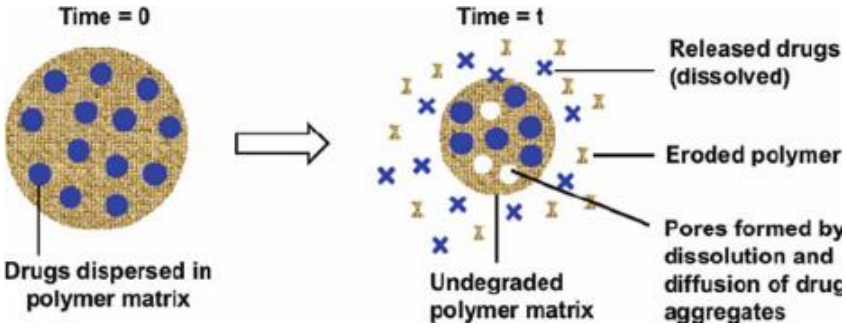

Figure 2.44. Drug release process from biodegradable polymeric fibers [114]

Drug loaded fibers fabricated from biodegradable polymers typically release the drugs by diffusion and erosion processes, as seen in Figure 2.44. The rate of drug release is governed jointly by the rate of diffusion of drug from the fibers and the rate of erosion of the polymer matrix in the fibrous structure. Factors such as the type of drug, type of polymer, fiber diameter and structure can affect the rate of diffusion and erosion, which will subsequently control the drug released [135].

Typically for a surface erosion-based polymer matrix (spherical, cylindrical or slab-like), drug release is expressed by the following equation [135]-

$$\frac{M_t}{M_\infty} = 1 - \left[1 - \frac{k_o.t}{c_o.a}\right]^n$$

M_t: Amount of drug released at time 't';

M_∞: Amount of drug released at infinite time

k_o: Erosion rate constant;

c_o: Initial drug concentration in the matrix

a: Radius / half-thickness;

n: Shape factor (spherical (n=3), cylindrical (n=2) or slab geometry (n=1))

There are several mathematical functions to use for kinetic modelling of drug release profiles for non-degradable polymer systems. There are different models which can be used to fit the drug release data, such as zero-order, first-order, linear regression, exponential regression, based on the type of system, drug, shape of the matrix, etc. [138].

The current trends in drug delivery systems show that biomedical textile structures are a key component for such devices. Fibrous non-woven and woven surfaces exhibit high porosity and surface area, and adjustable pore size distribution, which is desirable for the attachment of bioactive and therapeutic agents. These textile structures are also flexible in terms of processing, fabrication, functionalization and drug loading capabilities. They can be used to deliver a wide range of substances, such as antibiotics, anti-cancer drugs, proteins, cellular growth factors, etc. Thus, drug-releasing textile materials are considered to be a versatile system for drug delivery applications and provide attractive alternatives to conventional drug delivery systems [136].

CHAPTER 3 - THE EFFECT OF WET SPINNING CONDITIONS ON THE STRUCTURE AND PROPERTIES OF POLY-4-HYDROXYBUTYRATE FIBERS

3.1. INTRODUCTION

Polyhydroxyalkanoates (PHAs), also commonly known as bacterial polyesters, are considered to be novel polymers because of their biodegradability. A wide range of hydroxyalkanoate units, such as butyrates and valerates, are produced by bacterial fermentation, which can be polymerized and copolymerized with varying mechanical and structural properties [33]. Owing to the versatility of PHAs along with their biocompatibility and resorbability, they are promising candidates for biomedical applications such as implants, sutures, stents and tissue engineering scaffolds [38]. They are also under consideration for controlled release drug delivery applications involving a variety of therapeutic chemicals and drugs, particularly those that are thermally sensitive [3].

Poly-4-hydroxybutyrate (P4HB) is a type of polyhydroxyalkanoate that has been developed as an absorbable biomaterial for medical applications. It was first synthesized in the early 1990s using a fermentation process developed by researchers at Massachusetts Institute of Technology [139]. This biopolymer provides properties that has expanded the biomaterial design space, allowing for the development of new and improved resorbable medical products. It has already received approval from the United States FDA and EU regulatory agencies for use in clinical applications. Some of the products that are being developed using P4HB include vascular grafts, stents, patches, and sutures [50]. P4HB is a strong thermoplastic polymer and has significantly more flexibility than other synthetic absorbable polymers, such as polyglycolide (PGA) and poly-L-lactide (PLLA). It has a melting temperature around 60 °C, and a glass

transition temperature of −51 °C. P4HB is typically melt spun and drawn into filaments for various applications at temperatures between 180 – 210 °C, although higher molecular weight P4HB (>800 K) may require higher temperatures for processing due to its high melt viscosity [140]. The high processing temperatures of P4HB inhibits the possibility of incorporating drugs within the polymer during the spinning stage, as most drugs cannot sustain such high temperatures and hence require a post spinning incorporation process such as coating, absorption or surface conjugation [8]. This raises the need for a low temperature spinning process for bacterial polyesters that will address the major drawbacks associated with incorporating drugs in a post melt spinning process. Examples of such disadvantages include non-uniform absorption, and uneven and unpredictable release profiles [7].

Presently, there is no defined procedure to produce P4HB fibers through a solution or wet spinning process. Hence, this work focuses on identifying suitable wet spinning process conditions for poly (4-hydroxybutyrate) (P4HB) and developing a scalable method for the continuous extrusion of P4HB fibers. The process parameters studied in this project include the type of solvent and coagulant, spinneret size, spin dope concentration, coagulation bath temperature, and spin draw ratio. There are three main objectives to this study. (i) To analyze the process conditions for dissolution and coagulation of the P4HB polymer. (ii) To assess the effect of polymer concentration in the spin dope and the temperature of the coagulation bath on the spun fiber properties. (iii) To evaluate the effect of the spin draw ratio on the fiber structure and mechanical properties. Based on the results of this project, a suitable combination of these parameters will be used to further produce drug loaded P4HB monofilaments and study their fiber properties as well as their drug release profiles.

3.2. MATERIALS

The first step in this study was to determine a suitable dissolution and coagulation system for the P4HB polymer. Due to limitations related to intellectual property, P4HB could not be obtained in its polymeric form. However, 100% P4HB uncoated absorbable surgical sutures under the tradename Monomax® were obtained from B. Braun Surgical S.A. (Barcelona, Spain) and used as the raw polymer material for this study. These P4HB sutures had a molecular weight of approximately 300 kDa [141]. Potential solvents and coagulants for dissolving and coagulating P4HB were identified from the literature. A list of these chemicals, along with their supplier and grade is provided in Tables 3.1 and 3.2.

Table 3.1. Solvents studied for P4HB dissolution

Tetrahydrofuran	BDH	ACS Grade
Methylene dichloride	Sigma Aldrich	ACS Reagent, ≥ 95.5%
Chloroform	Fisher Scientific	ACS Grade
Ethyl lactate	Sigma Aldrich	ACS Grade

Table 3.2. Coagulants studied for P4HB coagulation

Methanol	Fisher Scientific	ACS Grade
Ethanol	Fisher Scientific	ACS Grade
Propanol	Fisher Scientific	ACS Grade
Reagent alcohol	Fisher Scientific	ACS Grade
Acetone	Fisher Scientific	ACS Grade
Hexane	Sigma Aldrich	ACS Grade

3.3. EXPERIMENTAL METHODS

3.3.1. Solvent Analysis

Potential solvents, such as tetrahydrofuran (THF), methylene dichloride, chloroform and ethyl lactate, were identified from the literature to study P4HB dissolution [59]. The primary criterion to compare the performance of each solvent was to measure the rate of polymer dissolution in each one at room temperature. A stopwatch was used to measure the time taken to dissolve 1 gram of dehydrated P4HB in 10 ml of each solvent stirring at 300 rpm, as shown in Figure 3.1. Additionally, the homogeneity and absence of turbidity of the polymer solution at different concentrations was also considered when choosing a suitable solvent.

Figure 3.1. Solvent analysis of P4HB for dissolution

3.3.2. Coagulation Study

Drop tests and spin trials using syringe-needle systems with various needle gauge sizes were used to study suitable coagulation conditions. The coagulants tested were methanol, ethanol, propanol, reagent alcohol, acetone and hexane. Polymer coagulation was studied at three coagulation temperatures: room temperature, 10º C and -10º C.

Multiple polymer solutions with 10% (w/v) concentration were prepared with either methylene dichloride or chloroform as solvents. One set of solutions, each containing methylene dichloride or chloroform, were tested directly for polymer coagulation. To the other set of polymer solutions, 10% (v/v) acetone was added to determine if the addition of a non-solvent to the spin dope affected the rate of polymer coagulation [142]. During the drop tests, the polymer solutions were added dropwise to potential coagulants in glass vials and a tweezer was used to stretch the polymer drop during coagulation (Figure 3.2). Syringe-needle systems, obtained from Sigma-Aldrich, were used to evaluate the polymer coagulation process by extruding the spin dope through a single spinneret hole with a small diameter, as shown in Figure 3.3. Needles with different gauge sizes ranging from 18 (0.838 mm inner diameter) to 25 (0.26 mm inner diameter) were tested to study the effect of spinneret hole size on polymer coagulation.

The polymer coagulated by both methods was assessed qualitatively for its structural integrity and rate of coagulation, as a faster rate of coagulation with immediate skin formation and a stretchable polymer structure is preferred for wet spinning. If the coagulated polymer could be pulled with a pair of tweezers without breaking, as shown in Figure 3.2, then this suggested that the polymer could be spun into continuous fibers in a coagulation bath. The ability of the coagulated polymer to elongate without breaking also indicated the potential for a higher spin draw ratio for the spun fibers [83].

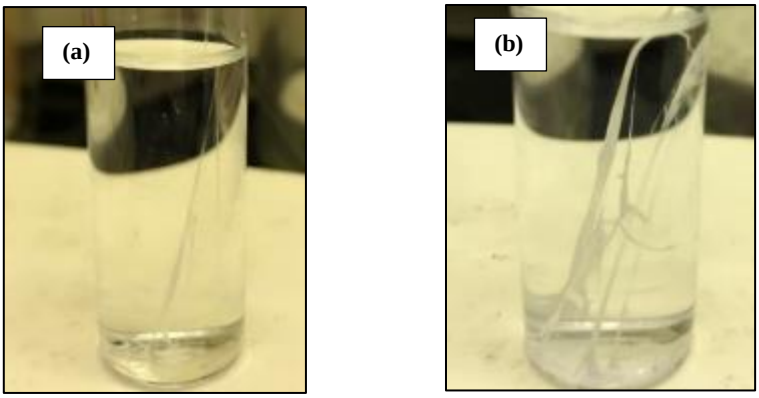

Figure 3.2. P4HB polymer solutions coagulated in (a) methanol (b) reagent alcohol

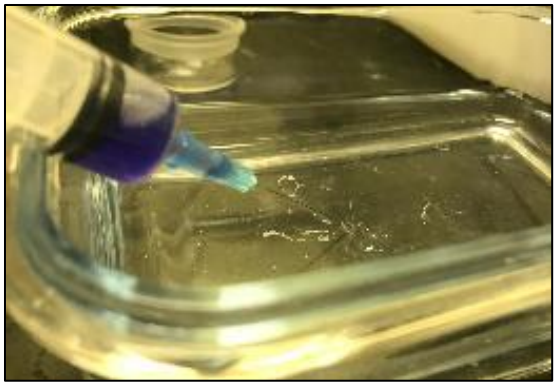

Figure 3.3. P4HB polymer solution coagulation trials using a syringe and needle

3.3.3. P4HB Fiber Spinning

Based on the suitable process conditions identified in the previous steps, P4HB fibers were spun with different spin dope concentrations, coagulation bath temperatures and spin draw ratios. P4HB polymer solutions of 10% and 15% (w/v) were prepared at room temperature using chloroform as the solvent with constant stirring at 300 rpm. After complete dissolution of the polymer, 10% (v/v) acetone was added to the polymer solution with constant stirring.

The 10% spin dopes were coagulated at two different coagulation bath temperatures: room temperature and 10 ºC, with a spin draw ratio of 12. In addition, 15% spin dopes were coagulated

at room temperature, but with two different spin draw ratios: 12 and 18. The coagulation bath contained reagent alcohol which was maintained at the preset temperature ±2 ºC. Other processing parameters, such as extrusion speed, needle gauge size, solvent system, coagulant and winding distance, were kept constant for all the spinning experiments.

Figure 3.4. (a) Wet spinning of P4HB monofilaments, (b) Stainless steel syringe-needle extrusion system, (c) Winding of as-spun P4HB monofilaments

A 50 ml stainless-steel syringe attached to a 25-gauge stainless steel needle (Sigma-Aldrich) was used to extrude the spin dope, as shown in Figures 3.4 (a) and (b). The linear displacement speed of the syringe was set at 0.15 mm/min for all spun samples. This corresponded to an approximate volumetric feed rate of the polymer solution in the syringe to be calculated at 119 mm^3/min, and the approximate linear flow rate through the needle was 2.2 m/min. The take-up speed on the winder was adjusted to 27 m/min and 40 m/min so as to obtain spin draw ratios of 12 and 18 respectively. Four sets of fibers were collected on multiple spools (Figure 3.4 (c)) and were stored in a sealed vacuum environment following removal of any residual solvent and/or coagulant. Table 3.3 summarizes the types of monofilaments spun and their various process conditions.

Table 3.3. Types of P4HB monofilaments spun with different process conditions

Sample Name	Spin Dope Concentration	Coagulation Temperature (T)	Spin draw ratio (R)
10T1	10%	10 ºC	12
10T2	10%	Room Temperature	12
15R1	15%	Room Temperature	12
15R2	15%	Room Temperature	18

3.4. CHARACTERIZATION METHODS FOR P4HB FIBERS

The spun monofilaments were subjected to multiple tests for measuring their diameter, linear density, crystallinity and birefringence. They were also tested for their mechanical properties, such as tenacity, elongation at break and tensile modulus, and their thermal properties, such as melting temperature and enthalpy or heat of fusion.

3.4.1. Fiber Diameter

A calibrated JSM Model 6010LA analytical scanning electron microscope (SEM) was used to view fiber samples from all four sets of monofilaments and to measure their diameters. The samples were mounted on carbon tape and were sputter coated with 60% gold / 40% palladium for 20 seconds (Figure 3.5). A magnification of 1700x was used to capture multiple images of each set of monofilaments. Image J software was used subsequently to measure the diameters of each set of monofilaments against a calibrated image. Twenty readings were taken for each set of monofilaments from different sections and multiple images.

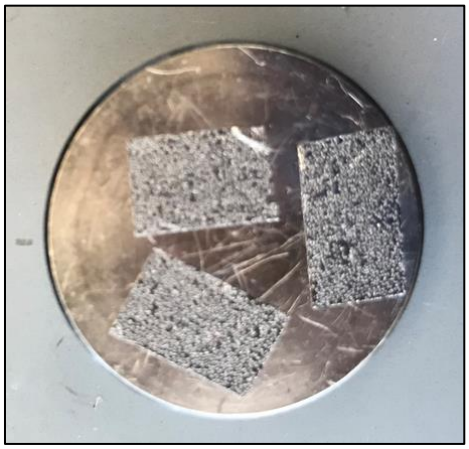

Figure 3.5. Sputter coated monofilament specimens mounted on a sample holder

3.4.2. Fiber Linear Density

All four types of monofilaments were tested on the Textechno Vibromat ME (Figure 3.6) using the ASTM D-1577 standard test method for measuring linear density with a vibroscope. A 55 mg clip was used with a pre-tension of 1 denier and fifteen readings were taken for each set of monofilaments.

Figure 3.6. P4HB monofilament specimen attached to the Vibromat instrument

3.4.3. Fiber Crystallinity

A Rigaku SmartLab x-ray diffractometer was used at 40kV and 44mA for measuring the degree of crystallinity of the P4HB fibers. Test specimens were prepared for each sample by fixing fibers parallel to each other over a 1-inch aluminum frame. The specimen was placed in the instrument between the x-ray tube and the detector, as shown in Figure 3.7. The 2Ɵ range was set to measure from 10 to 50 degrees, with a step rate of 3 seconds per 0.05 degrees.

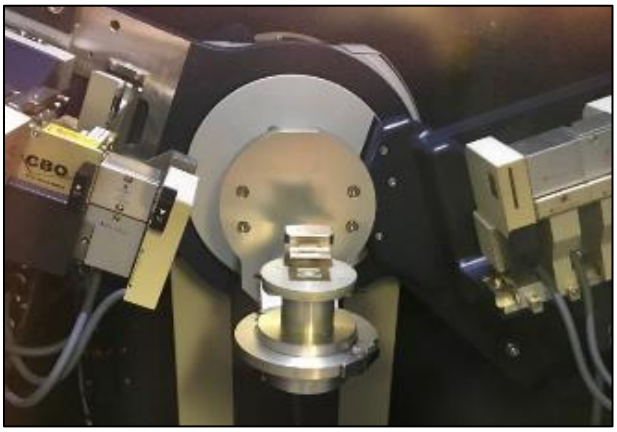

Figure. 3.7. Fiber specimen in the X-ray diffractometer

A peak fitting software called PDXL was used to analyze the data and determine the degree of crystallinity by calculating the area under the crystalline and amorphous peaks.

$$\% \text{ Crystallinity} = \frac{Ac}{Ac+Aa} \times 100 \qquad \text{Equation (i)}$$

Where, *Ac* = Total area under all crystalline peaks and *Aa* = Area of the amorphous region. In addition to the degree of crystallinity, the positioning and sharpness of crystalline peaks were also compared visually for the different fibers. Typically for polymers, broader peaks correspond to smaller crystallites, while narrower and sharper peaks denote bigger crystallites [143].

3.4.4. Mechanical Testing

An MTS Q-Test machine was used for the mechanical testing of the four monofilaments. ASTM D3822 standard test method with a 2N load cell was followed. The monofilaments were mounted across test card windows with a 1-inch gauge length (Figure 3.8) and extended at a constant rate of 15 mm/min until failure. Twenty-five readings were taken for each set of monofilaments, and the results were analyzed and compared for fiber tenacity, tensile modulus and elongation at break.

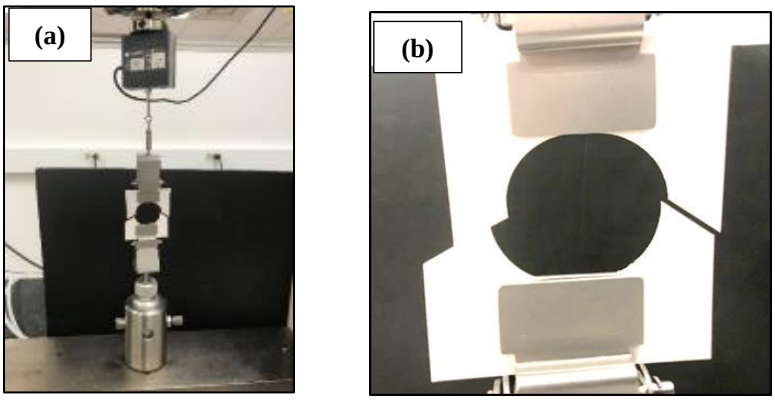

Figure 3.8. (a) Monofilament test specimen mounted across a card and clamped between the jaws, (b) Close-up view of the specimen ready to test

3.4.5. Thermal Testing

A Perkin Elmer Diamond differential scanning calorimetry (DSC) instrument was used to perform thermal analysis on all four P4HB monofilaments. Individual specimens were prepared by weighing 3 - 5 mg of the fiber in a crimped aluminum pan. The specimens were subjected to a heating cycle from room temperature to 100 ºC and then cooled down to about -40 ºC. The temperature was raised and cooled at the rate of 10 °C/min. The melting point and enthalpy or heat of fusion were calculated for each sample during the heating cycle, and the crystallization peak and crystallization enthalpy were measured during the cooling cycle.

3.4.6. Fiber Orientation

To assess the degree of orientation in the P4HB monofilaments, a birefringence test was conducted using a polarizing optical microscope at 400x magnification and a six-order quartz wedge (Figure 3.9 (a)). The birefringence values for the monofilaments were determined using the Michel Levy birefringence scale (Figure 3.9 (b)) [144]. Ten specimens of each monofilament were observed under the microscope.

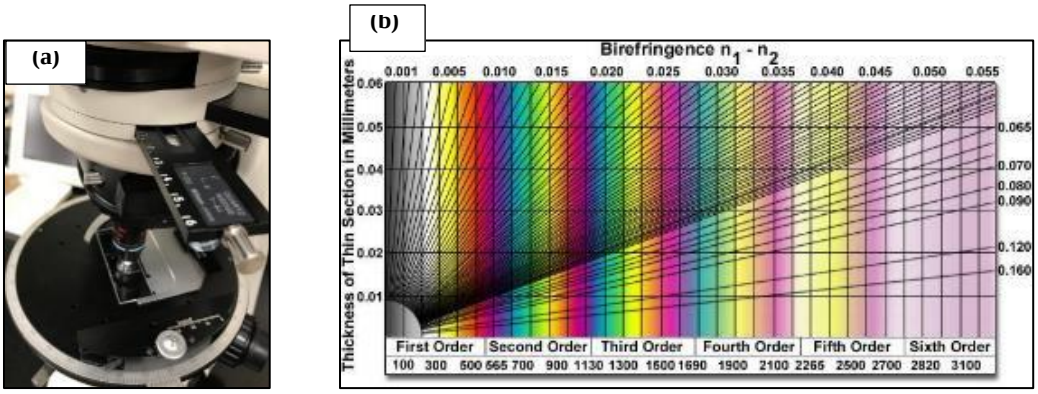

Figure 3.9. (a) Polarizing microscope with a six-order quartz wedge, and (b) Michel Levy birefringence scale

3.4.7. Statistical Analysis

The data obtained from all these test methods was subjected to statistical analysis to assess the effect of the polymer concentration, coagulation temperature and spin draw ratio on the properties and structure of the wet spun monofilaments. F-test, t-test and ANOVA statistical methods were used to compare fiber samples from 10T2 and 15R1 and identify any significant effect of polymer concentration. The effect of coagulation temperature was determined by comparing the results from fiber samples 10T1 and 10T2, while the data from fiber samples 15R1 and 15R2 were used to determine the effect of the spin draw ratio. A p-value less than 0.05 was assumed to identify a significant difference between the data sets.

3.5. RESULTS AND DISCUSSION

3.5.1. Solvent Analysis

Methylene dichloride and chloroform were narrowed down as the two most suitable solvents for P4HB due to their higher rate of dissolution as well as their ability to fully dissolve P4HB and form a clear polymer solution at room temperature. It was also found that 15% (w/v) was the maximum dissolution concentration for P4HB in either methylene dichloride or chloroform. Polymer concentrations higher than 15% did not produce a clear homogeneous solution. Tetrahydrofuran had a lower rate of dissolution and was not able to fully dissolve the polymer at concentrations higher than 10%. Ethyl lactate was unable to dissolve the P4HB polymer. Table 3.4 summarizes the results of the polymer dissolution experiments.

Table 3.4. Comparison between solvents for polymer dissolution

Solvent	Time for dissolution of 10% w/v solution	Time for dissolution of 15% w/v solution
Methylene dichloride	8 min	15 min
Tetrahydrofuran	26 min	Partially Soluble
Ethyl lactate	-	-
Chloroform	14 min	20 min

3.5.2. Coagulation Study

The qualitative results of the drop tests performed to study the coagulation of the P4HB polymer solutions with various solvent and coagulant systems are summarized in Table 3.5. A coagulated polymer sample which had good extensibility and didn't disintegrate when pulled with tweezers was considered to have good spinnability and drawability. Also, for wet spinning, a faster rate of coagulation was preferred because the extruded polymer needs to rapidly form a "skin" followed by subsequent coagulation of the core to generate the oriented fibrous structure for continuous spinning [83].

Table 3.5. Drop test qualitative results for polymer coagulation

Coagulation System and Temperature		Solvent System			
		Methylene dichloride	Methylene dichloride + Acetone	Chloroform	Chloroform + Acetone
Methanol	**RT**	Brittle, Slow	Stretchable, Slow	Brittle, Slow	Stretchable, Fast
	10º C	Brittle, Slow	Stretchable, Slow	Brittle, Slow	Stretchable, Fast
	-10º C	Stretchable, Slow	Stretchable, Fast	Stretchable, Slow	Stretchable, Fast
Ethanol	**RT**	Brittle, Slow	Stretchable, Slow	Brittle, Slow	Stretchable, Fast
	10º C	Brittle, Slow	Stretchable, Slow	Brittle, Slow	Stretchable, Fast
	-10º C	Stretchable, Slow	Stretchable, Fast	Stretchable, Slow	Stretchable, Fast
Propanol	**RT**	Brittle, Slow	Stretchable, Slow	Brittle, Slow	Stretchable, Fast
	10º C	Brittle, Slow	Stretchable, Slow	Brittle, Slow	Stretchable, Fast
	-10º C	Stretchable, Slow	Stretchable, Fast	Stretchable, Slow	Stretchable, Fast
Reagent alcohol	**RT**	Brittle, Slow	Stretchable, Slow	Brittle, Slow	Stretchable, Fast
	10º C	Brittle, Slow	Stretchable, Slow	Brittle, Slow	Stretchable, Fast
	-10º C	Stretchable, Slow	Stretchable, Fast	Stretchable, Slow	Stretchable, Fast
Acetone	**RT**	Brittle, Slow	Brittle, Slow	Brittle, Slow	Brittle, Slow
	10º C	Brittle, Slow	Brittle, Slow	Brittle, Slow	Brittle, Slow
	-10º C	Brittle, Slow	Brittle, Slow	Brittle, Slow	Brittle, Slow
Hexane	**RT**	Brittle, Slow	Brittle, Slow	Brittle, Slow	Brittle, Slow
	10º C	Brittle, Slow	Brittle, Slow	Brittle, Slow	Brittle, Slow
	-10º C	Brittle, Slow	Brittle, Slow	Brittle, Slow	Brittle, Slow

RT = Room temperature

Brittle – Coagulated polymer disintegrated when compressed with tweezers
Stretchable – Coagulated polymer structure remained intact upon pulling with tweezers
Slow – Polymer did not coagulate immediately after extrusion into coagulant
Fast – Polymer coagulated immediately upon extrusion into coagulant

Most solvent / coagulant combinations caused the polymer to coagulate slowly and / or to generate a brittle coagulated polymer structure, making them unsuitable for continuous fiber extrusion and wet spinning. However, it was found that the polymer solution prepared with the addition of acetone to chloroform coagulated in an alcohol-based bath forming a stretchable polymer structure at all three temperatures. This system worked well due to the miscibility of chloroform with alcohol. The addition of acetone to the spin dope appeared to increase the rate of coagulation for the polymer when extruded in the coagulation bath as it is a poor solvent for P4HB. This can be attributed to the effect of a non-solvent in the polymer solution, as it enhances the transition of the polymer from the solvent rich phase to the polymer rich phase during coagulation [145]. This can speed up the process of skin formation on the fiber surface and avoid the continuous filament breaking in the coagulation bath. A 25-gauge needle (0.26 mm internal diameter) was found to be the most suitable for P4HB extrusion. This is because the smaller size needle increases the surface area of the extruded filaments, thereby increasing the rate of skin formation and subsequent coagulation and the formation of extremely fine monofilaments (< 10 μm in diameter).

3.5.3. Fiber Diameter

The SEM images in Figure 3.10 and the mean diameter values from Figure 3.11 show that Sample 15R1 fibers had the largest diameter and Sample 10T1 fibers had the smallest diameter among the four types of monofilaments. The mean diameters and standard deviations for all four monofilaments are summarized in Table 3.6.

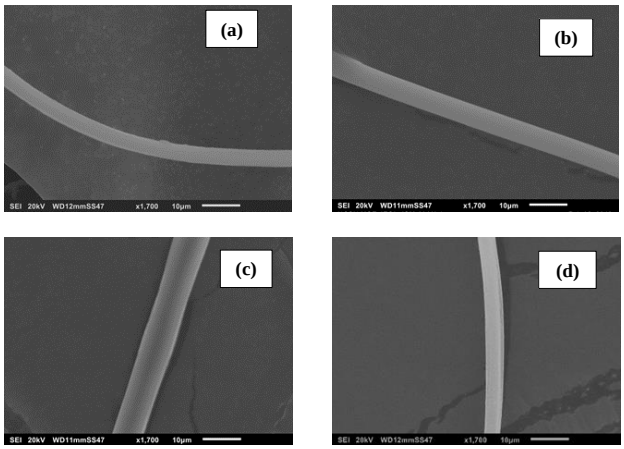

Figure 3.10. SEM images of (a) 10T1, (b) 10T2, (c) 15R1 and (d) 15R2 monofilaments

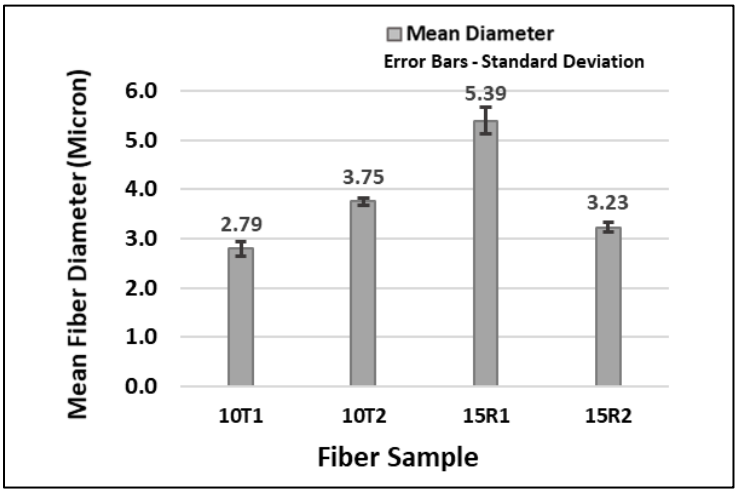

Figure 3.11. Mean fiber diameters for different spinning conditions

Table 3.6. Mean fiber diameters

Fiber Type	Mean Diameter (µm)	Standard Deviation (µm)
10T1	2.79	0.14
10T2	3.75	0.07
15R1	5.39	0.28
15R2	3.23	0.11

Statistical analysis of the data for all four fibers indicated that there were significant differences between the mean diameters of all the fibers spun under different processing conditions. The difference in diameter between the 10T2 and 15R1 samples ($p < 0.0001$) showed that the increase in spin dope polymer concentration from 10% to 15% led to more swelling of the extruded polymer as it leaves the needle. It was also found that the 10T2 fibers had a larger diameter than the 10T1 fibers coagulated at only 10º C ($p < 0.0001$), suggesting that a decrease in coagulation temperature reduced the amount of polymer swelling during extrusion. The comparison between the 15R1 sample and the 15R2 fibers supported the theory that an increase in draw ratio will decrease the diameter due to greater stretching of the fibers. It was also observed that even though the 15R2 fibers had a higher polymer concentration in the spin dope than 10T2 fibers, they still had a significantly lower diameter ($p < 0.0001$). This suggests that the spin draw ratio has a higher impact on the fiber diameter than the spin dope concentration.

3.5.4. Fiber Linear Density

As can be seen from Figure 3.12 and Table 3.7, the 15R1 fibers had the highest linear density compared to the other monofilaments. This can be attributed to them having the largest diameter and 15% polymer concentration in the spin dope. The linear density for 15R2 fibers was significantly lower than that for the 15R1 sample ($p < 0.0001$) due to the higher draw ratio. No significant difference was observed between the two sets of 10% monofilaments ($p = 0.12$), implying that the coagulation bath temperature did not have a significant effect on the linear density of the monofilaments.

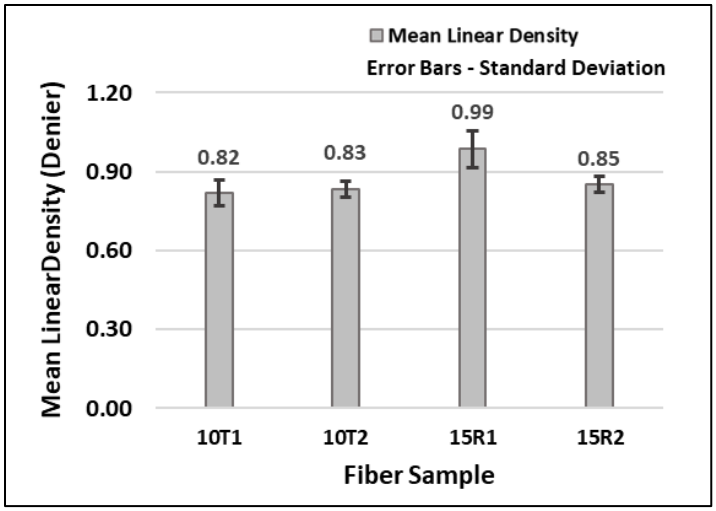

Figure 3.12. Fiber linear density for different spinning conditions

Table 3.7. Linear density of the fibers

Fiber Type	Mean Linear Density (Denier)	Standard Deviation (Denier)
10T1	0.820	0.053
10T2	0.831	0.037
15R1	0.985	0.075
15R2	0.853	0.034

A limitation of this test method was the use of 55 mg clips for weighing the fibers. While these were the lightest clips available, they appeared to be too heavy for the fine fibers being tested. Using lighter weight clips might have provided more accurate results. Also, due to the fineness of the fibers, some specimens might have been accidently stretched or distorted while mounting them onto the Vibromat for testing.

3.5.5. Fiber Crystallinity

Figure 3.13 depicts the x-ray diffractograms for all four different P4HB fibers spun with different spinning conditions. It can be seen that the 2Ɵ angle location of the peaks is similar for all four samples. However, the crystalline peaks for the 15R1 and 15R2 fibers were observed to be narrower than the peaks for the fibers spun with 10% spin dope concentration, implying a larger crystallite size [143]. The diffractogram for the 10T1 fibers also had a larger peak for the amorphous region compared to the other fibers which were coagulated at room temperature. It was also seen that the relative intensities of the two major peaks (relative peak intensity) was similar for all four fibers (approx. 47-52%).

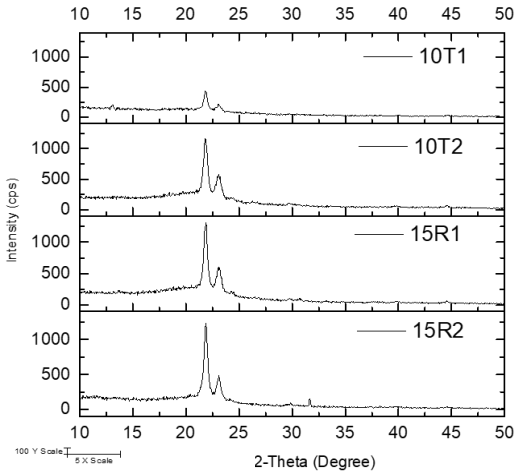

Figure 3.13. X-ray diffractograms for P4HB fibers with different spinning conditions

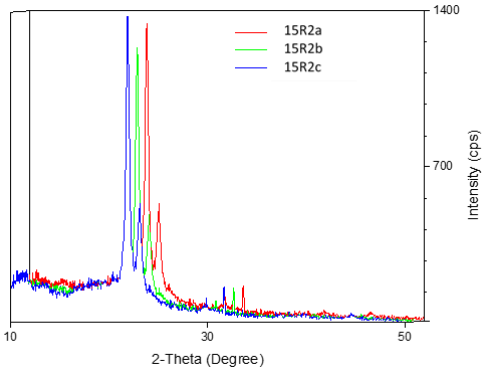

Figure 3.14. X-ray diffractograms for fiber Sample 15R2

Figure 3.14 is an overlay of the x-ray diffractograms for three specimens from the same 15R2 sample. This sample was measured in triplicate so as to determine the variability in crystallinity within any one fiber sample. It can be seen that the 2Θ angle location of the peaks is similar for all three specimens, except that there is some variation between relative peak heights. The mean crystallinity of the 15R2 fiber sample was calculated to be about 44.8% with a standard deviation of 2.8%. By measuring three replicate values for this one sample set, the level of uniformity for the degree of crystallinity appears to be satisfactory for all four spun fiber samples.

The experimentally measured degree of crystallinity for the fibers depicted in Figure 3.15 and Table 3.8, appears to be in agreement with the results obtained for the mechanical and thermal properties of the fibers. The fibers in Sample 15R2 had the highest degree of crystallinity due to their higher draw ratio of 18, compared to the other three fibers, which had a draw ratio of 12. Also, the 15R1 fibers had a higher crystallinity than the 10T1 and 10T2 samples due to the higher concentration of polymer in the spin dope, which increased the number of polymer chains present in the fiber. Lastly, the higher crystallinity of the 10T2 fibers showed that coagulation at room temperature is more favorable for polymer chain alignment.

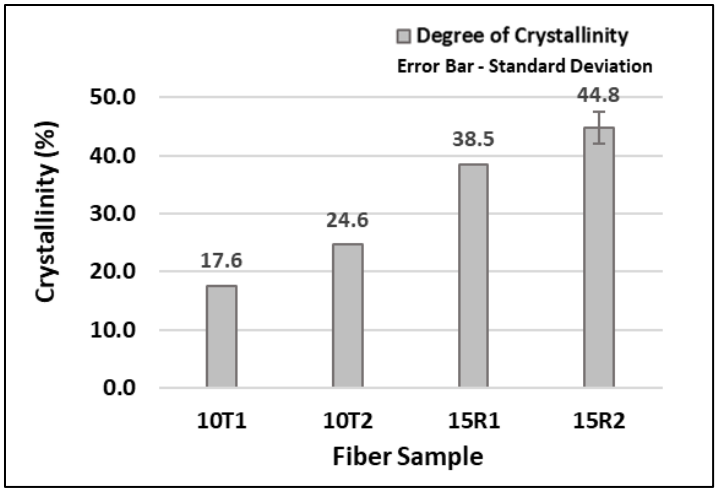

Figure 3.15. Fiber crystallinity for different spinning conditions

Table 3.8. Degree of crystallinity for P4HB fibers

Monofilament Type	Crystallinity (%)
10T1	17.6
10T2	24.6
15R1	38.5
15R2	44.8

3.5.6. Mechanical Testing

The results from mechanical testing were analyzed in terms of tenacity, elongation at break and tensile modulus for all four types of monofilaments. All three properties were compared statistically to determine if there were any significant differences between the four fiber samples. Table 3.9 summarizes the experimentally determined mean and standard deviation results for the mechanical properties of all four fiber types.

Table 3.9. Summary of mechanical test results

Fiber Type	Fiber Tenacity (gf/denier)		Elongation @ Break (%)		Fiber Modulus (gf/denier)	
	Mean	Standard Deviation	Mean	Standard Deviation	Mean	Standard Deviation
10T1	0.72	0.14	25.87	6.61	56.09	14.91
10T2	1.03	0.17	51.46	11.77	72.84	16.96
15R1	1.57	0.38	124.17	25.51	65.63	13.94
15R2	1.88	0.24	55.87	10.91	101.71	23.59

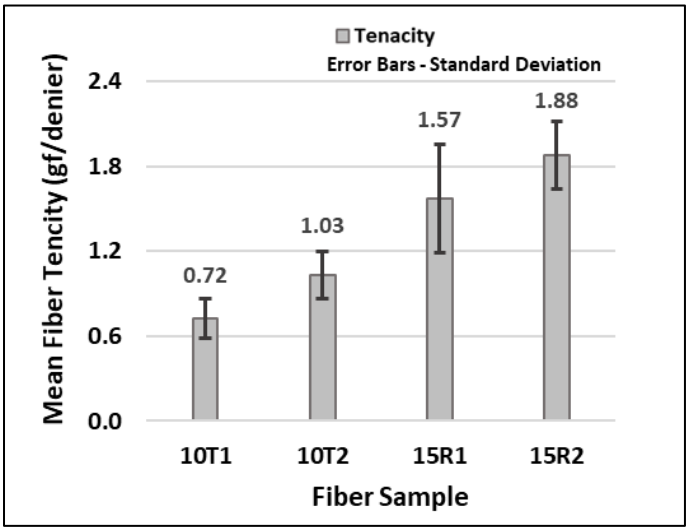

Figure 3.16. Mean fiber tenacity for different spinning conditions

It can be seen in Figure 3.16 that the 15R2 fibers had the highest tenacity among the four types of monofilaments. The difference in tenacity between 15R2 and 15R1 fibers was found to be significant ($p = 0.005$), which can be attributed to the higher draw ratio of the 15R2 fibers, which likely resulted in an increased polymer chain alignment and fiber crystallinity. Sample 15R1 also had a significantly higher tenacity than the fibers spun with a 10% spin dope concentration (p

< 0.0001), implying that the increase in polymer concentration had a direct effect on the strength of the monofilaments. The 10T2 fibers had a significantly higher tenacity than the 10T1 fibers (p = 0.038), suggesting that a lower coagulation temperature did not favor polymer chain alignment during the coagulation process.

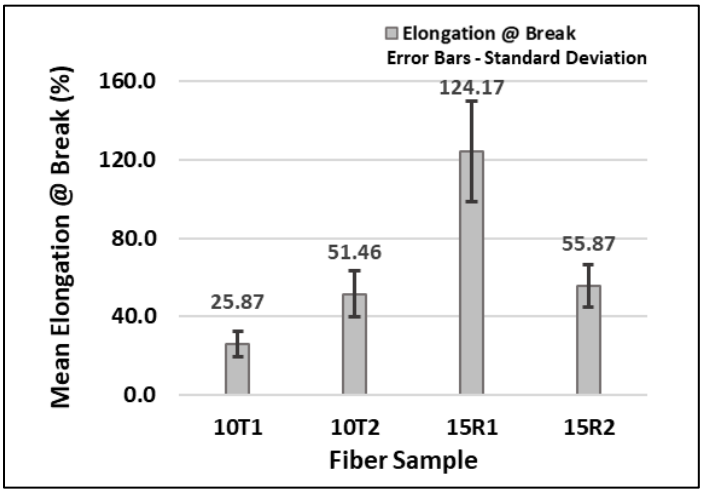

Figure 3.17. Fiber elongation at break for different spinning conditions

Based on the results for fiber elongation at break (Figure 3.17), it can be observed that the increase in draw ratio between the 15R2 and 15R1 fiber samples caused a reduction in the fiber elongation, due to an increase in the fiber crystallinity. The higher elongation of the 15R1 fibers can be attributed to the higher spin dope concentration which resulted in a fiber with more polymer chain entanglement than for the fibers spun with 10% polymer concentration. The significant difference in fiber elongation between Sample 10T1 and higher stretch Sample 10T2 was caused by the greater polymer swelling during coagulation at room temperature ($p < 0.0001$). No significant difference was observed between the elongation of the 10T2 and the 15R2 samples ($p = 0.13$).

Figure 3.18 shows the typical load-elongation profiles for the four different of P4HB fibers. It can be clearly seen that 15R2 has the steepest slope while 15R1 has the maximum elongation at break, supporting the findings from the quantitative analysis.

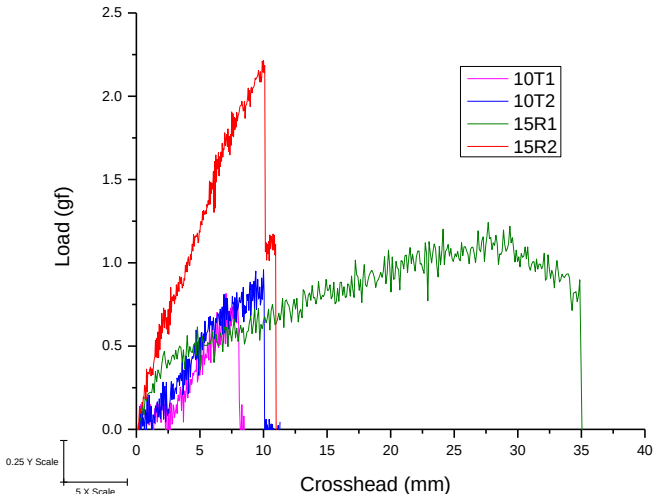

Figure 3.18. Typical load-elongation curves for the fibers

Differences in the fiber modulus caused by the variation in their spinning conditions can be clearly seen in Figures 3.19. The 15R2 fibers clearly had the highest modulus and steepest initial slope among all four types of spun fibers, suggesting that the higher draw ratio resulted in greater chain alignment for these fibers and an increase in fiber stiffness. The fiber modulus did not differ significantly between the 15R1 and 10T2 fiber samples ($p = 0.11$), implying that the spin dope concentration did not have a significant effect on the resulting fiber stiffness. However, a significant increase was observed in the fiber modulus between the 10T1 and 10T2 samples ($p = 0.0005$), which may have resulted from higher chain entanglement of the 10T2 fibers.

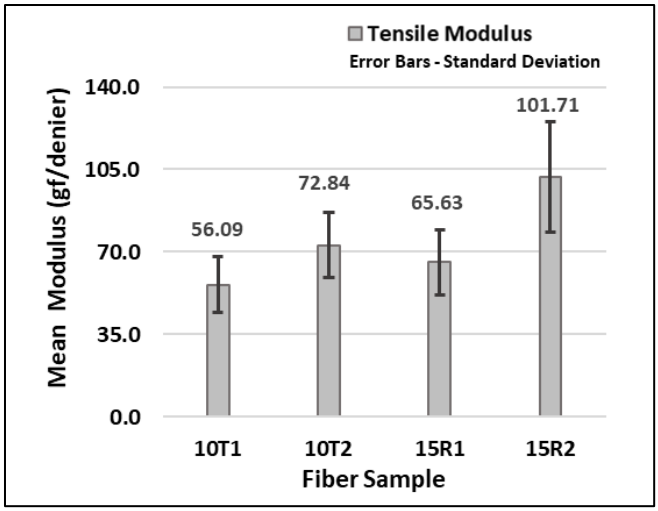

Figure 3.19. Mean fiber modulus for different spinning conditions

Certain technical limitations were faced during the measurement of these fiber mechanical properties which resulted in higher standard deviations than expected. A 2N swinging load cell was used on the MTS mechanical test instrument, which caused vibrations during testing, and resulted in a noisy stress/strain signal. It is believed that a smaller capacity load cell could have provided more accurate readings. Additionally, the fiber mounting process on the specimen cards contributed to the variability in the position of the fibers under test. Some handling error may have occurred during fiber mounting as some specimens may have been accidently stretched due to the fineness of the fibers.

3.5.7. Thermal Testing

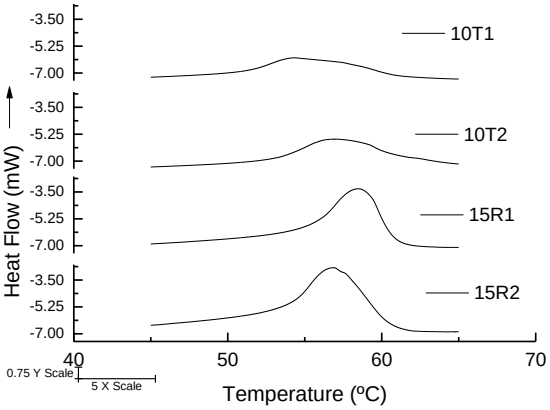

Figure 3.20. DSC heating curves for P4HB fibers

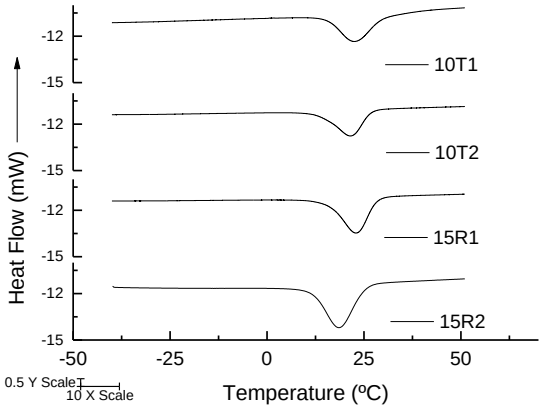

Figure 3.21. DSC cooling curves for P4HB fibers

Based on the DSC thermograms shown in Figures 3.20 and 3.21 and the test results summarized in Table 3.10, it is clear that the 15R2 monofilaments had the largest melting peak area, resulting in the highest melting enthalpy among the four types of P4HB monofilaments This could be attributed to the higher spin ratio which likely increased the polymer chain alignment in the fibers. The increase in spin dope concentration also had a significant effect on the melting enthalpy, suggesting that a higher polymer concentration resulted in an increase in the crystallinity

of the fibers. A higher melting enthalpy was also observed for the 10T2 fibers as compared to Sample 10T1, indicating an increase in chain alignment. These inferences also supported the findings of the x-ray diffraction and mechanical tests which showed that the increase in draw ratio, spin dope concentration and coagulation bath temperature directly affected the fiber tenacity as well as the fiber crystallinity.

Table 3.10. Summary of thermal test results

Sample	Melt Peak Temp. (°C)	Melt Enthalpy (J/g)	Melt Peak Area (mJ)	Crystallization Peak Temp. (°C)	Crystallization Enthalpy (J/g)	Crystallization Peak Area (mJ)
10T1	53.8	9.7	41.6	21.8	-20.3	-86.9
10T2	56.4	12.4	51.8	23.2	-26.6	-111.3
15R1	57.9	24.1	80.2	22.9	-32.1	-106.4
15R2	56.4	29.0	136.5	18.9	-32.1	-150.8

The trend observed in the crystallization enthalpy values during the cooling cycle was similar to the melting enthalpy results. Higher polymer concentration and coagulation temperature increased the crystallization enthalpy, implying a higher degree of crystallinity. However, there was no difference seen in the crystallization enthalpies for the 15R1 and 15R2 fibers, suggesting a lack of effect of the draw ratio on the degree of crystallinity in the polymer during the cooling cycle. This could be caused by the polymer chains in the crystalline regions getting more entangled during the melting phase of the heating cycle. On cooling, the polymer melt will reach the crystallization temperature and form a semi-crystalline structure, typically with a reduced degree of crystallinity compared to the original spun structure [146].

3.5.8. Fiber Orientation

The crossed polarized images in Figure 3.21 show a similar color pattern in the first order of the Michel Levy Birefringence Scale for all four fiber types. Due to the fiber fineness and low microscope magnification, only an approximate range of values for birefringence was obtained as shown in Table 3.11. For more precise results, a higher magnification is required. Nevertheless, as each fiber had a different diameter, they each had a different range of the birefringence values. Due to a lack of precision in the data, no statistical difference between the orientations of these four fibers could be determined.

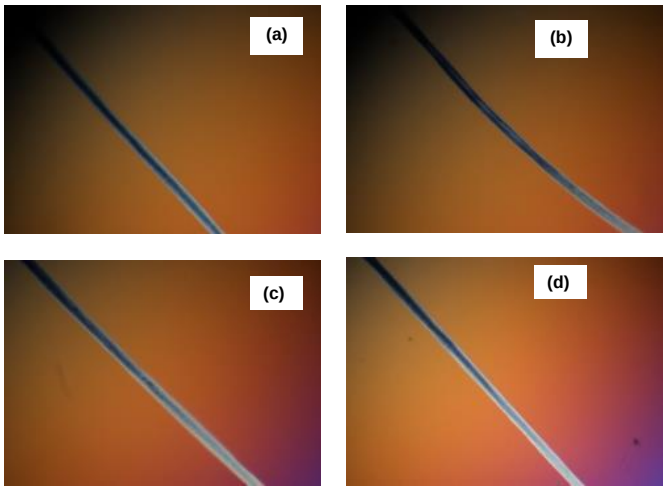

Figure 3.21. Polarized images of P4HB fibers (a) 10T1, (b) 10T2, (c) 15R1 and (d) 15R2

Table 3.11. Birefringence results for P4HB monofilaments

Monofilament Type	Birefringence Range
10T1	0.040 - 0.050
10T2	0.040 - 0.055
15R1	0.045 - 0.055
15R2	0.055 - 0.065

3.6. CONCLUSIONS

As mentioned earlier in the chapter, the primary focus of this study was to identify suitable process conditions for wet spinning P4HB fibers. The three objectives of the study were successfully accomplished in a series of steps in order to spin fibers suitable for drug delivery applications. First, chloroform and methylene dichloride were identified as suitable solvents for the P4HB polymer, with the addition of acetone to the polymer solution, as it aided in faster polymer coagulation following extrusion. An alcohol-based coagulation bath was determined to be suitable for spinning P4HB fibers due to its miscibility with the solvent system. The use of a 25-gauge needle as a spinneret provided a narrow diameter and larger surface area for the solvent / non-solvent exchange. These process conditions allowed for continuous extrusion of the P4HB fibers. After the suitable dissolution and coagulation conditions were identified, the effect of parameters such as the polymer concentration in the spin dope, the coagulation bath temperature and the spin draw ratio of the fibers were studied to assess their influence on the fiber properties and structure. These steps allowed further identification of other suitable wet spinning process parameters which can produce mechanically superior fibers. It was found that a polymer concentration of 15% in the spin dope and a coagulation bath at room temperature produced stronger fibers with a higher degree of chain alignment and crystallinity. The higher draw ratio also increased the fiber modulus and crystallinity while reducing the fiber elongation and diameter.

It was concluded from the results of this study that a polymer concentration of 15% and coagulation bath at room temperature should be used to spin fibers loaded with a drug at different concentrations to determine the drug loading capabilities of the fibers. Furthermore, in the future, the drug release profiles of these fibers will be studied to understand the effect of spinning conditions on drug retention and release.

CHAPTER 4 – THE EFFECT OF DRUG LOADING ON THE STRUCTURE AND PROPERTIES OF WET SPUN P4HB FIBERS

4.1. INTRODUCTION

Poly-4-hydroxybutyrate (P4HB) is an aliphatic polyester being developed as an absorbable material for implantable medical applications. P4HB is strong yet flexible and can provide novel properties for new biomedical opportunities. The chemical structure of P4HB is similar to other aliphatic absorbable polyesters, such as poly-lactic acid (PLA) and polycaprolactone (PCL). Owing to the biocompatibility and mechanical properties of P4HB, it can be used in a variety of medical applications, such as wound healing, orthopedic devices, drug delivery systems, and tissue engineering applications. Examples of some of the P4HB based medical devices being studied include sutures, hernia meshes, vascular grafts, cardiovascular patches, heart valves, stents, shunts, and cochlear implants [50].

A recent field of interest for P4HB is controlled drug delivery in medical devices. The absorbable polymer can be used as a drug carrier in the form of films, fibers and particles for targeted drug delivery applications. Several studies are ongoing on the potential applications of P4HB in drug delivery such as, aqueous shunts for glaucoma and cochlear implants coated with drugs for fibrosis prevention [3], microspheres for progesterone release and anti-tumor drugs for cancer therapy [5], and drug-coated stents for coronary applications [6].

Over the past few years, fibers have become an attractive carrier for drug delivery applications. They have an ideal morphology due to their cylindrical shape and high surface area to volume ratio, which means that they can release drugs over a large surface area. Fiber based delivery systems include surgical sutures, wound dressings, and tissue engineering scaffolds that

can be loaded with therapeutic drugs and other bioactive compounds for various treatments [7]. There are several methods to fabricate fibers as drug delivery systems. 1) The spun fibers can be coated with drugs by surface treatment or 2) the drugs can be added to the fibers during the spinning stage. Some common methods are wet spinning and electrospinning, where the drug is dissolved along with the polymer in a solvent and the solution is extruded to form drug-loaded fibers. Using these methods, fibers with fine diameters can be spun with a uniform distribution of the drug throughout the fiber [8].

A recent study on wet spun PLA micro-fibers containing dexamethasone (DXM), an anti-inflammatory agent, tested the effect of drug loading concentration on fiber properties as well the drug release mechanism. It was seen that the increase in drug concentration in the polymer solution resulted in the decrease of the amount drug actually encapsulated in the spun fibers. It was also found that beyond a certain limit, the increase in drug concentration in the polymer solution significantly decreased the drug encapsulation in the fibers [119].

The addition of drugs can affect the fiber structure and properties in various ways depending on the type of drug used, solvent and non-solvent interactions, the affinity of the drug for the polymer and the solvent. In some cases, during wet spinning, the addition of the drug can influence the mechanical strength and/or fiber crystallinity by solvent induced crystallization caused by the solvent-drug interactions. The mechanical properties can also be affected by secondary polymer-drug interactions, such as hydrogen bonding between the polymer lattice and drug particles [119]. On the other hand, the addition of drug can form defects in the fiber structure due to drug diffusion from the polymer during the coagulation stage. During wet spinning, when a homogeneous polymer solution is extruded from the spinneret, solvent non-solvent exchange

takes place, and the solvent diffuses out of the polymer solution and a skin-like layer is formed due to the fast polymer interaction with the non-solvent (Figure 4.1(a)).

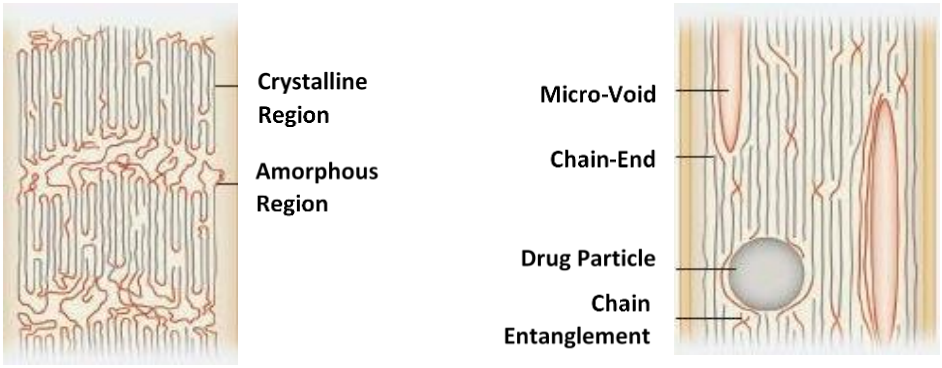

Figure 4.1. (a) Homogeneous polymer solution, and (b) drug-loaded fiber with micro-voids

However, with the drug dissolved/dispersed in the polymer solution, during extrusion the drug can leach out from the coagulating polymer with the solvent and can create micro-voids in the wet-spin filaments (Figure 4.1(b)) [147]. These micro-voids can increase in the penetration of the non-solvent into the polymer structure and increase the swelling of the fiber during coagulation. The presence of these micro-voids can act as stress-points between the polymer chains and reduce the mechanical strength and elongation of the fibers. The drawing of the fibers during or after the spinning stage can limit the effect of the micro-voids on the mechanical properties by inducing orientation and crystallinity in the polymer chains [148].

Figure 4.2. Antibacterial Coated Vicryl Suture by Ethicon®

Vicryl® Plus suture made by Ethicon is an example of a fiber-based drug delivery system made with an absorbable polymer: polyglactin, and coated with an antibacterial agent (Figure 4.2) [124]. Use of antibacterial agents in sutures and wound closure products can prevent post-surgical infections at the wound site, thus improving the healing process. Studies have been undertaken for electrospinning fibrous mats from PLA containing antibiotic drugs like ciprofloxacin, levofloxacin, moxifloxacin. Microfibers were produced with the drugs added to the spinning solution and the drug-loaded fibers were tested for their antibacterial capabilities. It was found that the presence of these fluroquinolone drugs inhibited the growth of bacteria and reduced the cell adhesion to the fibers [131].

Levofloxacin is a quinolone/fluroquinolone antibiotic drug with a broad spectrum of activity against Gram-positive and Gram-negative bacteria, and atypical respiratory pathogens. It is found as a yellowish white to bright yellow crystalline powder and has a molecular weight of 361.37 Da. It is freely soluble in glacial acetic acid and chloroform but has poor solubility in water and alcohol. The typical dosage of this drug is between 500-1500 mg per day for humans [149].

There are two main objectives for the completion of this study – (i) Evaluate the effect of drug concentration on structure and properties of P4HB fibers, and (ii) Study the effect of spin draw ratio on drug loaded P4HB fibers. Several P4HB fibers will be wet spun with different concentrations of drug in the spin dope and spin draw ratios using the method developed in the

previous chapter. Due to the efficacy of the drug and its high solubility in chloroform (10mg/ml), the solvent selected for wet spinning of P4HB, levofloxacin is chosen as a suitable drug for this study. The characterization results of the drug-loaded fibers will be compared to homogeneous control fibers containing no drug, spun with the same process parameters to determine the effect of drug on the fiber structure and properties. The drug-loading efficiency is also determined by measuring the amount of drug encapsulated in the spun fiber relative to the amount of drug added to the spin dope [119].

4.2. MATERIALS

Like the previous study, P4HB was obtained in the form of Monomax® absorbable surgical sutures, manufactured by B.Braun Surgical S.A. (Barcelona, Spain). These 100% P4HB sutures had a molecular weight of approximately 300 kDa [141]. Chloroform was used as a solvent to dissolve the polymer as well as the drug. Levofloxacin, the drug chosen for this study, was obtained from Sigma Aldrich as a 98% HPLC grade faint yellow powder. Acetone was used as a non-solvent additive to the spin dope while reagent alcohol was used as a coagulant for wet spinning the fibers.

4.3. EXPERIMENTAL METHODS

As determined from the previous study, a spin dope with 15% (wt./v) polymer concentration dissolved in chloroform with 10% acetone (v/v) added to the solution was found suitable for wet spinning P4HB fibers in a reagent alcohol coagulation bath at room temperature. These process parameters were used similarly for also producing drug loaded fibers with different

concentrations of drug added to the spin dope. Levofloxacin was dissolved in chloroform at three concentrations relative to the polymer - 2%, 5% and 10% (wt./wt.). The drug solutions were added to the polymer solutions to form heterogeneous spin dopes which were coagulated at two different spin draw ratios: 12 and 18. Other process parameters such as extrusion speed, needle gauge size, coagulation bath and winding distance were kept constant for all the spinning experiments. A 50 ml stainless-steel syringe attached to a 25-gauge stainless steel needle (both obtained from Sigma-Aldrich) was used for extrusion of the spin dope. The speed at which the syringe was pushed in the spinning machine was set at 0.15 mm/min for all the fibers. The volumetric feed rate of the polymer solution in the syringe was calculated to be 119 mm^3/min (approx.) and the linear flow rate through the needle was found to be 2.2 m/min (approx.). The take-up speed on the winder was adjusted to 27 m/min and 40 m/min to obtain spin draw ratios of 12 and 18 respectively. Six sets of fibers were collected onto multiple spools and were kept in a sealed environment for removal of any residual solvent and/or coagulant. Table 4.1 summarizes the types of drug-loaded monofilaments spun and their variable process conditions.

Table 4.1. Types of drug loaded P4HB fibers spun with different conditions

Monofilament Type	Drug Concentration (wt.% polymer)	Spin Draw Ratio (D)
2D1	2	12
2D2	2	18
5D1	5	12
5D2	5	18
10D1	10	12
10D2	10	18

4.4. CHARACTERIZATION METHODS FOR P4HB FIBERS

The drug-loaded monofilaments were characterized for their drug-loading efficiency, diameter, linear density and crystallinity. They were also tested for their mechanical properties such as tenacity, elongation at break and tensile modulus, and thermal properties such as melting temperature and enthalpy. These results were compared to the homopolymer control fibers spun with the same processing conditions as described in the previous chapter, 15R1 and 15R2.

4.4.1. Drug-Loading Efficiency

UV Spectroscopy was used to quantify the amount of drug loaded in the P4HB fibers. Multiple standard solutions with different drug concentrations were prepared with chloroform and reagent alcohol in volumetric flasks. It was determined that the polymer did not affect the absorbance for the drug in the chloroform and reagent alcohol solutions. Calibration equations in two different concentration ranges were obtained for both chloroform and reagent alcohol. It was found that the calibration equations deviated from the Beer-Lambert Law, most likely due to instrument failure to follow certain conditions of the Beer-Lambert Law. Fundamentally, the Beer-Lambert Law requires that "*every photon of light striking the detector must have an equal chance of absorption*". However, a spectrometer has a finite spectral resolution, implying that the intensity reading at a specific wavelength is really an average over a small spectral interval [150].

Five fiber samples from different sections of the spools were dissolved in chloroform in a standard volumetric flask. The drug concentration in these solutions were measured to quantify the wt.% of drug present in the fibers. The drug-loading efficiency is determined by measuring the amount of drug encapsulated in the fiber relative to the amount of drug added to the spin dope [119].

$$Drug\ Loading\ Efficiency\ (\%) = \frac{Amount\ of\ Drug\ in\ Fiber\ (wt\%)}{Amount\ of\ Drug\ in\ Spin\ Dope\ (wt\%)}\ x\ 100$$

Apart from the drug loading efficiency, the amount of drug present in the coagulation bath after the spinning process was also measured by testing five samples of the coagulant. This was done to determine the amount of drug which diffused out of the polymer solution during extrusion.

4.4.2. Fiber Diameter

A calibrated JSM Model 6010LA analytical scanning electron microscope (SEM) was used to view fiber samples from all six sets of drug-loaded monofilaments and to measure their diameters. The samples were mounted on conductive carbon tape and were sputter coated with 60% gold / 40% palladium for 20 seconds. A magnification of 1700x was used to capture multiple images of each set of monofilaments. The Image J software was used subsequently to measure the diameters of each set of monofilaments. Twenty readings were taken for each set of monofilaments from different sections and multiple images.

4.4.3. Fiber Linear Density

All six types of drug-loaded monofilaments were tested on the Textechno Vibromat ME using the ASTM D-1577 test method for measuring linear density with a Vibroscope. A 55 mg clip was used with a pre-tension of 1 denier and fifteen readings were taken for each set of monofilaments.

4.4.4. Fiber Crystallinity

A Rigaku SmartLab x-ray diffractometer was used at 40kV and 44mA for measuring the degree of crystallinity of the P4HB fibers. Test samples were prepared by fixing fibers parallel to each other over a 1-inch aluminum frame. The sample was placed in the instrument between the x-ray tube and the detector. The 2Θ range was set to measure from 10 to 50 degrees, with a step rate of 3 seconds per 0.05 degrees. PDXL, a peak fitting software was used to analyze the data and determine the degree of crystallinity by calculating the area under the crystalline and amorphous peaks.

$$\% \text{ Crystallinity} = \frac{Ac}{Ac+Aa} \times 100$$

Where, *Ac* = Total area under all crystalline peaks and *Aa* = Area under amorphous region.

Besides the degree of crystallinity, the positioning and sharpness of the crystalline peaks were also compared visually for the different fibers. Typically for polymers, broader peaks correspond to smaller crystallites while narrower and sharper peaks denote bigger crystallites [143].

4.4.5. Mechanical Testing

An MTS Model Q-Test machine was used for mechanical testing of all six monofilaments. ASTM D3822 standard test method with a load cell of 2N was followed where the monofilaments were mounted onto the test cards with a 1-inch gauge length and extended at a constant rate of 15 mm/min until broken. Twenty-five readings were taken for each set of monofilaments and the results were analyzed and compared for fiber tenacity, modulus and elongation at break.

4.4.6. Thermal Testing

A Perkin Elmer Model Diamond differential scanning calorimetry (DSC) instrument was used to perform thermal analysis on all six P4HB monofilaments. Individual specimens were prepared by weighing 3 - 5 mg of the fiber in a crimped aluminum pan. The specimens were subjected to a heating cycle from room temperature to 100 ºC and then cooled down to about -40 ºC. The temperature was raised and cooled at the rate of 10 °C/min. The melting point and enthalpy were calculated for each sample during the heating cycle and the crystallization peak and crystallization enthalpy was measured during the cooling cycle.

4.4.7. Statistical Analysis

The data obtained from all these test methods were analyzed statistically to assess the effect of the drug concentration and spin draw ratio on the drug-loading of these monofilaments. The results were also compared to those of the homogeneous control fibers without any drug to determine the effect of drug loading on the structure and properties of the fibers. A p-value less than 0.05 was considered as a significant difference between the data sets.

4.5. RESULTS AND DISCUSSION

4.5.1. Drug Loading Efficiency

The calibration equations for the levofloxacin in chloroform and reagent alcohol are shown in Figure 4.3 and Table 4.2. Chloroform equations were in the concentration ranges of 0.0004 – 0.004 mg/ml and 0.004 – 0.009 mg/ml. Reagent alcohol had equations in the concentration ranges of 0.0002 – 0.0009 mg/ml and 0.0012 – 0.009 mg/ml. All four equations had $R^2 > 0.999$.

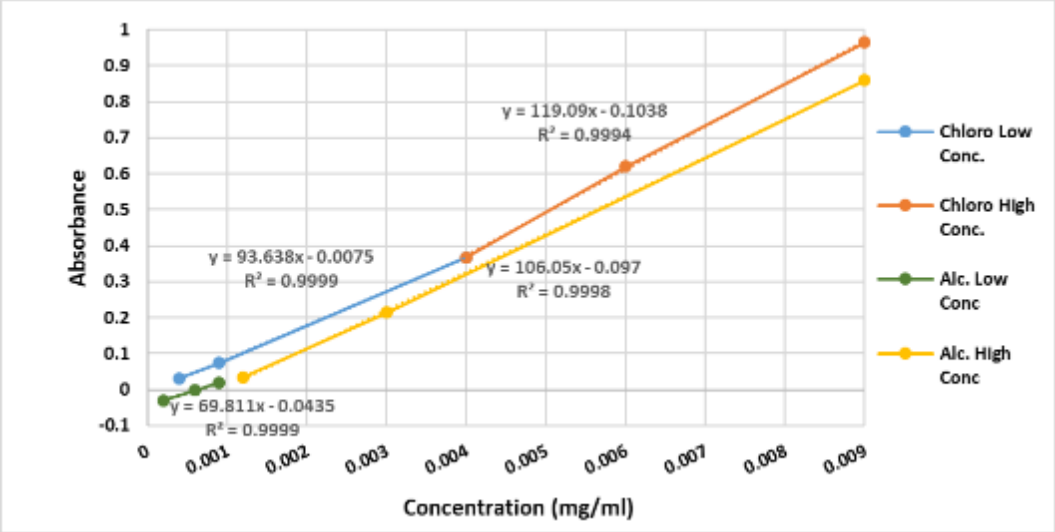

Figure 4.3. Calibration curves for levofloxacin in chloroform and reagent alcohol

Table 4.2. Calibration equations for levofloxacin in chloroform and reagent alcohol

Solution	Concentration Range	Calibration Equation	R^2
Chloroform	0.0004 – 0.0040 mg/ml	Abs = 93.638*Conc -0.0075	0.9999
Chloroform	0.0040 – 0.0090 mg/ml	Abs = 119.09*Conc -0.1038	0.9994
Reagent Alcohol	0.0002 – 0.0009 mg/ml	Abs = 69.811*Conc -0.097	0.9999
Reagent Alcohol	0.0012 – 0.0090 mg/ml	Abs = 106.05*Conc -0.097	0.9998

Figure 4.4. depicts the drug distribution in the spun fibers and the alcohol coagulation bath for different drug concentrations in the spin dope and spin draw ratios. It was observed that the fibers spun with 2 wt.% drug concentration had a drug-loading efficiency of over 90% in the fibers. The fibers spun with 5 wt.% drug concentration had drug loading efficiencies between 75-85% while fibers spun from 10 wt.% drug concentration had less than 40% loading efficiency. Thus, an

increase in the spin dope drug concentration reduced the overall drug loading efficiency. Based on the drug distribution, over 97% of the drug was accounted for either in the fiber or in the coagulation bath, for each of the spinning processes. The drug which was not measured could have been lost during the process or some calculation error during the measurements.

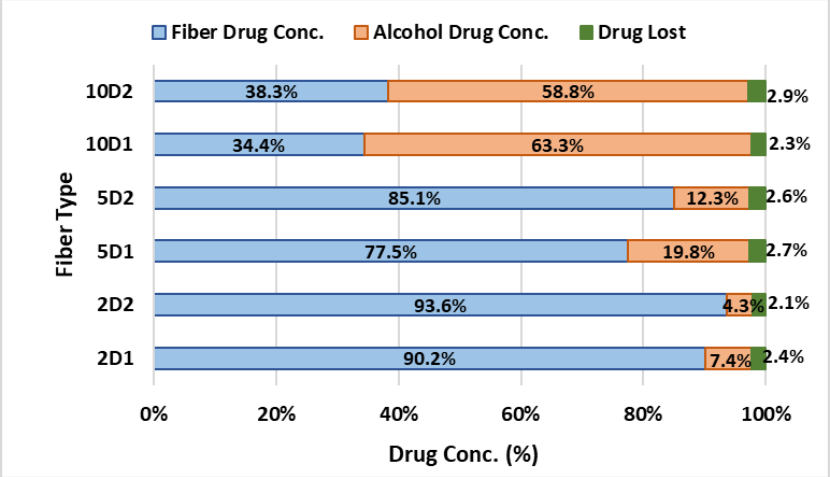

Figure 4.4. Drug distribution in fiber and coagulation bath after spinning

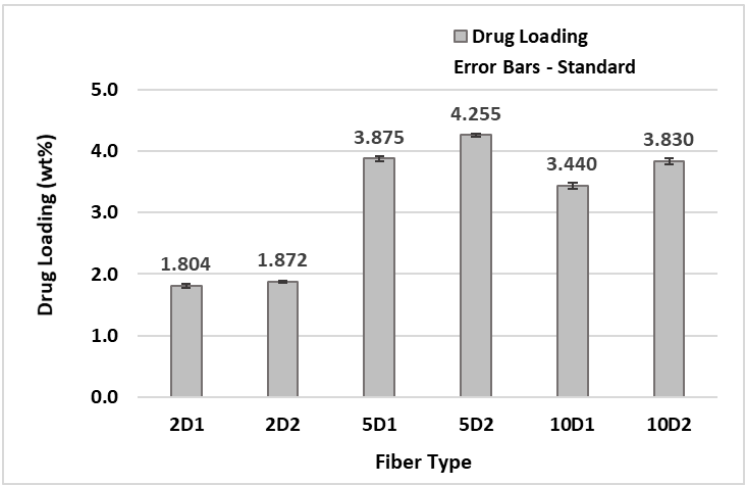

Figure 4.5. Fiber drug loading (wt.%) for different P4HB fibers

Table 4.3. Fiber drug loading for different P4HB fibers

Fiber Sample	Mean Drug Loading (wt.%)	Standard Deviation (wt.%)
2D1	1.804	0.029
2D2	1.872	0.023
5D1	3.875	0.036
5D2	4.255	0.030
10D1	3.440	0.051
10D2	3.830	0.046

As seen in Figure 4.5 and Table 4.3, the fibers spun from 5 wt.% drug concentration had the maximum drug loading (wt.%) among the three spin dope drug concentrations, implying that the quantity of drug that was loaded onto the 5D1 and 5D2 fibers was significantly higher than for the 2D1 and 2D2 fibers ($p < 0.0001$). The drug loading decreased significantly for 10D1 and 10D2 fibers as compared to 5D1 and 5D2 fibers ($p < 0.0001$), suggesting that the fibers had reached their limit for drug loading, which was closer to the 5 wt.% concentration. Also, it was observed that fibers with a higher spin draw ratio retained more drug during the spinning process ($p < 0.0001$). This suggests that the higher winding speed of the fibers decreased the residence time in the coagulation bath, reducing the drug diffusion from the polymer solution during extrusion. The low standard deviations (< 1.5%) for the fiber drug loading measurements indicated that the drug was distributed uniformly throughout the length of the fiber samples.

4.5.2. Fiber Diameter

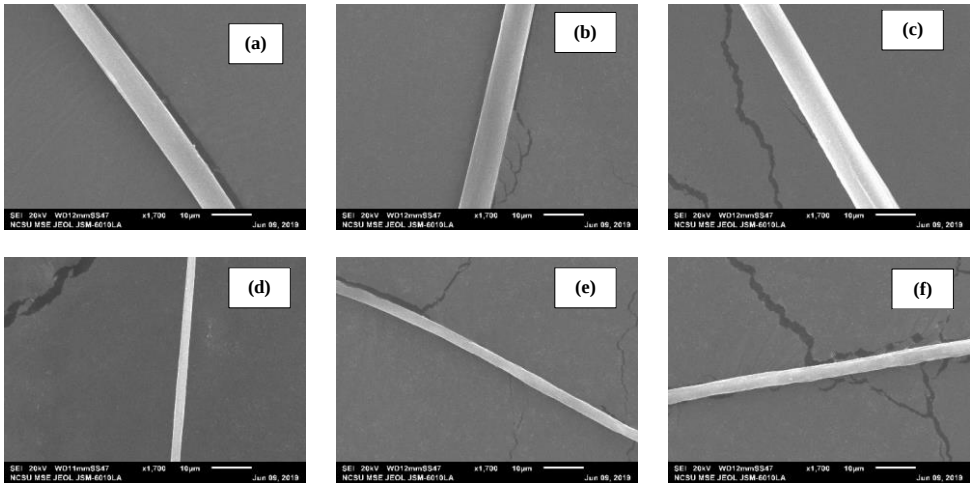

Figure 4.6. SEM images at x1700 magnification of (a) 2D1, (b) 5D1, (c) 10D1, (d) 2D2, (e) 5D2, and (f) 10D2 fibers

The SEM images of the drug-loaded fibers are shown in Figure 4.6. The mean diameters and standard deviations of all six drug-loaded fibers and the two control fibers are graphically represented in Figure 4.7. and summarized in Table 4.4. The statistical analysis of the diameter measurements showed that there was no significant difference in the diameters of the fibers loaded with 2% and 5% drug concentration and the blank homogeneous fibers ($p > 0.05$). 2D1 and 5D1 fibers had diameters similar to 15R1 fibers while the 2D2 and 5D2 fibers were similar in thickness to the 15R2 fibers. The results imply that no significant effect of the drug was observed on the diameter of these fiber. However, both sets of fibers spun with 10% drug concentration had significantly higher diameters compared to all the other fibers, including the homogeneous fibers ($p < 0.0001$). The significant change in diameter for the 10D1 and 10D2 fibers could be attributed to increased swelling during coagulation, caused by higher drug diffusion from the polymer

solution when the solvent-non solvent exchange occurred. The low standard deviations (< 5.2%) implies that all the fibers were uniformly cylindrical in shape throughout the length of the sample.

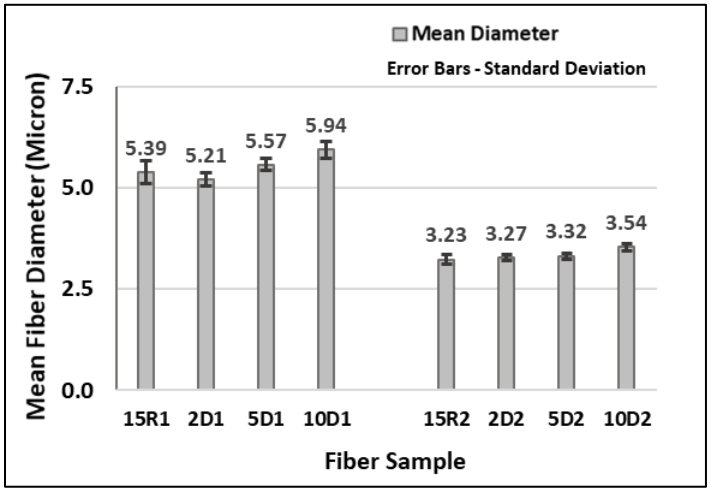

Figure 4.7. Mean diameter for different P4HB fibers

Table 4.4. Mean diameters for the fibers

Fiber Type	Mean Diameter (µm)	Standard Deviation (µm)
2D1	5.21	0.16
2D2	3.27	0.08
5D1	5.57	0.15
5D2	3.32	0.07
10D1	5.94	0.21
10D2	3.54	0.09
15R1	5.39	0.28
15R2	3.23	0.11

4.5.3. Fiber Linear Density

Figure 4.8 and Table 4.5. clearly show that the 10D1 fibers have the highest linear density, which can be attributed to them having the largest diameter. No significant difference ($p > 0.05$) was observed between the linear densities of the fibers except for the 10D1 and 15R1 fibers, which had significantly different linear densities ($p < 0.001$). These differences could be a result of the changes in fiber structure caused by the addition of the drug.

A limitation of this test method was the use of 55mg clip for weighing the fibers. This clip seemed too heavy for the fiber and it was concluded that using a lighter weighing clip might provide more accurate results. Also, due to the fineness of the fibers, some specimens might have accidently been damaged or stretched while handling them and clamping them onto the Vibromat tester.

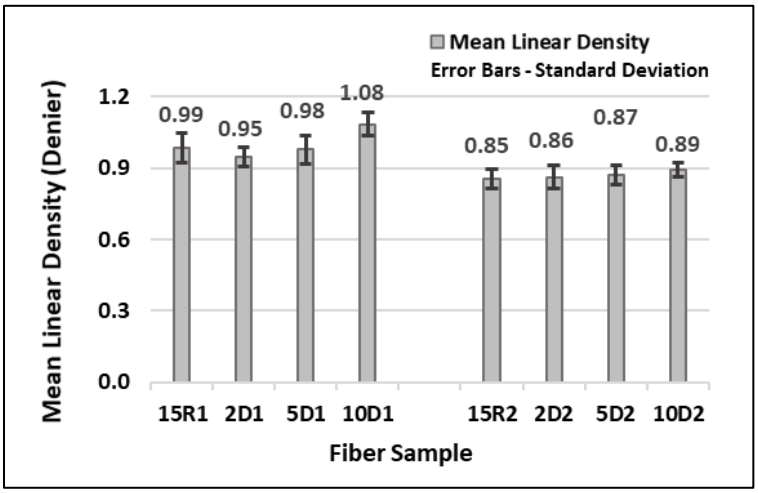

Figure 4.8. Mean linear density for different P4HB fibers

Table 4.5. Mean linear density of the fibers

Fiber Type	Mean Linear Density (Denier)	Standard Deviation (Denier)
2D1	0.947	0.043
2D2	0.862	0.052
5D1	0.977	0.066
5D2	0.871	0.045
10D1	1.084	0.054
10D2	0.892	0.032
15R1	0.985	0.068
15R2	0.853	0.047

4.5.4. Fiber Crystallinity

The x-ray diffractograms for the drug-loaded and homogeneous control fibers are depicted in Figure 4.9. The peak positions of all the samples were similar with respect to the 2Θ angle. It can be observed that the peaks for the fibers spun with a higher spin draw ratio are sharper and narrower, implying larger crystallite size [143]. This corresponds to the theory that a higher draw ratio increases the polymer chain alignment, which leads to increased crystallinity. This can also be seen in Figure 4.10 and Table 4.6, where fibers with higher spin draw ratios have higher crystallinity. It was also noticed that the 10D1 and 10D2 fibers had a lower degree of crystallinity as compared to the other drug-loaded fibers. This could be caused by the formation of micro-voids in the fiber during coagulation when the drug diffused out of the polymer solution with the solvent [148].

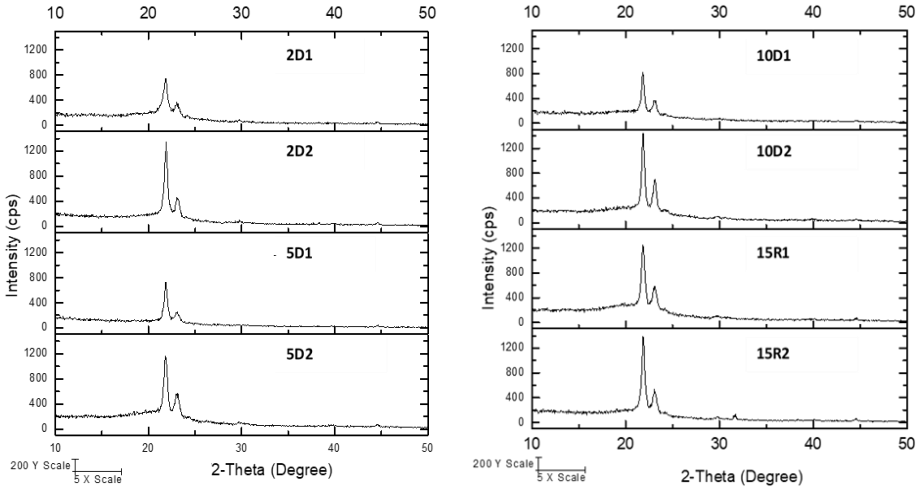

Figure 4.9. X-ray diffractograms for different P4HB fibers

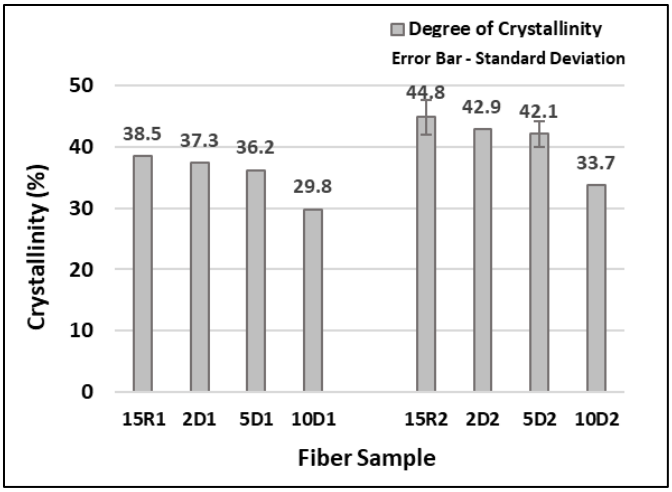

Figure 4.10. Crystallinity for different P4HB fibers

Three samples of 15R2 fibers and 5D2 fibers were tested to determine the variability in the degree of crystallinity for these two fibers. The mean crystallinity of the 15R2 fiber samples was calculated to be about 44.8% with a standard deviation of 2.8% while 5D2 fibers had a mean crystallinity of 42.1% with a standard deviation of 2.1%. The low standard deviation of the crystallinity of these two sets of fibers indicated that the fibers had a uniform alignment of polymer

chains. There was no significant difference found in the crystallinity of these two fibers ($p = 0.0534$), suggesting that the addition of up to 5 wt.% drug in the 5D2 fibers did not have a significant effect on the fiber structure and polymer chain alignment. Resource and time limitations restricted the testing of multiple samples from each set of fibers in order to determine statistical differences for the crystallinity of these fibers.

Table 4.6. Degree of crystallinity for the fibers

Monofilament Type	Crystallinity (%)
2D1	37.3
2D2	42.9
5D1	36.2
5D2	42.1
10D1	29.8
10D2	33.7
15R1	38.5
15R2	44.8

3.5.5. Mechanical Testing

The results from the mechanical testing (Table 4.7) were analyzed for tenacity, elongation at break and elastic modulus for all six types of drug loaded monofilaments. The mechanical properties of the drug loaded fibers were compared to the homogeneous control fibers to determine if there were significant differences between the fiber types.

Table 4.7. Summary of mechanical test result analysis

Fiber Type	Fiber Tenacity (gf/denier)		Elongation @ Break (%)		Tensile Modulus (gf/denier)	
	Mean	Standard Deviation	Mean	Standard Deviation	Mean	Standard Deviation
2D1	1.44	0.34	108.41	21.76	58.43	9.36
2D2	1.75	0.22	52.28	13.12	92.11	16.47
5D1	1.39	0.29	94.24	28.07	56.36	15.51
5D2	1.71	0.25	51.02	12.51	90.03	17.12
10D1	1.23	0.31	78.49	22.20	50.14	13.39
10D2	1.59	0.23	49.13	14.41	81.21	18.93
15R1	1.57	0.38	124.17	25.51	65.63	13.94
15R2	1.88	0.24	55.87	10.91	101.71	23.59

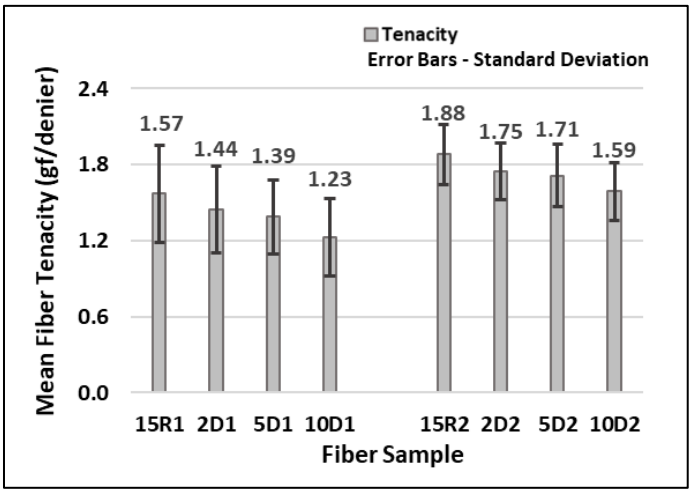

Figure 4.11. Mean tenacity for different P4HB fibers

It can be seen from Figure 4.11 that the 15R2 fibers had the highest tenacity among all the fiber types. It is also observed that the fibers with a higher draw ratio had significantly higher tenacity compared to their counterparts with a lower draw ratio ($p < 0.0001$). This could be

attributed to the increase in crystallinity and chain alignment induced by the higher draw ratio. Statistical analysis of the data showed that there was no significant difference in the fiber tenacity among the 2D1, 5D1 and 15R1 fibers ($p = 0.1173$) and the 2D2, 5D2 and 15R2 fibers ($p = 0.2472$), indicating that the addition of up to 5 wt.% drug in the fibers did not have a significant effect on the fiber tenacity. However, there was a significant difference in the tenacity between 10D1 and 15R1 and between 10D2 and 15R2 fibers ($p < 0.001$), which could be caused by micro-voids created due to the drug diffusion from the polymer solution during the coagulation process. These micro-voids can act as stress points between the polymer chains and lead to premature mechanical failure [148].

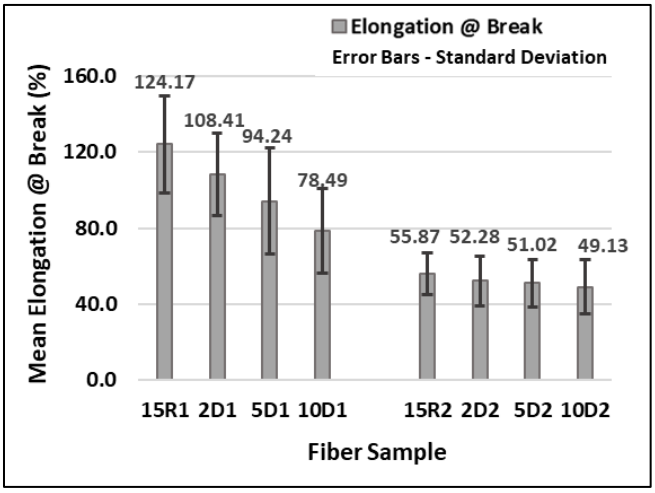

Figure 4.12. Mean elongation at break for different P4HB fibers

Based on the results for elongation at break (Figure 4.12), it was found that the addition of the drug lowered the elongation for some of the fibers. All three drug loaded fibers spun at a lower draw ratio had a significantly lower elongation at break than the control fibers with the same draw ratio ($p < 0.001$). This indicated that the addition of the drug decreased the fiber swelling and chain

entanglement which led to a lower elongation at break. It was also observed that all four fiber samples which were spun at a higher draw ratio, namely 2D2, 5D2, 10D2 and 15R2, had similar values for elongation at break ($p = 0.0695$). This suggested that at a higher draw ratio, the addition of the drug did not seem to have a significant effect on these fibers, as the reduced residence time in the coagulation bath minimized fiber swelling and chain entanglement.

Figure 4.13 depicts typical load-elongation profiles for the drug loaded fibers and the control fibers. It can be seen that the fibers with a higher spin draw ratio have a steeper slope and lower elongation as compared to the fibers spun at a lower draw ratio. These graphs support the quantitative analysis of the fiber mechanical properties.

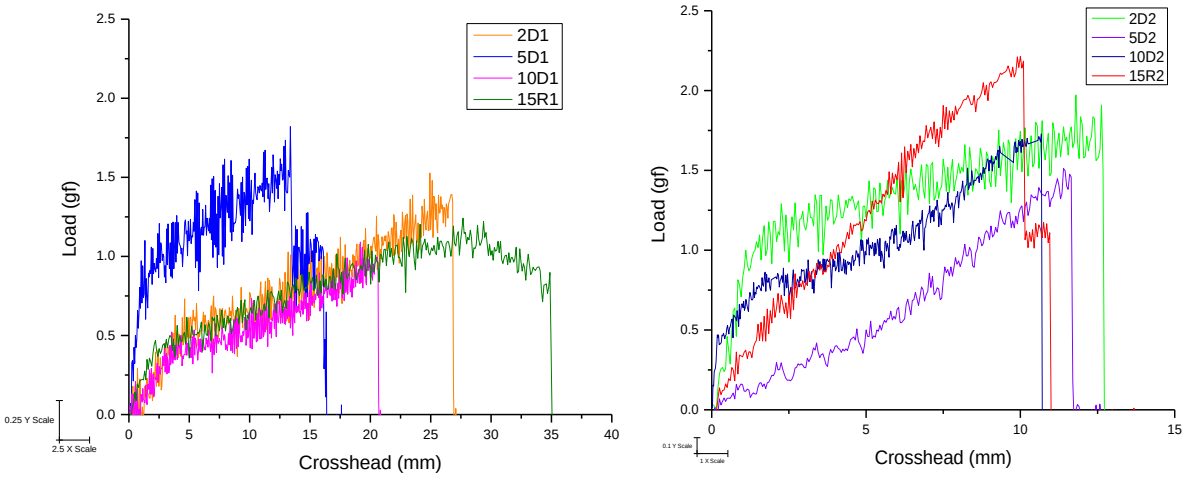

Figure 4.13. Typical load-elongation curves for different P4HB fibers

The results observed for tensile modulus (Figure 4.14) have similar trends to the results for the fiber tenacity. It was found that there was no significant difference in the tensile modulus between the 2D2, 5D2 and 15R2 fibers ($p = 0.0807$), implying that the addition of up to 5 wt.% of the drug did not have a significant effect on the fiber stiffness at higher draw ratios. However,

the 10D2 fibers had a significantly lower tensile modulus compared to the 15R2 fibers ($p = 0.0016$). For fibers spun at a lower draw ratio, the tensile modulus did not decrease significantly with the increase in drug concentration from 2 wt.% to 5 wt.% ($p > 0.05$). This suggests that an increase in the drug concentration of the spin dope has more effect on the fiber stiffness at lower draw ratios due to the increased residence time in the coagulation bath.

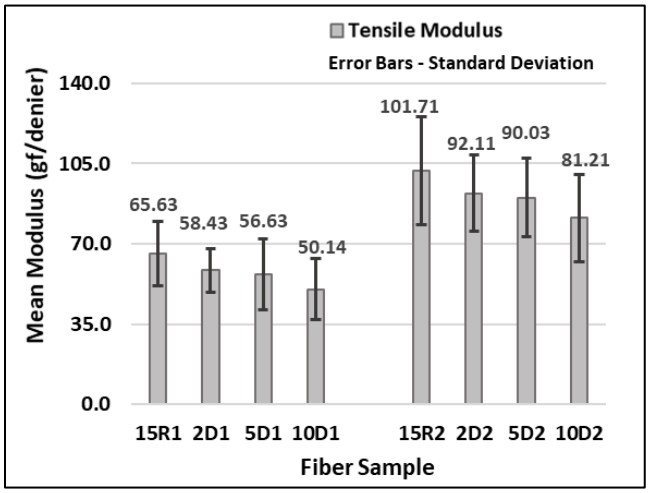

Figure 4.14. Mean tensile modulus for different P4HB fibers

Certain process and method limitations were faced in the measurement of the fiber mechanical properties which resulted in higher standard deviations for the readings. A 2N swinging load cell was used on the MTS instrument, which caused vibrations in the fiber during testing and resulted in measurements with a noisy signal. It is also believed that a lower capacity load cell could have provided more accurate readings. Additionally, the fiber mounting process on the specimen cards imparts an inherent variability in the positioning of the fibers. Some error may also have occurred during the fiber mounting as some specimens might have been accidently damaged or stretched during handling due to the fineness of the fibers.

4.5.6. Thermal Testing

From the heating curves in Figure 4.15 it can be seen that the melting peaks for the fibers spun with 2 wt.% and 5 wt.% drug concentration are taller and narrower than the peaks for the fibers spun with 10 wt.% drug concentration. The broader and flatter peaks of the 10D1 and 10D2 fibers suggested that they had lower crystallinity than the other fibers. This corresponded to the values for the melting peak area as well as the results from the XRD and mechanical testing.

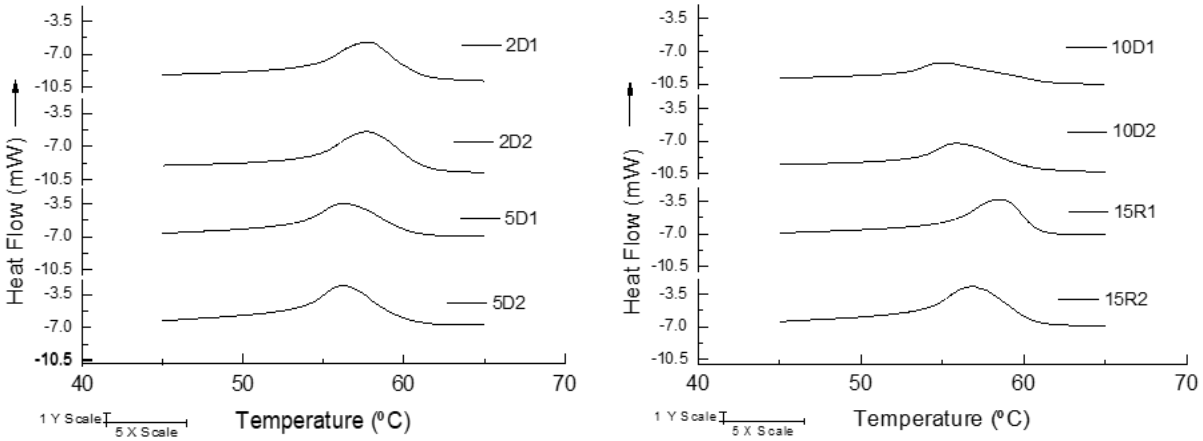

Figure 4.15. DSC heating curves for P4HB fibers

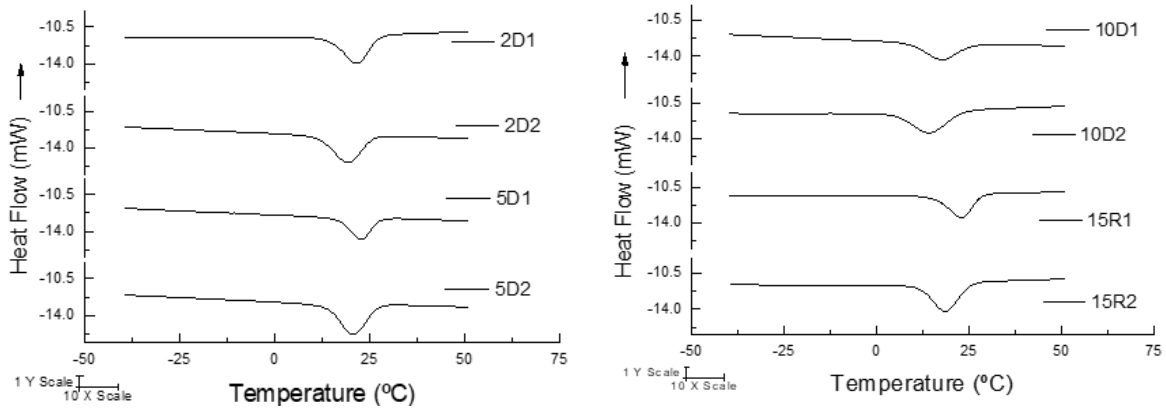

Figure 4.16. DSC cooling curves for P4HB fibers

The results obtained from the analysis of the heating and cooling curves (Figure 4.16) of the DSC thermograms are summarized in Table 4.8. It was observed that the melting peak temperatures for all the fiber samples were in the range of 54 – 58 °C. The 5D1 and 5D2 fibers had a closer melting temperature to the homogeneous control fibers than any of the other fibers. It was also seen that the melting enthalpy values for the 2 wt.% and 5 wt.% drug concentration fibers were similar to the homogeneous control fibers, suggesting that the addition of the drug did not affect the thermal properties of these fibers.

Table 4.8. Summary of the DSC test result analysis

Sample	Melt Peak Temp. (°C)	Melt Enthalpy (J/g)	Melt Peak Area (mJ)	Crystallization Peak Temp. (°C)	Crystallization Enthalpy (J/g)	Crystallization Peak Area (mJ)
2D1	55.8	19.8	93.3	23.7	-26.4	-78.7
2D2	55.7	24.2	111.5	21.3	-30.7	-98.4
5D1	57.4	22.4	98.3	22.5	-27.2	-81.3
5D2	57.2	23.8	111.7	19.1	-29.8	-100.6
10D1	54.6	15.1	48.6	23.2	-19.5	-46.5
10D2	55.4	20.2	64.7	15.1	-22.8	-53.2
15R1	57.9	24.1	80.2	18.4	-28.2	-106.4
15R2	56.4	29.0	136.5	19.8	-32.1	-150.8

4.6. CONCLUSION

As mentioned earlier in the chapter, the main aim of this study was to understand the effect of drug loading on wet spun P4HB fibers. The two objectives of the study were accomplished by following the spinning method developed in the previous study and using relevant literature for explaining the results obtained.

It was found that an increase in drug concentration in the spin dope increased the fiber drug loading of the spun fibers up to a certain limit. However, beyond 5 wt.% drug in the polymer solution, the drug loading efficiency of the fibers decreased significantly. It was also observed that more drug was loaded in the fibers at a higher draw ratio, suggesting that the decrease in residence time in the coagulation bath reduced the extent of drug diffusion from the polymer solution. The low standard deviation for the fiber drug loading measurements indicated that the drug was distributed uniformly along the length of the fibers. The fibers spun with 2 wt.% drug concentration in the spin dope did not have any significant effect on the spun fiber mechanical properties, diameter or crystallinity. The fibers spun with 5 wt.% drug concentration at a higher draw ratio also had similar mechanical properties, diameter and crystallinity as compared to homogeneous control fibers. However, the fibers spun with 10 wt.% drug concentration had a significant effect on mechanical properties, diameter and crystallinity. All six drug-loaded fibers will be subjected to a drug release study to determine how the drug is released from these fibers over a period of time. The effect of different drug-loading concentrations and spin draw ratios on the drug release profiles will be determined.

CHAPTER 5 – DRUG RETENTION AND RELEASE PROFILES FOR DRUG LOADED P4HB FIBERS

5.1. INTRODUCTION

In the recent years, the interest in polymeric drug delivery systems has led to the design and development of therapeutically active fibers for various applications, from surgical sutures and wound dressings to tissue engineering scaffolds. From the many techniques to fabricate textile fibers incorporated with drugs, a suitable method is to produce drug loaded fibers via wet spinning. Due to the ambient spinning conditions and the incorporation of drugs in the polymer dope prior to fiber spinning, the drugs maintain their stability by being loaded into and are released from the fibers uniformly. The wet spinning method can also produce fibers which can be woven, knitted and braided into different structures [119]. Many research studies have been undertaken to understand the effect of drug incorporation on fiber properties, as well as the drug release profiles from these fibers. It has been found that multiple factors, such as polymer composition, molecular weight and structure, type of drug and drug concentration, and fiber processing methods, can affect the drug release profiles for such drug loaded fibers [151].

For an efficient controlled drug delivery system, a predictable drug release profile is essential to prevent non-uniform dosage. At concentrations higher than the maximum therapeutic level, the drug can cause toxic side effects, while at concentrations lower than the minimum effective level, the drug will not have a sufficient therapeutic effect (Figure 5.1). To maintain the required drug concentration at the targeted location for as long as needed, the drug delivery system should be able to control the drug release rate and duration. In order to do so, the system generally needs to release part of the dose rapidly to attain the effective therapeutic concentration followed

by a defined release rate which can maintain the drug concentration at the therapeutic dose level [138]. Hence, it is necessary to study the drug release profiles for fibers incorporated with drugs in conditions which simulate the targeted drug release environment to ensure uniformity in the drug release profile. An *in vitro* experimental method with phosphate buffer solution (PBS) at 37 °C and 7.4 pH is commonly used for simulating the systemic conditions of the human body [119].

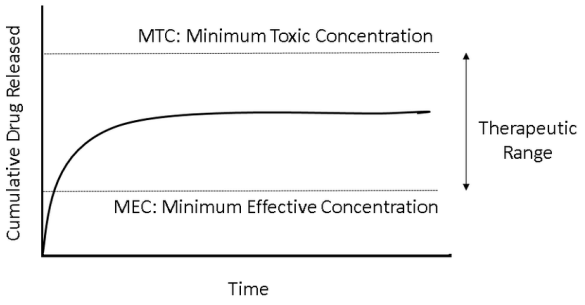

Figure 5.1. Cumulative drug release to deliver therapeutic dose [152]

There are several methods which can be used to obtain the drug release profiles from different drug delivery systems. Some of them are based on kinetic modeling with established methods, such as zero-order and first-order release kinetics. They may also follow the Higuchi model or the Hopfenberg model. These can be applied to various drug delivery systems based on the matrix type, structure and drug release mechanism. Another way to investigate the drug release profiles is to apply statistical methods, such as exploratory data analysis or a multivariate analysis approach and using regression models to obtain a predictable release profile for the drugs [138].

In this study, the primary focus was to analyze the drug release profiles for levofloxacin incorporated in wet spun poly-4-hydroxybutyrate (P4HB) fibers over a period of 5 days. Additionally, the drug retention within the P4HB fibers was studied over the same period of time so as to understand the uniformity and predictability of the drug loading and release from these

fibers. There were two main objectives for this study: (i) To assess the effect of drug loading concentration on the drug retention in, and release profiles from P4HB fibers, and (ii) To evaluate the effect of spin draw ratio on the drug retention in, and release profiles from P4HB fibers.

5.2. MATERIALS

The drug release and retention studies were carried out with six sets of levofloxacin loaded fibers produced in the previous project by wet spinning (Table 5.1). Chloroform was used to dissolve the fibers and the drug in the solution was measured to determine drug retention in the fibers. A phosphate buffer solution (PBS) at pH 7.4 was used to study drug release from the fibers.

Table 5.1. Types of wet spun drug loaded P4HB fibers

Fiber Sample	Drug Concentration (wt.% polymer)	Spin Draw Ratio (D)
2D1	2	12
2D2	2	18
5D1	5	12
5D2	5	18
10D1	10	12
10D2	10	18

5.3. EXPERIMENTAL METHODS

5.3.1. In-Vitro Drug Release

A five-day drug release study was conducted for each of the six drug loaded fiber samples. Thirty specimens of 10 mg for each type of fiber were immersed in 5 ml of phosphate buffer solution (PBS) at 7.4 pH in individual glass vials for removal after different time intervals. The glass vials were kept in a shaker bath at 37 °C with an agitation of 25 rpm (Figure 2). The pH was

monitored regularly with a pH meter. No variations in the solution pH were observed over the course of the study. The time intervals for the study were 1 hour, 2 hours, 4 hours, 8 hours, 12 hours, 24 hours, 48 hours, 72 hours, 96 hours and 120 hours for each fiber type. After every time interval, three specimens for each fiber sample were removed from the shaker bath, placed in a clean petri-dish and stored under vacuum for drying. The fibers and the PBS solutions were further tested to measure the amount of drug released in PBS as well as the amount of drug still retained in the fiber.

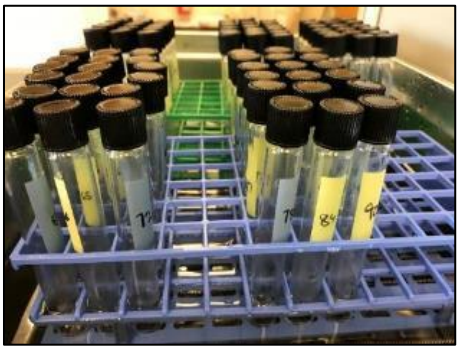

Figure 5.2. Drug loaded P4HB fibers immersed in PBS for i*n vitro* drug release study

5.3.2. Drug Quantification

Ultra-violet (UV) spectroscopy was used for quantifying the amount of drug in the PBS released solution and in the fibers after dissolving them in a chloroform solution. The drug had a UV absorbance at a wavelength of 290-303 nm, which was not affected by the presence of the polymer or other chemicals. Standard solutions with different drug concentrations were prepared from chloroform and PBS in volumetric flasks. Calibration equations in two concentration ranges were obtained for both chloroform and PBS. After the calibration equations were obtained, the samples from the *in vitro* release study were tested and the amount of drug quantified.

After each time interval, the fiber samples were removed from the vials and kept in petri dishes for drying. The dried fibers were weighed and dissolved in chloroform in separate standard volumetric flasks. The solutions were tested in a UV spectrophotometer (Agilent Technologies, Cary 300 UV-Vis) and the amount of drug present in each solution was measured. The data was used to calculate the average amount of drug retained by each fiber sample at different times during the five-day study. The PBS in the glass vials was also tested for the amount of drug released from the different fibers. Each specimen from a glass vial was diluted with fresh PBS in a standard volumetric flask and tested with the UV spectrophotometer. The data was used to calculate the average amount of drug released by each fiber sample at different times during the five-day study.

Exploratory data analysis was used to determine statistically the drug release kinetics for the polymer/drug combination in this study. This method is used to understand the approximate drug release kinetics for controlled drug delivery systems, especially for new and relatively lesser known delivery systems. The release data was depicted graphically by plotting the mean values at each dissolution time point and error bars with two times standard error. The numerical data for the release profiles was evaluated at each time point statistically with a confidence interval of 95%, and a regression analysis was used to determine the predictability of the drug release data obtained from the *in vitro* study [138].

5.3.3. Statistical Analysis

As specified earlier, there were three specimens for each of the six fiber samples at each time interval. The results obtained from the PBS in the vials were used to understand the drug release study, while the data from the testing of the fibers in the chloroform solution were used to explain the drug retention performance. Both data sets were subjected to statistical analysis using

analysis of variance (ANOVA) and Bartlett's Test for determining significant differences in drug release and drug retention between the different fiber samples at each time interval.

ANOVA was used to compare significant differences in the amount of drug released and the amount of drug retained by the different fibers. On the other hand, Bartlett's Test was used to compare variances in the drug release data and drug retention data for the different fiber samples. A p-value of 0.05 was used to determine significant differences between the data sets for both statistical tests.

5.4. RESULTS AND DISCUSSION

5.4.1. Drug Calibration Equations

The calibration equations for the levofloxacin in chloroform and in PBS are shown in Figure 5.3 and Table 5.2. The chloroform equations were in the concentration ranges of 0.0004 – 0.004 mg/ml and 0.004 – 0.009 mg/ml. The PBS solutions had equations in the concentration ranges of 0.0002 – 0.002 mg/ml and 0.002 – 0.009 mg/ml. All four equations had $R^2 > 0.999$.

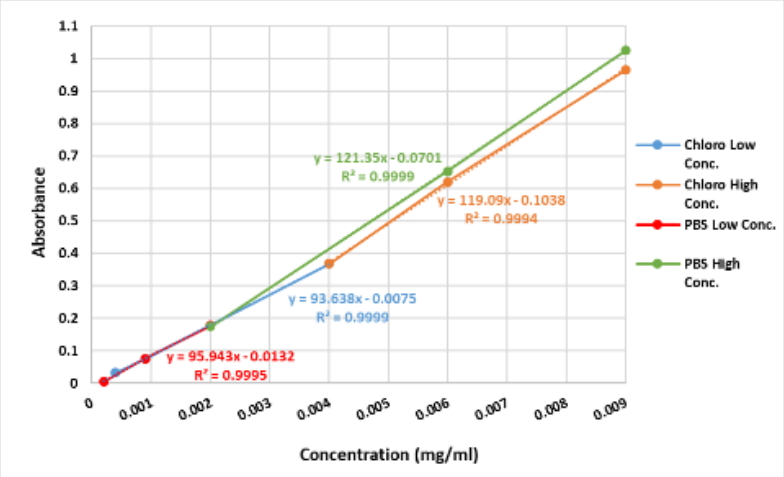

Figure 5.3. Calibration curves for levofloxacin in chloroform and PBS

Table 5.2. Calibration equations for levofloxacin in chloroform and PBS

Solution	Concentration Range	Calibration Equation	R^2
Chloroform	0.0004 – 0.0040 mg/ml	Abs = 93.638*Conc - 0.0075	0.9999
Chloroform	0.0040 – 0.0090 mg/ml	Abs = 119.09*Conc - 0.1038	0.9994
PBS	0.0002 – 0.0020 mg/ml	Abs = 95.943*Conc - 0.0132	0.9995
PBS	0.0020 – 0.0090 mg/ml	Abs =121.35*Conc - 0.0701	0.9999

5.4.2. Drug Loading Efficiency

Figure 5.4 depicts the drug loading efficiency (wt.%) of the six P4HB fiber samples loaded with levofloxacin during the wet spinning process. These results were acquired by the methods and measurements described in the previous chapter. These data represent the total amount of drug (wt.%) present in the fiber samples before the *in vitro* drug release experiment began.

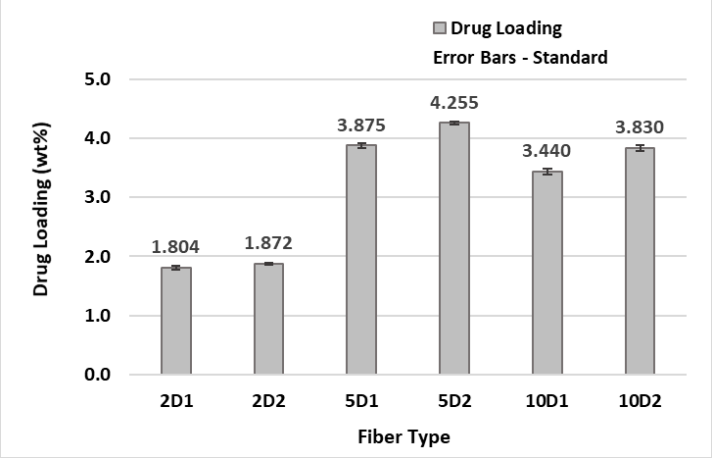

Figure 5.4. Fiber drug loading (wt.%) for different P4HB fiber samples

5.4.3. Drug Release Study

Figure 5.5 depicts the drug release profiles for the drug loaded P4HB fiber samples over a period of 5 days (120 hours). It can be seen that the fibers have a logarithmic regression with $R^2 > 0.98$ for the drug release of all six samples. The regression analysis implies a good level of predictability assuming first order release kinetics for these fiber samples as the experimental data fits closely to the regression curves.

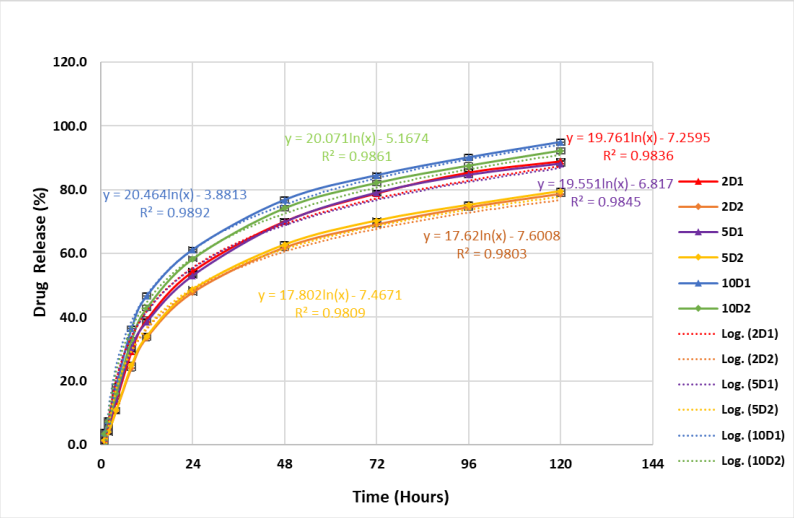

Figure 5.5. Drug release profiles for different P4HB fiber samples

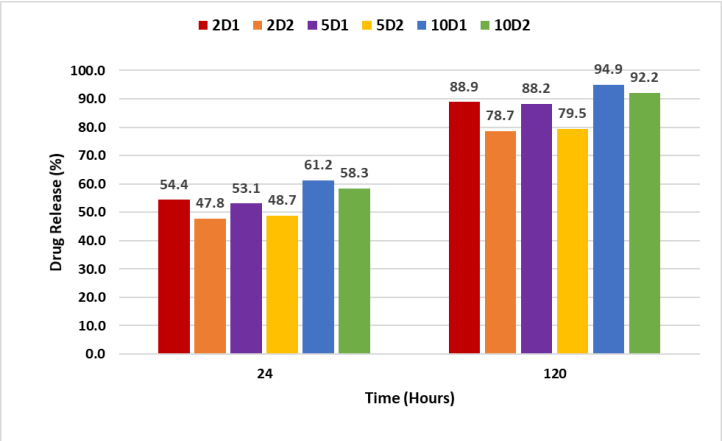

Figure 5.6. Percent drug released (%) after 24 hours and 120 hours for P4HB fiber samples

It was found that the fibers spun with 10 wt.% drug concentration in the spin dope had the fastest release rate while the 2D2 and 5D2 fiber samples had the slowest release rate. The release profiles showed that there was an initial fast release of the drugs, with 47 – 61% being released in the first 24 hours, as seen in Figure 5.6. The release rates were found to be much slower over the next few days, with less than 80% total drug release observed for the 2D2 and 5D2 fiber samples after 120 hours. On the other hand, the 10D1 and 10D2 fiber samples released over 90% of the total drug loaded, while 2D1 and 5D1 fiber samples released around 88% of the drug during the 5-day study. A significant difference ($p < 0.0001$) was observed in the drug release between 24 hours and 120 hours for all 6 fiber samples. However, similar amounts of drug release were observed for the 2D1 and 5D1 fiber samples ($p = 0.2167$ & 0.2281) and for the 2D2 and 5D2 fiber samples ($p = 0.0847$ & 0.0938) both at 24 hours and at 120 hours respectively. Based on the characterization results of these fibers from the previous chapter, it is known that the 2D2 and 5D2 fiber samples had the highest degree of crystallinity, about 42%. The 2D1 and 5D1 fiber samples had a crystallinity of 36 – 37%, while the 10D1 and 10D2 fiber samples had a crystallinity in the range of 30 - 33%. As a result, it was observed that an increase in crystallinity significantly reduced the fiber drug release rate, even though the fibers had a higher wt.% drug loading. This suggests that the degree of crystallinity in the fibers has a stronger effect on the drug release rates than the total wt.% drug loading. Table 5.3 summarizes the means and standard deviations of the drug release data for all the fiber samples at each time point. It also lists the results for the Bartlett's test which compares the variances between the different fiber samples at each time point. All the comparisons have a p-value > 0.05, which shows that there is no significant difference among the variances in the data. This suggests that the drug release was even for all the fibers, implying that the drug had a uniform distribution along the length of the fiber samples.

Table 5.3. Results from the Drug Release Study

Time Interval (Hours)	Fiber Type	Mean (%)	SD (%)	Bartlett's Test p-value
1	2D1	1.8	0.404	0.7218
	2D2	1.2	0.423	
	5D1	1.9	0.416	
	5D2	1.3	0.409	
	10D1	3.9	0.414	
	10D2	3.4	0.438	
2	2D1	5.6	0.329	0.8733
	2D2	3.9	0.361	
	5D1	5.8	0.343	
	5D2	4.1	0.355	
	10D1	7.6	0.369	
	10D2	7.2	0.332	
4	2D1	13.7	0.428	0.7981
	2D2	10.6	0.442	
	5D1	14.3	0.419	
	5D2	10.8	0.431	
	10D1	18.2	0.425	
	10D2	16.1	0.453	
8	2D1	29.2	0.412	0.8845
	2D2	24.1	0.427	
	5D1	30.4	0.405	
	5D2	24.9	0.419	
	10D1	36.4	0.431	
	10D2	32.8	0.428	
12	2D1	39.3	0.418	0.9249
	2D2	33.6	0.432	
	5D1	38.6	0.424	
	5D2	34.1	0.411	
	10D1	46.7	0.447	
	10D2	42.9	0.429	
24	2D1	54.4	0.278	0.8487
	2D2	47.8	0.301	
	5D1	53.1	0.293	
	5D2	48.7	0.285	
	10D1	61.2	0.306	
	10D2	58.3	0.276	
48	2D1	70.1	0.420	0.7748
	2D2	61.9	0.436	
	5D1	69.9	0.413	
	5D2	62.8	0.427	
	10D1	76.8	0.440	
	10D2	74.2	0.437	
72	2D1	78.9	0.336	0.9014
	2D2	69.1	0.348	
	5D1	79.1	0.330	
	5D2	70.3	0.342	
	10D1	84.5	0.352	
	10D2	82.1	0.349	
96	2D1	85.4	0.462	0.7926
	2D2	74.5	0.479	
	5D1	84.7	0.454	
	5D2	75.2	0.470	
	10D1	90.1	0.484	
	10D2	87.5	0.480	
120	2D1	88.9	0.412	0.8525
	2D2	78.7	0.427	
	5D1	88.2	0.405	
	5D2	79.5	0.419	
	10D1	94.9	0.431	
	10D2	92.2	0.428	

5.4.4. Drug Retention Study

The drug retention profiles depicted in Figure 5.7 show the concentration of drug retained by the fiber during the five-day *in vitro* study. The analysis of these profiles resulted in logarithmic regression curves with $R^2 > 0.98$ for all six fiber samples, suggesting predictability assuming first order release kinetics. It can also be seen that the curves obtained for the drug retention in fibers is complementary to those for the drug release in the PBS medium, signifying uniformity in the drug distribution and drug release. The trends observed in the drug retention profiles of the fiber samples mirror those from the drug release profiles, which implies consistency in the experimental methods and the test results. As seen in Figure 5.8, around 50% of the drug was retained by the 2D2 and 5D2 fiber samples after 24 hours, while 10D1 and 10D2 fiber samples retained less than 40% of the drug after 24 hours. Similarly, after 120 hours 10D1 and 10D2 fiber samples retained only 3-7% of the drug while the 2D2 and 5D2 fibers retained about 18% of the total drug loaded.

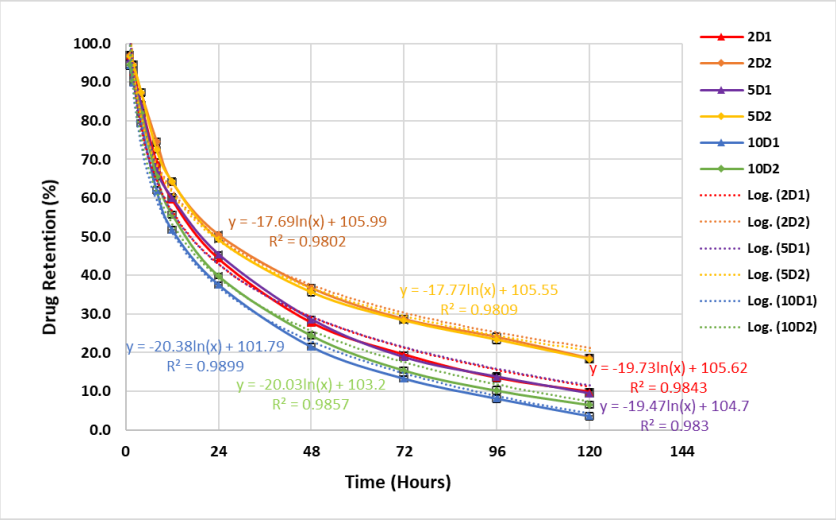

Figure 5.7. Drug retention profiles for different P4HB fiber samples

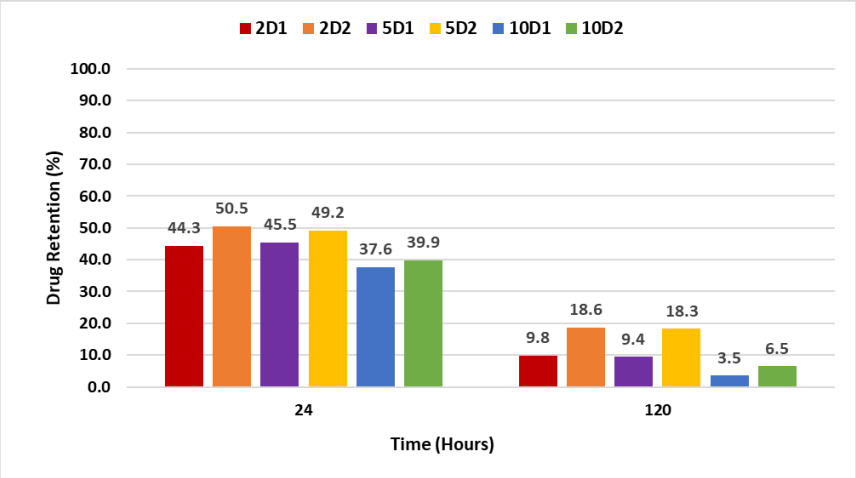

Figure 5.8. Percent drug retained (%) after 24 hours and 120 hours for P4HB fiber samples

A significant difference ($p < 0.0001$) was observed in the percent drug retention between 24 hours and 120 hours for all 6 fiber samples. On the other hand, no significant differences were found in the drug retention between the 2D1 and 5D1 fiber samples ($p = 0.2527$ & 0.3072) and between the 2D2 and 5D2 fiber samples ($p = 0.0735$ & 0.0812) both at 24 hours and at 120 hours respectively. This suggests that an increase in the fiber draw ratio and a higher crystallinity results in higher drug retention over time. In fact, it appears that the degree of crystallinity has a greater effect on the drug retention profile than the initial amount of drug loaded into the fibers. Table 5.4 summarizes the means and standard deviations for the drug retention profiles for all six fibers at each time interval. It also lists the results for the Bartlett's test which compares the variances between the different fiber samples at each time point. As seen, the p-value > 0.05 for all the data sets, implying that there is no significant difference in the variances for the drug retention of the fibers. This suggests that all six fiber samples have uniform drug distribution along their length.

Table 5.4. Results from drug retention study

Time Interval (Hours)	Fiber Type	Mean (%)	SD (%)	Bartlett's Test p-value
1	2D1	96.8	0.338	0.8224
	2D2	97.1	0.351	
	5D1	95.9	0.333	
	5D2	96.6	0.344	
	10D1	94.3	0.354	
	10D2	94.7	0.351	
2	2D1	92.7	0.381	0.8177
	2D2	94.7	0.416	
	5D1	91.4	0.393	
	5D2	94.5	0.381	
	10D1	89.9	0.393	
	10D2	90.4	0.411	
4	2D1	84.2	0.376	0.7632
	2D2	87.3	0.414	
	5D1	84.1	0.385	
	5D2	87.4	0.395	
	10D1	79.4	0.409	
	10D2	82.0	0.404	
8	2D1	69.2	0.342	0.7741
	2D2	74.7	0.354	
	5D1	67.5	0.336	
	5D2	72.5	0.348	
	10D1	61.9	0.328	
	10D2	65.6	0.355	
12	2D1	59.5	0.396	0.6825
	2D2	64.1	0.442	
	5D1	60.1	0.408	
	5D2	64.3	0.396	
	10D1	51.8	0.408	
	10D2	55.7	0.442	
24	2D1	44.3	0.384	0.7435
	2D2	50.5	0.398	
	5D1	45.5	0.377	
	5D2	49.2	0.390	
	10D1	37.6	0.401	
	10D2	39.9	0.399	
48	2D1	27.7	0.392	0.6992
	2D2	36.8	0.427	
	5D1	28.6	0.404	
	5D2	35.6	0.399	
	10D1	21.5	0.414	
	10D2	24.4	0.407	
72	2D1	19.4	0.412	0.9028
	2D2	28.7	0.429	
	5D1	18.8	0.408	
	5D2	28.3	0.419	
	10D1	13.3	0.431	
	10D2	15.4	0.424	
96	2D1	13.4	0.438	0.7658
	2D2	24.1	0.452	
	5D1	13.7	0.429	
	5D2	23.3	0.443	
	10D1	8.1	0.456	
	10D2	10.2	0.433	
120	2D1	9.8	0.451	0.8099
	2D2	18.6	0.470	
	5D1	9.4	0.446	
	5D2	18.3	0.461	
	10D1	3.5	0.467	
	10D2	6.5	0.454	

5.4.5. Drug Release Kinetic Model

The drug retention data for the fibers was plotted as a log cumulative percentage of drug remaining vs. time and it was found to be a linear profile (Figure 5.9). The linear regression curves for all six fibers had an $R^2 > 0.979$, suggesting a good fit for the first order kinetic model, which can be used to express the elimination of the drugs from these fibers. In this model, the release of the drugs is expressed as the following equation [138]:

$$log_{10}\frac{C_t}{C_0} = \frac{-kt}{2.303}$$

Where, Co = initial drug concentration, Ct = drug concentration at time t and k = rate constant.

Typically, this first-order kinetic model is used for drug absorption/diffusion through a non-degradable matrix. However, it is believed that during the five-day *in vitro* study period the drug loaded fibers did not undergo any resorption and hence the drug was released via this mechanism.

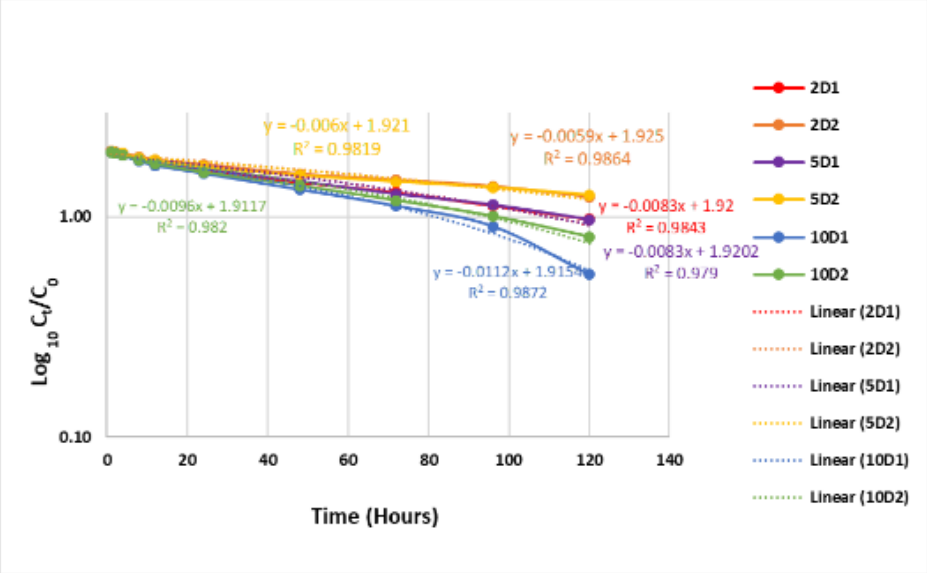

Figure 5.9. First-order kinetic model for drug remaining in the fibers

5.4.6. Drug Distribution

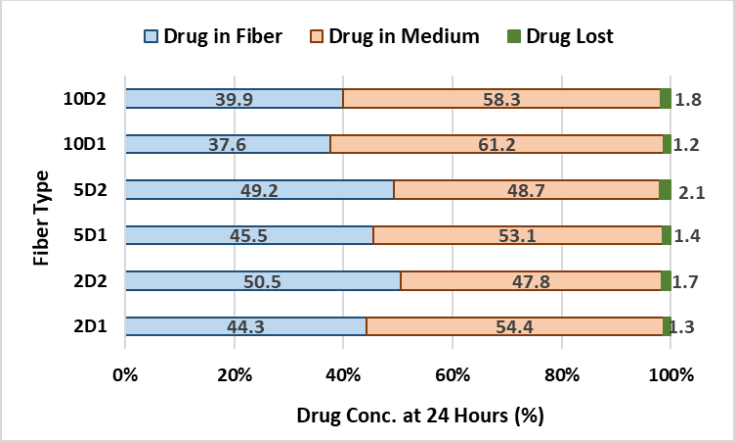

Figure 5.10. Total drug distribution after the 24-hour *in vitro* study

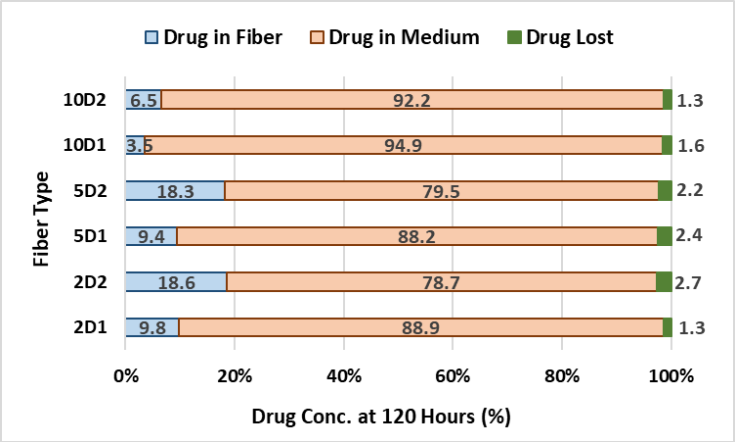

Figure 5.11. Total drug distribution after the 120-hour *in vitro* study

Figures 5.10 and 5.11 show the total drug distribution after 24 hours and 120 hours respectively during the drug release *in vitro* study. It can be seen that during the study, over 97% of the drug was either released into the PBS medium or retained in the fiber. About 1-3% of the drug was lost during the *in vitro* experiments, handling and testing procedures. At each time point, when the fibers were removed from the vials and transferred to the petri dishes for drying, some

of the PBS solution containing the drug was most likely lost. It is also possible that some error in fiber weighing may have occurred, as the weighing balance had a precision of 0.1mg, not less. A more precise weighing balance would probably have improved the accuracy of the measurements. Alternatively, increasing the number of test specimens for all six fiber samples at each time point could have provided more precise results for the drug release and drug retention studies.

5.5. CONCLUSIONS

Based on the results of the *in vitro* experimental study using exploratory data analysis, it was found that the drug release and retention rates are predictable in terms of a logarithmic relationship with a regression coefficient, $R^2 > 0.98$. The data can be predicted from a first-order kinetic model with a 98% confidence. A large proportion of the drug was released in the first 24 hours, followed by a gradual release of the remaining drug. It was also found that the fibers with a higher degree of crystallinity had a slower drug release rate, even though some of these fibers had a higher initial wt.% drug loading. This implies that the fiber crystallinity has a stronger effect on the drug release profile and retention rates than the total drug concentration loaded into the fibers. The initial rapid release of the drug is likely to be caused by the dissolution of the drug closer to the fiber surface. When implanting the P4HB fibers surgically as a medical device, the rapid release in the initial time frame is considered desirable, so as to generate an effective antimicrobial activity greater than the minimum effective concentration, and thus lower the risk of bacterial infection during the surgical procedure.

CHAPTER 6 – CONCLUSIONS, LIMITATIONS AND FUTURE WORK

6.1. CONCLUSIONS

As stated in the beginning of this dissertation, P4HB has potential applications in controlled release drug delivery systems. One of those applications could be in the form of incorporating a drug within textile fibers which can be used for several different medical products, such as sutures and tissue engineering scaffolds. The primary goal of this study was to develop a scalable wet spinning process for producing drug loaded P4HB fibers. To achieve this goal, the study was divided into three main projects, described in Chapter 1. The following section summarizes the findings and conclusions for each of the three projects.

The first project was to study the effect of wet spinning conditions on the structure and properties of P4HB fibers. Three wet spinning process conditions were studied each at two levels: polymer concentration in the spin dope, the temperature of the coagulation bath, and the as-spun draw ratio. Using characterization tests, such as SEM, XRD, DSC and mechanical testing, it was found that an increase in spin dope concentration and a higher spun draw ratio resulted in stronger fibers which possessed a higher degree of crystallinity. It was also found that fibers spun at a higher coagulation temperature had increased polymer chain alignment. It was also found that all the fibers had a uniform cylindrical structure. Based on this project, it was concluded that a spin dope concentration of 15%, and a coagulation bath at room temperature should be used to spin drug loaded P4HB fibers.

The second project was focused on studying the effect of drug loading on the structure and properties of the wet spun P4HB fibers. The chosen antibiotic drug for the study, levofloxacin, was added to the spin dopes at three different concentrations (2%, 5% & 10% by weight) with

respect to the polymer. The fibers were spun using the three different drug concentrations and two spun draw ratios (12 & 18). It was determined that the fibers spun at a higher spun draw ratio with 5 wt.% drug in the spin dope had the highest amount of drug (4.26 wt.%) incorporated into the wet-spun fibers, with about 85% drug loading efficiency. It was also found that the fibers spun with 2 wt.% and 5 wt.% drug concentrations at higher spun draw ratios did not seem to have a significant effect on the mechanical and structural properties of the fibers, as compared to the properties of the control fibers. Based on all the drug loading results from this study, it was determined that the fibers had a maximum drug loading limit between 2-5 wt.%. It was also concluded that the higher spun draw ratio increased the drug loading efficiency of the fibers.

The third project was to study the drug retention and drug profiles of the drug loaded P4HB fibers. The *in vitro* method carried for five days provided a fairly consistent profile for all six types of drug loaded fibers. It was found that the fibers had a burst drug release in the first twenty-four hours, followed by a slower release rate. A logarithmic regression equation was determined for the drug release and retention profiles, with a $R^2 > 0.98$, suggesting a certain level of predictability. It was found that the drug remaining in the fibers followed a first-order kinetic model which is typically used to predict drug elimination/diffusion from a matrix. No significant differences were found in the percent drug release and percent drug retention between the fibers at different time points, indicating a uniform distribution of the drug in all the fibers. However, it was found that the fiber with a higher degree of crystallinity had a significantly slower drug release rate, even when they had a higher amount of drug wt.% in the fiber. This suggested that the fiber structure and crystallinity had a more significant contribution to the drug release profile than the total drug loading concentration of the fiber.

6.2. LIMITATIONS

The primary limitation in this study was the unavailability of P4HB in its polymeric form. Therefore 100% P4HB uncoated absorbable surgical sutures were used as the raw material for preparing the spin dopes. It is possible that using polymer pellets instead of the sutures could produce homogeneous polymer solutions at concentrations higher than 15%. Some other limitations were related to the characterization tests for the wet spun fibers produced in this study. The Vibromat used for measuring the fiber linear density did not have weighing clips lighter than 55 mg, which appeared to be too heavy for the fibers tested. Also, the mechanical testing was carried out on an MTS instrument with a 2N swinging load cell, which caused vibrations during testing and resulted in a noisy stress/strain signal. It is believed that a lighter weighing clip for the Vibromat and a smaller capacity load cell for the MTS instrument could have provided more accurate data on the properties of these fibers. Additionally, time and resource constraints limited the XRD testing of multiple samples for each type of fiber, restricting the statistical analysis for the crystallinity of the fibers. Lastly, the weighing balance used for some of the steps had a minimum measurement precision of 0.1mg, which may have caused certain measurement errors in the study.

6.3. FUTURE WORK

The design and development of P4HB based wet spun drug loaded fibers is a big step which requires much more conclusive data on the effect of processing parameters on the fiber properties and drug loading and release profiles than currently available. This doctoral study is a step towards attaining a preliminary understanding of the wet spinning process of P4HB fibers and its

applicability in controlled release drug delivery systems. Additional work in this area needs to be done to gain a better understanding of these wet spun drug loaded P4HB fibers. This includes studying some of the other wet spinning process parameters, such as extrusion speed, type of spinneret, length of the coagulation bath and evaluating their effect on the spun and drawn fiber properties. Another area which needs to be focused on is the drug loading of the fibers by narrowing down the optimum concentration of the drug which can provide close to 100% loading efficiency. Additionally, a more in-depth study of the drug release profiles along with studying the efficacy of the drug loaded fibers over a period of time (such as using gram-positive or gram-negative antimicrobial testing) can provide a better understanding of the release kinetics for these fibers. Furthermore, incorporation of different types of drugs in P4HB fibers, such as anti-inflammatory drugs to prevent severe immune response or anti-coagulant drugs to prevent thrombosis, can also be studied.

CHAPTER 7 – REFERENCES

[1] E. Devaux, " Understanding the behaviour of synthetic polymer fibres during spinning," in *Advances in Filament Yarn Spinning of Textiles and Polymers*, Cambridge, Woodhead Publishing Ltd., 2014, pp. 31-47.

[2] I. Chodak, "Polyhydroxyalkanoates: Origin, Properties and Applications," in *Monomers, Polymers and Composites from Renewable Resources*, M. Belgacem and A. Gandini, Eds., Elsevier, 2008, pp. 451-477.

[3] S. Williams, S. Rizk and D. Martin, "Poly-4-hydroxybutyrate (P4HB): A new generation of resorbable medical devices for tissue repair and regeneration," *Biomedizinische Technik*, vol. 58, no. 5, pp. 1-14, 2013.

[4] Tepha Medical Devices, "Tepha Products Overview," Tepha Inc., [Online]. Available: https://www.tepha.com/products/overview/. [Accessed 23 01 2018].

[5] A. Shrivastav, H. Kim and Y. Kim, "Advances in the Applications of Polyhydroxyalkanoate Nanoparticles for Novel Drug Delivery System," *BioMed Research International*, 2013.

[6] L. Lei, S. Guo, W. Chen, H. Rong and F. Lu, "Stents as a platform for drug delivery," *Expert Opinion on Drug Delivery*, vol. 8, no. 6, pp. 813-831, 2011.

[7] F. Sharifi, A. C. Sooriyarachchi, H. Altural, R. Montazami, M. N. Rylander and N. Hashemi, "Fiber Based Approaches as Medicine Delivery Systems," *ACS Biomater. Sci. En*, vol. 2, pp. 1411-1431, 2016.

[8] Y. Qin, "Medical textile materials with drug-releasing properties," in *Medical Textile Materials*, Woodhead Publishing, 2016, pp. 175-189.

[9] D. P. Martin, S. Rizk, A. Ahuja and S. F. Williams, "Polyhydroxyalkanoate Medical Textiles and Fibers". United States Patent US008O3427OB2, 11 October 2011.

[10] G. Q. Chen, "A microbial polyhydroxyalkanoates (PHA) based bio- and materials industry," *Chemical Society Review*, vol. 38, no. 8, pp. 2434-46, 2009.

[11] C. S. Reddy,, R. Ghai, R. and V. C. Kalia, "Polyhydroxyalkanoates: an overview," *Bioresource Technology*, vol. 87, pp. 137-146, 2003.

[12] G. Braunegg, G. Lefebvre and K. Genser, "Polyhydroxyalkanoates, biopolyesters from renewable resources: physiological and engineering aspects," *Journal of Biotechnology*, vol. 65, pp. 127-161, 1998.

[13] P. M. Visakh, "Polyhydroxyalkanoates (PHAs), their Blends, Composites and Nanocomposites: State of the Art, New Challenges and Opportunities," in

Polyhydroxyalkanoate (PHA) Based Blends, Composites and Nanocomposites, I. Roy and V. P. M., Eds., Royal Society of Chemistry, 2015, pp. 1-17.

[14] A. A. Chowdhury, "Poly-β-hydroxybutyric acid-degrading bacteria and exoenzyme," *Archives. Microbiol.*, vol. 47, no. 2, pp. 167-200, 1963.

[15] G. de Koning, "Prospects of bacterial poly[(R)-3-(hydroxyalkanoates)]," Eindhoven: Technische Universiteit Eindhoven, 1993.

[16] S. Garge, "PHBV," Alchetron, [Online]. Available: https://alchetron.com/PHBV#-. [Accessed 20 01 2018].

[17] G. Braunegg, "Sustainable Poly(Hydroxyalkanoate) (PHA) Production," in *Degradable Polymers - Principles and Applications*, S. G., Ed., Dordrecht/Boston/London, Kluwer Academic Publisher, 2002, pp. 235-293.

[18] J. Asrar and K. J. Gruys, "Biodegradable Polymer (Biopol®)," in *Biopolymers Online*, Wiley, 2005, pp. 53-86.

[19] I. C. Business, "Monsanto to buy Biopol from Zeneca," ICIS, 1996.

[20] J. H. Schut, "Where is Metabolix's PHA biopolymer?," Plastics Engineering Blog, 2011.

[21] G. Chen, "Industrial Production of PHA," in *Plastics from Bacteria: Natural Functions and Applications*, Berlin, Springer, 2010, pp. 121-132.

[22] M. Annuar, I. Tan and K. Ramachandran, "Evaluation of nitrogen sources for growth and production of medium-chain-length poly-(3-hydroxyalkanoates) from palm kernel oil by Pseudomonas putida," *J Mol Biol Biotechnol*, vol. 16, no. 1, pp. 11-15, 2008.

[23] A. M. Gumel, M. S. M. Annuar and Y. Chisti, "Recent Advances in the Production, Recovery and Applications of Polyhydroxyalkanoates," *J Polym Environ*, vol. 21, pp. 580-605, 2013.

[24] M. Mohammadi and M. Ghaffari-Moghaddam, "Recovery and Extraction of Polyhydroxyalkanoates (PHAs)," in *Polyhydroxyalkanoate (PHA) Based Blends, Composites and Nanocomposites*, The Royal Society of Chemistry, 2015, pp. 47-65.

[25] B. Kunasundari and K. Sudesh, "Isolation and recovery of microbial polyhydroxyalkanoates," *eXPRESS Polymer Letters*, vol. 5, no. 7, pp. 620-634, 2011.

[26] C. Peña, T. Castillo, A. García, M. Millán and D. Segura, "Biotechnological strategies to improve production of microbial poly-(3-hydroxybutyrate): a review of recent research work," *Microbiology Biotechnology*, vol. 7, no. 4, pp. 278-293, 2014.

[27] M. Koller and G. Braunegg, "Potential and Prospects of Continuous Polyhydroxyalkanoate (PHA) Production," *Bioengineering*, vol. 2, no. 2, pp. 94-121, 2015.

[28] B. D., "Polyhydroxyalkanoates," in *Plastics from microbes: microbial synthesis of polymers and polymer precursors*, D. P. Mobley, Ed., Munich, Hanser, 1994, pp. 5-33.

[29] N. Berezina and S. M. Martelli, "Polyhydroxyalkanoates: Structure, Properties and Sources," in *Polyhydroxyalkanoate (PHA) Based Blends, Composites and Nanocomposites*, I. Roy and V. P. M., Eds., The Royal Society of Chemistry, 2015, pp. 18-46.

[30] M. Zinn and R. Hany, "Tailored material properties of polyhydroxyalkanoates through biosynthesis and chemical modification," *Advanced Engineering Materials,* vol. 7, pp. 408-411, 2005.

[31] G. Tan, C. Chen, L. Li, L. Ge, L. Wang, I. Razaad, Y. Li, L. Zhao and J. Wang, "Start a Research on Biopolymer Polyhydroxyalkanoate (PHA): A Review," *Polymers,* vol. 6, no. 3, pp. 706-754, 2014.

[32] A. AJ and D. EA, "Occurrence, metabolism, metabolic role, and industrial uses of bacterial polyhydroxyalkanoates," *Microbiology Review,* vol. 54, pp. 450-472, 1990.

[33] F. Wang and S. Lee, "Poly(3-hydroxybutyrate) production with high productivity and high polymer content by a fed-batch culture of Alcaligenes latus under nitrogen limitation," *Applied Environmental Microbiology,* vol. 63, pp. 3703-3706, 1997.

[34] S. Shahid, R. Mosrati, J. Ledauphin, C. Amiel, P. Fontaine, J.-L. Gaillard and D. Corroler, "Impact of carbon source and variable nitrogen conditions on bacterial biosynthesis of polyhydroxyalkanoates," *Bioscience and Bioengineering,* vol. 116, pp. 302-308, 2013.

[35] S. Valappil, A. Boccaccini, C. Bucke and I. Roy, "Polyhydroxyalkanoates in Gram-positive bacteria," *Antonie Van Leeuwenhoek,* vol. 91, pp. 1-17, 2007.

[36] E. N. Pederson, C. W. J. McChalicher and F. Srienc, "Bacterial synthesis of PHA block copolymers," *Biomacromolecules,* vol. 7, no. 6, pp. 1904-1911, 2006.

[37] R. Davis, R. Kataria, F. Cerrone, T. Woods, S. Kenny, A. O'Donovan, M. Guzik, H. Shaikh, G. Duane, V. K. Gupta, M. G. Tuohy, R. B. Padamatti, E. Casey and K. E. O'Connor, "Conversion of grass biomass into fermentable sugars and its utilization for medium chain length polyhydroxyalkanoate (mcl-PHA) production by Pseudomonas strains," *Bioresource Technology,* vol. 150, pp. 202-209, 2013.

[38] S. Khanna and A. K. Srivastava, "Recent advances in microbial polyhydroxyalkanoates," *Process Biochemistry,* vol. 40, pp. 607-619, 2005.

[39] S. Chanprateep, "Current trends in biodegradable polyhydroxyalkanoates," *Bioscience and Bioengineering,* vol. 110, no. 6, pp. 621-632, 2010.

[40] H. Ramachandran, S. Kannusamy, K. Huaong, R. Mathava and A. Amirul, "Blends of Polyhydroxyalkanoates (PHAs)," in *Polyhydroxyalkanoate (PHA) Based Blends, Composites and Nanocomposites,* The Royal Society of Chemistry, 2015, pp. 66-97.

[41] M. Shibata, Y. Inoue and M. Miyoshi, "Mechanical properties, morphology, and crystallization behavior of blends of poly (L-lactide)," *Polymer,* vol. 47, no. 10, pp. 3557-3564, 2006.

[42] D. Lovera, L. Márquez, V. Balsamo, A. Taddei, C. Castelli and A. J. Müller, "Crystallization, Morphology, and Enzymatic Degradation of Polyhydroxybutyrate/Polycaprolactone (PHB/PCL) Blends," *Macromolecular Chemistry and Physics,* vol. 208, no. 9, pp. 924-937, 2007.

[43] G. Chen and Tsinghua, "Polyhydroxyalkanoates Blends and Composities," in *Biodegradable Polymer Blends and Composites from Renewable Resources*, Hoboken, New Jersey, John Wiley & Sons, 2008, pp. 1-191.

[44] L. Yu, K. Dean and L. Li, "Polymer blends and composites from renewable resources," *Progress in Polymer Science,* vol. 31, pp. 576-602, 2006.

[45] J. Mozejko-Ciesielska and R. Kiewisz, "Bacterial polyhydroxyalkanoates: Still fabulous?," *Microbiological Research,* vol. 192, pp. 271-282, 2016.

[46] E. Kosior, R. M. Braganca and P. Fowler, "Lightweight compostable packaging:," *The Waste & Resource Action Program,* vol. INN003/26, pp. 1-48, 2006.

[47] L. Yee and L. Foster, "Polyhydroxyalkanoates as Packaging Materials: Current Applications and Future Prospects," in *Polyhydroxyalkanoate (PHA) Based Blends, Composites and Nanocomposites*, I. Roy and V. P. M., Eds., The Royal Society of Chemistry, 2015, pp. 183-207.

[48] S. Rathbone, P. Furrer, J. L. ̈bben, M. Zinn and S. Cartmell, "Biocompatibility of polyhydroxyalkanoate as a potential material for ligament and tendon scaffold material," *Journal of Biomedical Materials Research Part A,* vol. 93, no. 4, pp. 1391-1403, 2009.

[49] E. I. Shishatskaya, "Biomedical Investigations of Biodegradable PHAs," *Macromolecular Symposia,* vol. 269, pp. 65-81, 2008.

[50] D. P.Martin and S. F.Williams, "Medical applications of poly-4-hydroxybutyrate: a strong flexible absorbable biomaterial," *Biochemical Engineering Journal,* vol. 16, no. 2, pp. 97-105, 2003.

[51] J. Lee, S. Jung, C. Park, H. Kim, C. Batt and Y. Kim, "Tumor-specific hybrid polyhydroxybutyrate nanoparticle," *Bioorg Med Chem Lett,* vol. 21, no. 10, pp. 2941-2944, 2011.

[52] A. Bohl, H. W. Rohm, P. Ceschi and G. Paasche, "Development of a specially tailored local drug delivery system for the prevention of fibrosis after insertion of cochlear implants," *Material Science: Materials in Medicine,* vol. 23, pp. 2151-2162, 2012.

[53] S. D. Waddington, "Polyhydroxyalkanoates and film formation therefrom". US Patent 5578382 A, 1 February 1996.

[54] A. Elias, P. Anbukarasu and D. Sauvageau, "Polyhydroxyalkanoate film formation using alkanoic acids". US Patent 20160230039 A1, 10 february 2016.

[55] I. Chodak and R. S. Blackburn, "Sustainable synthetic fibres: the case of poly(hydroxyalkanoates) (PHA) and other fibres," in *Sustainable textiles*, Woodhead, 2009, pp. 88-112.

[56] R. Hufenus, F. A. Reifler, M. P. Fernandez-Ronco and M. Heuberger, "Molecular orientation in melt-spun poly(3-hydroxybutyrate) fibers: Effect of additives, drawing and stress-annealing," *European Polymer Journal*, vol. 71, pp. 12-26, 2015.

[57] E. B. Bond, "Fiber Spinning Behavior of a 3-Hydroxybutyrate/3-Hydroxyheanoate Copolymer," *Macromolecular Symposia*, vol. 197, pp. 19-31, 2003.

[58] D. P. Martin, K. Gua, S. Rizk and S. F. Williams, "Ultrafine Electrospun Fibers of Poly-4-hydroxybutyrate and copolymers thereof". USA Patent US 20140277572A1, 18 September 2014.

[59] R. Cahil, K. Gua, D. P. Martin and S. Rizk, "Medical Devices Containing Dry Spun Non-Wovens of Poly-4-hydroxybutyrate and copolymers". USA Patent US 20120150285A1, 14 June 2012.

[60] F. Acevedo, P. Villegas, V. Urtuvia, J. Hermosilla, R. Navia and M. Seeger, "Bacterial polyhydroxybutyrate for electrospun fiber production," *International Journal of Biological Macromolecules*, vol. 106, pp. 692-697, 2018.

[61] W. Cui, Y. Zhou and J. Chang, "Electrospun nanofibrous materials for tissue engineering and drug delivery," *Science and Technology of Advanced Materials*, vol. 11, 2010.

[62] N. G. Gaylord and H. M. Hulburt, "Fiber Spinning," in *Processing of Thermoplastic Polymers*, Reinhold, Krieger, 1974, pp. 257-3304.

[63] H. Yoon, " Melt Spinning of High Performance Poly(ethylene terephthalate) (PET) via Utilizing a Horizontal Isothermal Bath (HIB) in the Threadline," North Carolina State University, Raleigh, 2012.

[64] N. Bhardwaj and S. C. Kundu, "Electrospinning: A fascinating fiber fabrication technique," *Biotechnology Advances*, vol. 28, pp. 325-347, 2010.

[65] J. Hagewood, "Technologies for the manufacture of synthetic polymer fibers," in *Advances in Filament Yarn Spinning of Textiles and Polymers*, Cambridge, Woodhead Publishing Ltd., 2014, pp. 48-71.

[66] G. Bhat and V. Kandagor, "Synthetic polymer fibers and their processing requirements," in *Advances in Filament Yarn Spinning of Textiles and Polymers*, Cambridge, Woodhead Publishing Ltd., 2014, pp. 3-30.

[67] D. Peiffer, "Degrees of freedom of polymeric molecules and their effect on physical-properties," *Macromolecular Science-Physics*, vol. B15, no. 4, pp. 595-611, `978.

[68] A. Kim and J. Musfeldt, "Understanding chemical structure physical property relationships in polymers through molecular modeling and thermal analysis techniques," *Chemical Education,* vol. 75, no. 7, pp. 893-896, 1998.

[69] P. Patel and D. Bogue, "The effect of molecular-orientation on the mechanical-properties of fibre-filled amorphous polymers," *Journal of Rheology,* vol. 25, no. 4, pp. 461-462, 1981.

[70] S. Cheng, "Materials science: polymer crystals downsized," *Nature,* vol. 448, no. 7157, pp. 1006-1007, 2007.

[71] G. Cook, Handbook of textile fibers: Man-made Fibers, Cambridge: Woodhead Publishing Ltd., 1984.

[72] "Fiber and Filament Production (Spinning)," Encyclopedia of Enginnering, 16 03 2015. [Online]. Available: http://www.mechscience.com/fiber-and-filament-production-spinning/. [Accessed 22 01 2018].

[73] A. Rawal and S. Mukhopadhyay, "Melt spinning of synthetic polymeric filaments," in *Advances in Filament Yarn Spinning of Textiles and Polymers*, Cambridge, Woodhead Publishing Ltd., 2014, pp. 75-99.

[74] B. Wulfhorst, T. Gries and D. Veit, "Raw Materials," in *Textile technology*, Munich, Hanser, 2006, pp. 13-73.

[75] Y. Murase and A. Nagai, "Melt Spinning," in *Advanced Fiber Spinning Technology*, Cambridge, Woodhead Publishing Ltd., 2004, pp. 25-64.

[76] "Fiber and Filament Production," Textile Innovation Knowledge Platform, [Online]. Available: http://www.tikp.co.uk/knowledge/technology/fibre-and-filament-production/. [Accessed 21 01 2018].

[77] A. Ziabicki, Fundamentals of Fibre Formation: the Science of Fibre Spinning and Drawing, New York: John Wiley & Sons, 1976.

[78] Y. Imura, R. Hogan and M. Jaffe, "Dry spinning of synthetic polymer fibers," in *Advances in Filament Yarn Spinning of Textiles and Polymers*, Cambridge, Woodhead Publishing Ltd., 2014, pp. 187-202.

[79] Textile Engineer@ Blogspot, "Types of Spinning (Man-Made Fibers)," 23 10 2010. [Online]. Available: http://textileengineerr.blogspot.com/2010/10/types-of-spinning-man-made-fibers.html. [Accessed 22 01 2018].

[80] D. V. Krevelen and K. Nijenhuis, Properties of Polymers Fourth Edition, Amsterdam: Elsevier, 2009.

[81] S. Eichhorn, J. Hearle, M. Jaffe and T. Kikutani, Handbook of Textile Fibre Structure Volume 1: Fundamentals and Manufactured Polymer Fibres, Cambridge: Woodhead Publishing Ltd., 2009.

[82] S. Gogolewski and A. Pennings, "High-modulus fibers of nylon-6 prepared by a dry-spinning method," *Polymer,* vol. 26, pp. 1394-1400, 1985.

[83] B. Ozipek and H. Karakas, "Wet spinning of synthetic polymer fibers," in *Advances in Filament Yarn Spinning of Textiles and Polymers*, Cambridge, Woodhead Publishing Ltd., 2014, pp. 174-186.

[84] A. L. Ahmad, T. A. Otitoju and B. S. Ooi, "Hollow fiber (HF) membrane fabrication: A review on the effects of solution spinning conditions on morphology and performance," *Journal of Industrial and Engineering Chemistry,* vol. 70, pp. 35-50, 2019.

[85] H. Yasuda, K. Ban and Y. Ohta, "Gel Spinning Processes," in *Advanced Fibre Spinning Technology,* Cambridge, Woodhead Publishing Ltd., 1994, pp. 172-186.

[86] C. Kuo and W. Lan, "Gel spinning of synthetic polymer fibres," in *Advances in Filament Yarn Spinning of Textiles and Polymers*, Cambridge, Woodhead Publishing Ltd., 2014, pp. 100-112.

[87] J. Yao, C. W. M. Bastiaansen and T. Peijs, "High Strength and High Modulus Electrospun Nanofibers," *Fibers,* vol. 2, pp. 158-187, 2014.

[88] Y. Termonia, P. Meakin and P. Smith, "Theoretical study of the influence of the molecular weight on the maximum tensile strength of polymer fibers," *Macromolecules,* vol. 18, no. 11, pp. 2246-2252, 1985.

[89] Q. Q. Ni, X. D. Jin, H. Xia and F. Liu, " Electrospinning, processing and characterization of polymer-based nano-composite fibers," in *Advances in Filament Yarn Spinning of Textiles and Polymers*, Woodhead Publishing, 2014, pp. 128-148.

[90] H. Kadavil, Z. Moustafa, A. Elzatahry and T. Altahamouni, "Sputtering of Electrospun Polymer-Based Nanofibers for Biomedical Applications: A Perspective," *Nanomaterials* , vol. 9, no. 1, pp. 77-107, 2019.

[91] J. Doshi and D. H. Renekar, "Electrospinning process and applications of electrospun fibers," *Journal of Electrostatics,* vol. 35, pp. 151-156, 1995.

[92] B. Narasimhan and S. Mallapragada, "Dissolution of amorphous and semicrystalline polymers: mechanisms and novel applications," *Recent Res Dev Macromol Res,* vol. 3, no. 2, pp. 311-324, 1998.

[93] B. A. Miller, "A review of polymer dissolution," *Progress in Polymer Science,* vol. 28, pp. 1223-1270, 2003.

[94] E. D. Horton, "Polymer dissolution, Fractionation, Gas permeation".

[95] S. B. Grassino, "Polymer Solutions," University of Southern Mississippi, [Online]. Available: http://pslc.ws/macrog/property/solpol/ps1.htm. [Accessed 24 01 2018].

[96] H. Morita and M. Doi, "Mesoscale simulation of line-edge structures based on polymer chains in development and rinse processes," *Journal-of-Micro/Nanolithography,-MEMS,-and-MOEMS*, vol. 9, no. 4, p. 412 - 413, 2010.

[97] M. J. Covitch and K. J. Trickett, "How Polymers Behave as Viscosity Index Improvers in Lubricating Oils," *Advances in Chemical Engineering and Science*, vol. 5, pp. 134-151, 2015.

[98] Y. Termonia, "Fundamentals of Polymer Coagulation," *Polymer Science: Part B*, vol. 33, no. 2, pp. 279-288, 1995.

[99] T. Tsurumi, "Solution Spinning," in *Advanced Fiber Spinning Technology*, Cambridge, Woodhead Publishing ltd., 1994, pp. 65-104.

[100] L. Eykens, K. De Sitter, L. Stoops, C. Dotremont, L. Pinoy and B. Van der Bruggen, "Development of polyethersulfone phase-inversion membranes for membrane distillation using oleophobic coatings," *Journal of Applied Polymer Science*, vol. 134, p. 45516, 2017.

[101] J. Chen, W. Chenguo, D. Xingguang and L. Huanzhang, "Study on coagulation mechanism of wet spinning PAN fibers," *Polymer Research*, vol. 13, no. 6, pp. 515-519, 2006.

[102] A. J. Domb, J. Kost and D. M. Wiseman, Handbook of Biodegradable Polymers., Harwood Academic Publishers, 1997.

[103] C. R. Gajjar and M. W. King, Resorbable Fiber-Forming Polymers for Biotextile Applications, Springer, 2014, pp. 1-5.

[104] N. Campbell, Biology: 10th ed., Benjamin, Ed., Menlo Park, California: Cummings, 2013.

[105] L. Fambri, C. Migliaresi, K. Kesenci and E. Piskin, "Biodegradable Polymers," in *Integrated Biomaterials Science*, R. Barbucci, Ed., Kluwer Academic, 2002, pp. 119-187.

[106] Y. Huang, "Hydrolytic behavior of poly(lactic acid) films with different architecture modified by poly(dodecafluorheptyl methylacrylate)," *European Polymer Journal*, vol. 59, pp. 189-199, 2014.

[107] F. vonBurkersroda, LuiseSchedl and AchimGöpferich, "Why degradable polymers undergo surface erosion or bulk erosion," *Biomaterials*, vol. 23, no. 21, pp. 4221-4231, 2002.

[108] P. Atkins, The Elements of Physical Chemistry, New York: W. H. Freeman, 1997.

[109] A. Gopferich, "Mechanisms of polymer degradation and erosion," *Biomaterials*, vol. 17, pp. 103-114, 1996.

[110] I. Taniguchi, "Materials for Biomedical Applications," Spring 2006. [Online]. Available: http://ocw.mit.edu/courses/materials-science-and-engineering/3-051j-materials-forbiomedical-applications-spring-2006/lecture-notes/lecture4_2.pdf.. [Accessed 04 02 2018].

[111] S. Lyu and D. Untereker, "Degradability of Polymers for Implantable Biomedical Devices," *International Journal of Molecular Sciences,* vol. 10, pp. 4033-4065, 2009.

[112] B. D. Ratner, A. S. Hoffman, F. J. Schoen and J. E. Lemons, "Degradation of Materials in the Biological Environment," in *Biomaterials Science*, Elsevier, 2012, pp. 243-259.

[113] M. A. Souza, K. Y. Sakamoto and L. H. Mattoso, "Release of the Diclofenac Sodium by Nanofibers of Poly(3-hydroxybutyrate-co-3-hydroxyvalerate) Obtained from Electrospinning and Solution Blow Spinning," *Journal of Nanomaterials,* vol. 2014, p. 8, 2014.

[114] C. T. Huynh and D. S. Lee, "Controlled Release," *Encyclopedia of Polymeric Nanomaterials,* 2014.

[115] D. Halpern, "POLYMERS IN MEDICINE AND SURGERY-A SURVEY.s," *Annals of the New York Academy of Sciences,* vol. 146, pp. 193-202, 1968.

[116] W. O. Herrmann and H. Wolfram, "Surgical and medical preparations". US Patent 2155658, 25 Apr 1939.

[117] E. R. Kenawy, F. I. Abdel-Hay, M. H. El-Newehy and G. E. Wnek, "Processing of polymer nanofibers through electrospinning as drug delivery systems," *Materials Chemistry and Physics,* vol. 113, no. 1, pp. 296-302, 2009.

[118] W.-W. Yang and E. Pierstorff, "Reservoir-Based Polymer Drug Delivery Systems," *Journal of Laboratory Automation,* vol. 17, no. 1, pp. 50-58, 2012.

[119] D. M. Lavin, R. M. Stefani, L. Zhang, S. Furtado, R. A. Hopkins and E. Mathiowitz, "Multifunctional polymeric microfibers with prolonged drug delivery and structural support capabilities," *Acta Biomaterialia,* vol. 8, pp. 1891-9000, 2012.

[120] C. K. Pillai and C. P. Sharma, "Absorbable Polymeric Surgical Sutures: Chemistry, Production, Properties, Biodegradability, and Performance," *Journal of Biomaterials Applications,* vol. 25, no. 4, pp. 291-366, 2010.

[121] O. Catanzano, S. Acierno, P. Russo, M. Cervasio, . M. D. B. De Caro, A. Bolognese, G. Sammartino, L. Califano, G. Marenzi, A. Calignano , D. Acierno and F. Quaglia, "Melt-spun bioactive sutures containing nanohybrids for local delivery of anti-inflammatory drugs," *Materials Science and Engineering C,* vol. 43, pp. 300-309, 2014.

[122] C. J. Rozzelle, J. Leonardo and V. Li, "Antimicrobial suture wound closure for cerebrospinal fluid shunt surgery: a prospective, double-blinded, randomized controlled trial," *Journal of Neurosurgery:Pediatrics,* vol. 2, no. 2, pp. 111-117, 2008.

[123] V. A. Zhukovskii, "Problems and prospects for development and production of surgical suture materials," *Fibre Chemistry,* vol. 40, no. 3, pp. 208-216, 2008.

[124] Ethicon US, "Coated VICRYL® Plus Antibacterial (polyglactin 910) Suture," [Online]. Available: https://www.jnjmedicaldevices.com/en-US/product/coated-vicryl-plus-antibacterial-polyglactin-910-suture. [Accessed 28 01 2019].

[125] K. J. Rambhia and P. X. Ma, "Controlled drug release for tissue engineering," *Journal of Controlled Release,* vol. 219, pp. 119-128, 2015.

[126] J. Jeong, S. I. Jeong, J. Park, H. Gwon, S. Ahn, H. Shin, J. Y. Lee and Y. Lim, "Development and characterization of heparin-immobilized polycaprolactone nanofibrous scaffolds for tissue engineering using gamma-irradiation," *RSC Advances,* vol. 7, no. 15, pp. 8963-8972, 2017.

[127] A. I. G. Varela, M. Aymerich, D. N. Garcia, Y. C. Martin, P. A. Beule, E. Alvarez, C. Bao-Varela and M. T. Flores-Arias, "Sol-Gel Glass Coating Synthesis for Different Applications: Active Gradient-Index Materials, Microlens Arrays and Biocompatible Channels," in *Recent Applications in Sol-Gel Synthesis*, IntechOpen, 2017, pp. 231-252.

[128] I. Alghoraibi, "Different methods for nanofibers design and fabrication," in *Handbook of Nanofibers*, Springer, 2018.

[129] Weistron Instruments, "Electrospinning Technique," [Online]. Available: http://www.weistron.com/tech-abc/electrospinning-tech/. [Accessed 05 02 2019]

[130] C. B. J. Manuel, V. G. Jesus and S. M. Aracely, "Electrospinning for Drug Delivery Systems: Drug Incorporation Techniques," in *Electrospinning - Material, Techniques, and Biomedical Applications*, IntechOpen, 2016, pp. 141-155.

[131] A. Toncheva, D. Paneva, V. Maximova, N. Manolova and I. Rashkov, "Antibacterial fluoroquinolone antibiotic-containing fibrous materials from poly(L-lactide-co-D,L-lactide) prepared by electrospinning," *European Journal of Pharmaceutical Sciences,* vol. 47, pp. 642-651, 2012.

[132] H. Gao, Y. Gu and Q. Ping, "The implantable 5-fluorouracil-loaded poly(L-lactic acid) fibers prepared by wet-spinning from suspension," *Journal of Controlled Release,* vol. 118, pp. 325-332, 2007.

[133] D. G. Yu, X. X. Shen, Y. Zheng, Z. H. Ma, L. M. Zhu and C. Branford-White, "Wet-spinning medicated PAN/PCL fibers for drug sustained release," *2nd International Conference on Bioinformatics and Biomedical Engineering*, pp. 1375-1378, 2008.

[134] D. L. Wise, Handbook of Pharmaceutical Controlled Release Technology, New York: Marcel Dekker Inc., 2000.

[135] Y. Fu and W. J. Kao, "Drug Release Kinetics and Transport Mechanisms of Nondegradable and Degradable Polymeric Delivery Systems," *Expert Opin Drug Deliv.*, vol. 7, no. 4, pp. 429-444, 2010.

[136] T. Shah and S. Halacheva, "Drug-releasing textiles," in *Advances in Smart Medical Textiles*, Elsevier, 2016, pp. 119-154.

[137] B. B. Crow, A. F. Borneman, D. L. Hawkins, G. M. Smith and K. D. Nelson, "Evaluation of in Vitro Drug Release, pH Change, and Molecular Weight Degradation of Poly(L-lactic acid) and Poly(D,L-lactide-co-glycolide) Fibers," *Tissue Engineering*, vol. 11, no. 7, pp. 1077-1084, 2005.

[138] S. Dash, P. N. Murthy, L. Nath and P. Chowdhury, "Kinetic Modeling on Drug Release from Controlled Drug Delivery Systems," *Acta Poloniae Pharmaceutica - Drug Research*, vol. 67, no. 3, pp. 217-223, 2010.

[139] Galatea Surgical, "History of P4HB™ Biopolymer," [Online]. Available: https://www.galateasurgical.com/surgical-scaffolds/history/. [Accessed 29 08 2018].

[140] D. P. Martin, S. Rizk, A. Ahuja and S. F. Williams, "Polyhydroxyalkanoate Medical Textiles and Fibers". United States Patent US008O3427OB2, 11 October 2011.

[141] H. Cong, "Studies of Barbed Surgical Sutures Associated with Materials, Anchoring," North Carolina State University, Raleigh, 2018.

[142] A. K. Agrawal, "National Programme on Technology Enhanced Learning (NPTEL)," 17 September 2013. [Online]. Available: https://nptel.ac.in/courses/116102010/. [Accessed 08 27 2018].

[143] P. Rizzo, "Polymer Technology Group," [Online]. Available: http://www.polymertechnology.it/bacheca/NanocompositeForm/page5/page5.html. [Accessed 28 04 2019]

[144] R. Hoffman and M. W. Davidson, "Olympus Corporation," [Online]. Available: https://www.olympus-lifescience.com/en/microscope-resource/primer/techniques/polarized/michel/. [Accessed 21 11 2018].

[145] R. Cox, "Acrylic Fibers," in *Synthetic Fibres: Nylon, Polyester, Acrylic, Polyolefin*, J. E. McIntyre, Ed., Cambridge, Woodhead Publishing Ltd., 2005, pp. 167-234.

[146] G. Strobl, "Laws controlling crystallization and melting in bulk polymers," *Reviews of Modern Physics*, vol. 81, no. 3, pp. 1287-1300, 2009.

[147] C. Lu, C. Blackwell, Q. Ren and E. Ford, "Effect of the Coagulation Bath on the Structure and Mechanical Properties of Gel-Spun Lignin/Poly(vinyl alcohol) Fibers," *ACS Sustainable Chem. Eng*, vol. 5, pp. 2949-2959, 2017.

[148] S. Knowledge, "Making Strong Fibers," [Online]. Available: 2008. http://sciencemags.blogspot.com/2008/05/making-strong-fibers.html. [Accessed 28 02 2019]

[149] Elsevier Ltd., "Levofloxacin," *Tuberculosis*, vol. 88, no. 2, pp. 119-121, 2008.

[150] T. O'Haver, "Instrumental Deviation from Beer's Law," January 2016. [Online]. Available: https://terpconnect.umd.edu/~toh/models/BeersLaw.html. [Accessed 10 07 2019].

[151] F. Alexis, "Factors affecting the degradation and drug-release mechanism of poly(lactic acid) and poly[(lactic acid)-co-(glycolic acid)]," Polymer International, vol. 54, pp. 36-46, 2005.

[152] R. Upadhyay, "An experimental and computational study of Bioceramic porosity on Drug Release Kinetics," University of North Carolina, Charlotte, 2016.